APPENDIX A-4:

TEMPERATURE TECHNICAL ANALYSIS

APPENDIX A-4: TEMPERATURE TECHNICAL ANALYSIS
TABLE OF CONTENTS

LIST OF FIGURES

LIST OF IMAGES

LIST OF TABLES

CURRENT CONDITIONS

Available Temperature Data

Vast amounts of temperature data have been collected in the Umatilla Basin. Two types of temperature data exist for the Umatilla River and tributaries: continuous measurements (typically recorded hourly) and forward looking infrared radiometer (FLIR) thermal imagery.

Continuous Temperature Measurements

Continuous hourly temperature data was collected in the Umatilla Basin during the summer of 1998 by the following agencies or groups:

- ✓ *Agricultural Research Service (ARS)*
- ✓ *Confederated Tribes of the Umatilla Indian Reservation (CTUIR)*
- ✓ *Oregon Department of Environmental Quality (ODEQ)*
- ✓ *Oregon Department of Fish and Wildlife (ODFW)*
- ✓ *Umatilla Sub-Basin TMDL Technical Committee*
- ✓ *United States Forest Service (USFS)*

The *maximum* 7-day statistics for 1998 are presented in **Table A-1**. **Figure A-1** displays the temperature monitoring locations.

Figure A-1. Temperature Monitoring Locations and Associated 7-day Maximums (1998)

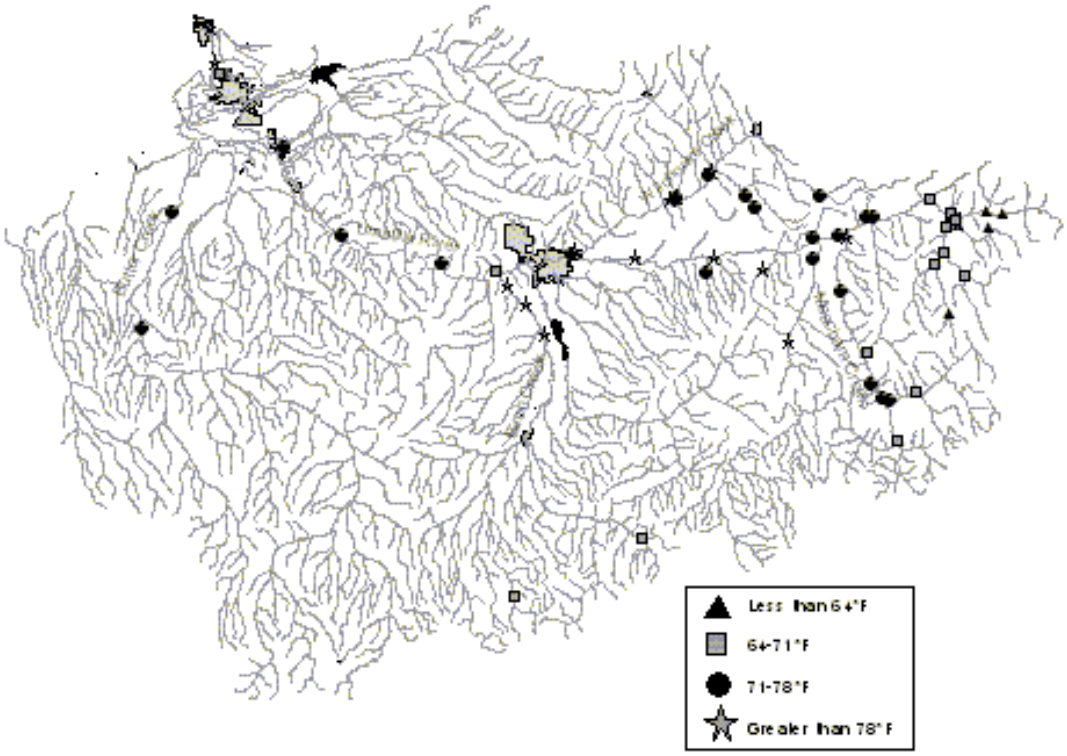

Table A-1. Calculated Water Temperature Statistics for the Umatilla River in 1998.

Temperature Site	*Start Date*	*End Date*	*Max Temp. (Date)*	*(°F)*	*7-Day Stat. (Date)*	*(°F)*
Birch Ck RM 1.5	6/1	8/14	7/28	92.1	7/24	89.1
Birch Ck RM 3.5	6/1	10/30	7/27	91.8	7/24	89.6
Birch Ck RM 6.5	6/1	10/30	7/28	89.4	7/24	86.7
Buck Ck at mouth	6/1	10/25	7/28	62.4	7/24	61.3
Buck Ck RM 3.3	5/1	12/19	7/27	63.0	7/23	61.7
Buckaroo Ck RM 2.0	5/13	10/18	7/27	84.7	7/23	81.7
Butter Ck at Madison Brg	7/2	10/20	8/14	80.8	8/9	75.7
Butter Ck at Pine City Brg	7/2	10/20	7/18	78.1	7/6	75.4
Camp Ck RM 0.5	4/8	12/15	8/3	67.8	7/31	65.7
East Birch Ck at Westgate	6/1	8/11	8/5	70.2	7/24	69.1
East Meacham Ck RM 0.2	4/8	12/15	8/3	70.3	7/23	68.9
Greasewood Ck at mouth	5/19	10/12	7/28	79.7	7/24	77.4
Meacham Ck at River Road	6/17	10/26	7/26	82.2	7/24	79.9
Meacham Ck below NF Meacham Ck	6/17	10/26	8/4	75.9	8/2	73.2
Meacham Ck RM 13.0	4/8	12/15	8/3	72.7	7/23	71.2
Meacham Ck RM 5.25	5/29	10/12	7/28	78.1	8/9	76.5
Moonshine Ck RM 1.1	5/14	10/11	7/28	79.3	7/24	77.0
N. Hermiston Drain at 12th St Brdg	7/1	10/21	9/4	66.9	8/31	66.4
N. Hermiston Drain at mouth	4/10	12/14	9/3	71.8	8/30	70.7
NF Meacham Ck at Forest Bound.	6/25	10/4	7/28	72.0	7/16	70.2
NF Meacham Ck RM 0.5	4/8	12/15	8/3	72.7	7/23	71.2
NF Umatilla R. at Umatilla Springs C.G.	6/17	10/26	8/5	61.3	7/16	60.8
NF Umatilla R. RM 2.7	4/21	12/19	7/27	61.2	7/15	60.3
NF Umatilla R. RM 4.0	4/21	12/19	7/27	58.8	7/23	57.7
SF Umatilla R. above Buck Creek	6/1	10/24	7/28	72.7	7/24	71.1
SF Umatilla R. at Gauge	12/1	8/15	7/28	70.5	7/24	69.3
SF Umatilla R. below Buck Creek	6/1	10/26	7/28	72.5	7/24	70.7
Shimmiehorn Ck (upper)	6/19	9/15	7/28	62.6	7/24	61.2
Shimmiehorn Ck at mouth	6/30	9/16	7/28	66.9	7/24	65.3

Table A-1 (continued). Calculated Water Temperature Statistics for the Umatilla River in 1998

Temperature Site	*Start Date*	*End Date*	*Max Temp. (Date)*	*Max Temp. (°F)*	*7-Day Stat. (Date)*	*7-Day Stat. (°F)*
Spring Ck at mouth	6/23	9/16	7/28	68.4	7/24	66.4
Spring Hollow Ck RM 3.5	5/19	10/11	7/27	75.4	7/24	73.2
Spring Hollow Ck RM 4.5	4/10	12/14	7/27	79.3	7/24	76.1
Squaw Ck RM 2.0	5/14	10/12	7/28	79.7	7/24	77.5
Stanfield Drain at mouth	4/10	12/14	7/27	75.2	7/23	73.8
Thomas Ck RM 0.25	4/8	12/15	7/27	66.6	7/23	65.5
Umatilla R. above Ryan Creek	4/9	12/16	7/28	74.8	7/16	73.0
Umatilla R. at Bingham Springs	4/9	11/18	7/28	71.4	7/16	70.0
Umatilla R. at Campbell RM 42.5	4/11	12/14	7/16	73.6	7/12	72.5
Umatilla R. at Cayuse	5/7	12/14	7/27	81.7	7/23	79.9
Umatilla R. at Cayuse Brdg	6/17	10/26	7/28	86.2	8/9	83.3
Umatilla R. at Corporation	6/17	10/26	7/28	66.4	7/16	65.8
Umatilla R. at Hermiston WWTP	7/1	10/21	7/28	80.2	7/24	78.4
Umatilla R. at Mission Brdg	6/17	10/25	7/28	85.5	7/24	83.5
Umatilla R. at Pendleton Gauge	7/1	10/24	8/4	78.3	7/24	76.5
Umatilla R. at Squaw Creek	5/14	10/18	7/28	79.2	7/24	77.0
Umatilla R. at Stanfield Dam	5/8	12/14	7/15	76.5	7/11	75.2
Umatilla R. at Umatilla Gravel Pit	7/8	9/11	7/27	92.3	7/22	89.1
Umatilla R. below Birch	7/1	10/21	7/16	70.7	7/10	70.0
Umatilla R. below Meacham	7/1	10/25	7/28	76.5	7/24	74.5
Umatilla R. below Ryan Creek	5/13	10/12	7/28	74.8	7/16	72.9
West Birch Ck RM 15	6/1	10/30	8/5	66.4	7/24	65.1
Wildhorse Ck above Greasewood	7/12	10/4	7/17	88.2	7/12	86.0
Wildhorse Ck at Lower Adams Brdg	7/11	10/3	7/28	76.5	7/24	74.1
Wildhorse Ck at mouth	5/13	10/12	7/26	87.1	7/24	84.4
Wildhorse Ck at North Adams Bridge	7/12	10/5	7/28	83.5	7/24	80.6
Wildhorse Ck below Greasewood	7/11	10/3	7/28	81.0	7/24	78.3
Wildhorse Ck RM 26.0	5/13	10/11	8/5	72.9	7/24	71.2

Figures A-2, A-3, and A-4 display diurnal temperature profiles of the Umatilla River above McKay Creek, the Umatilla River below McKay Creek, and several tributaries, respectively. In each of the Umatilla River figures, the longitudinal (downstream) heating pattern is readily apparent. In **Figure A-4**, McKay Creek has a less pronounced diurnal variation because the flow volume of the creek is nearly 200 cfs.

Figure A-2. Diurnal Temperature Profiles of the Umatilla River Upstream of McKay Creek

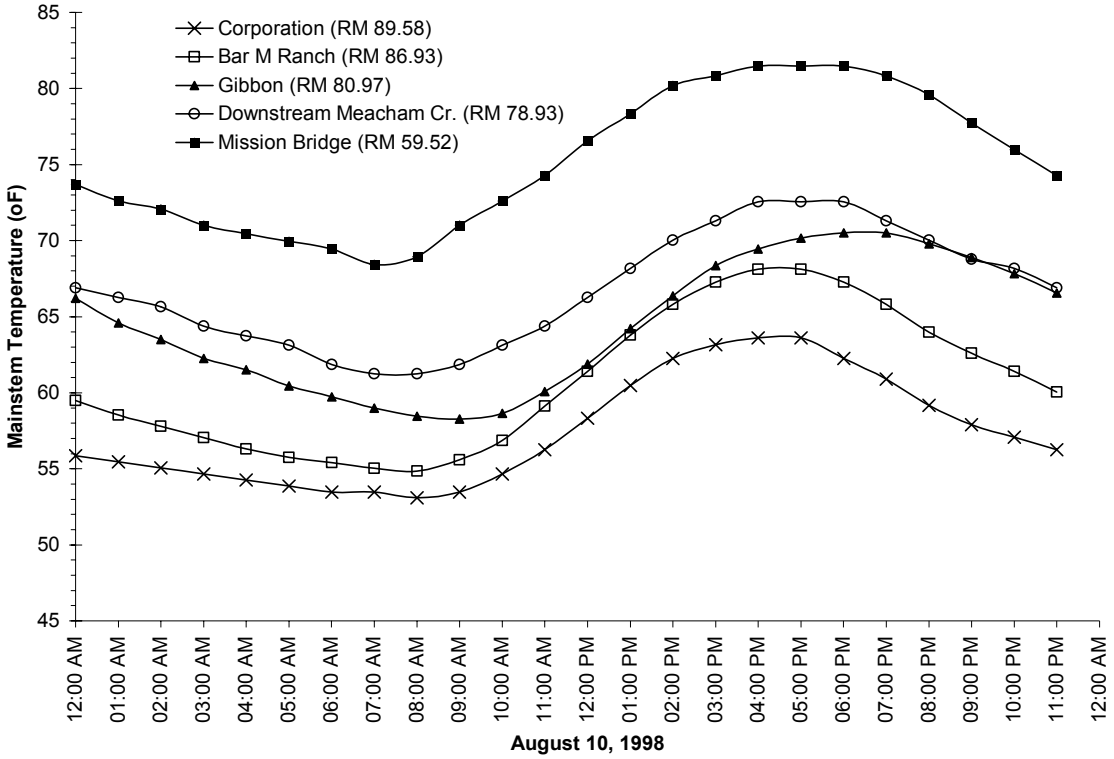

Figure A-3. Diurnal Temperature Profiles of the Umatilla River Downstream of McKay Creek

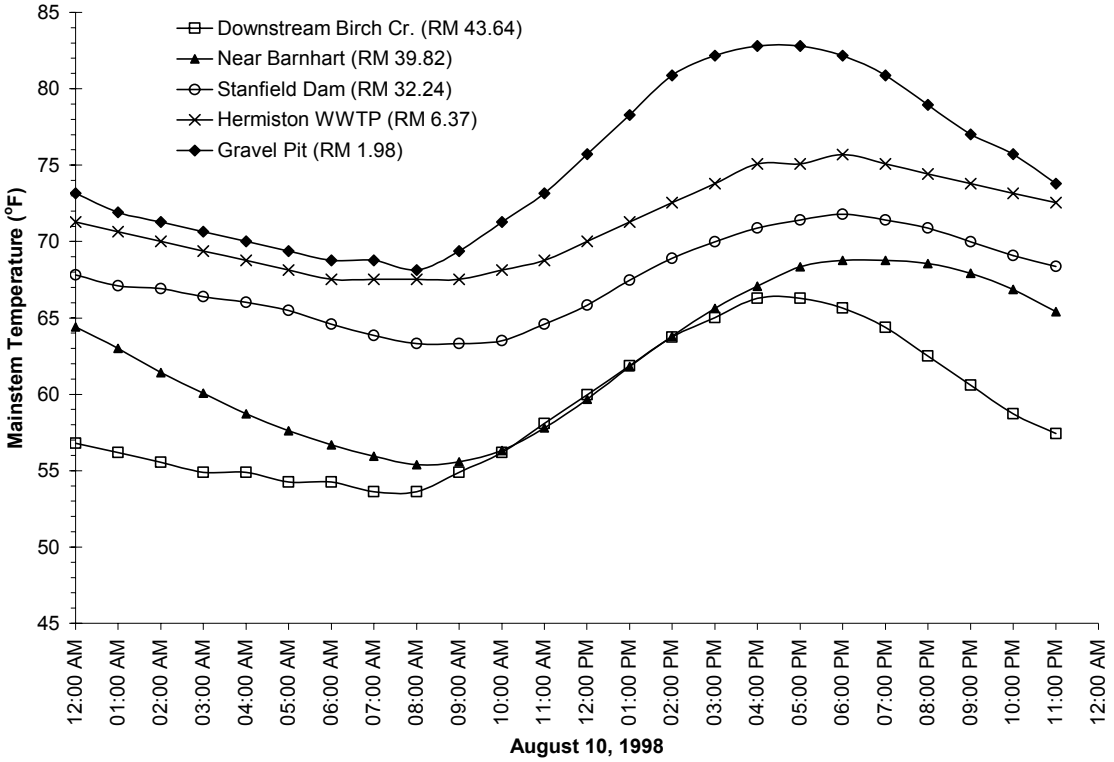

Figure A-4. Dirunal Temperature Profiles of Selected Tributaries (near their mouths)

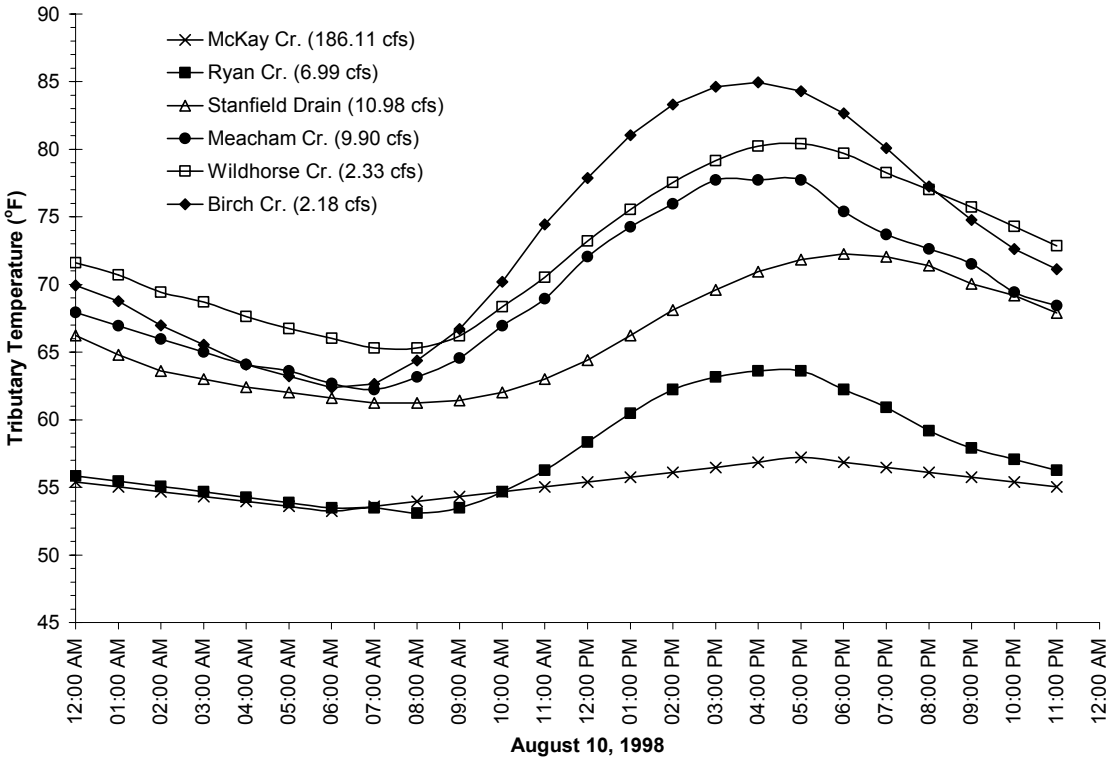

Seasonal Variability

Section 303(d)(1) requires this TMDL to be "established at a level necessary to implement the applicable water quality standard with seasonal variations." Both stream temperature and flow vary seasonally from year to year. Water temperatures are coolest in winter and early spring months. Stream temperatures exceed State water quality standards in summer and early fall months (June, July, August and September). Warmest stream temperatures correspond to prolonged solar radiation exposure, warm air temperature, low flow conditions and decreased groundwater contribution. Seasonal variability of the daily maximum temperatures for the Umatilla River mainstem is presented in **Figure A-5** and **Figure A-6**.

The warmest stream temperatures appear to occur in late July and early August. Upper reaches of the Umatilla River warm rapidly in the downstream direction to *sub-lethal* (64°F to 74°F) and *incipient lethal* (74°F to 80°F) levels for salmonids (recall **Table 2** of the Umatilla Basin TMDL). Most tributaries where data was collected also have 7-day maximums within or near the sub-lethal and incipient lethal levels for salmonids.

Figure A-5. Umatilla River Daily Maximum Temperatures Upstream of Pendleton.

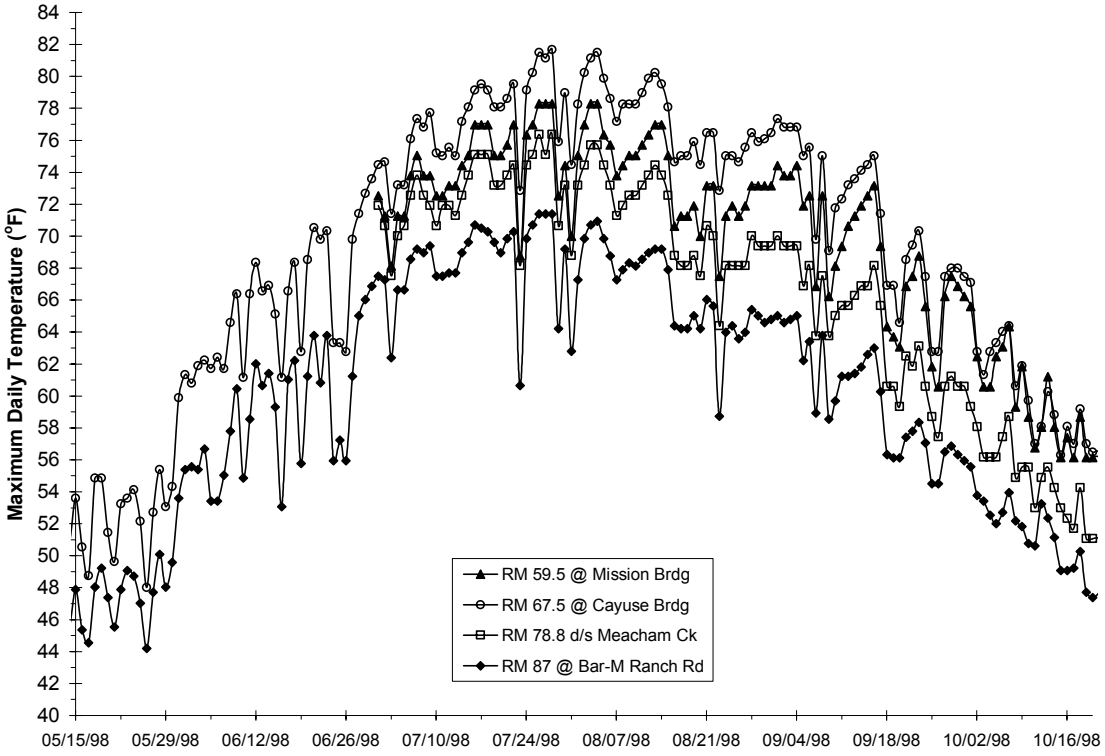

Figure A-6. Umatilla River Maximum Daily Temperatures Downstream of McKay Creek.

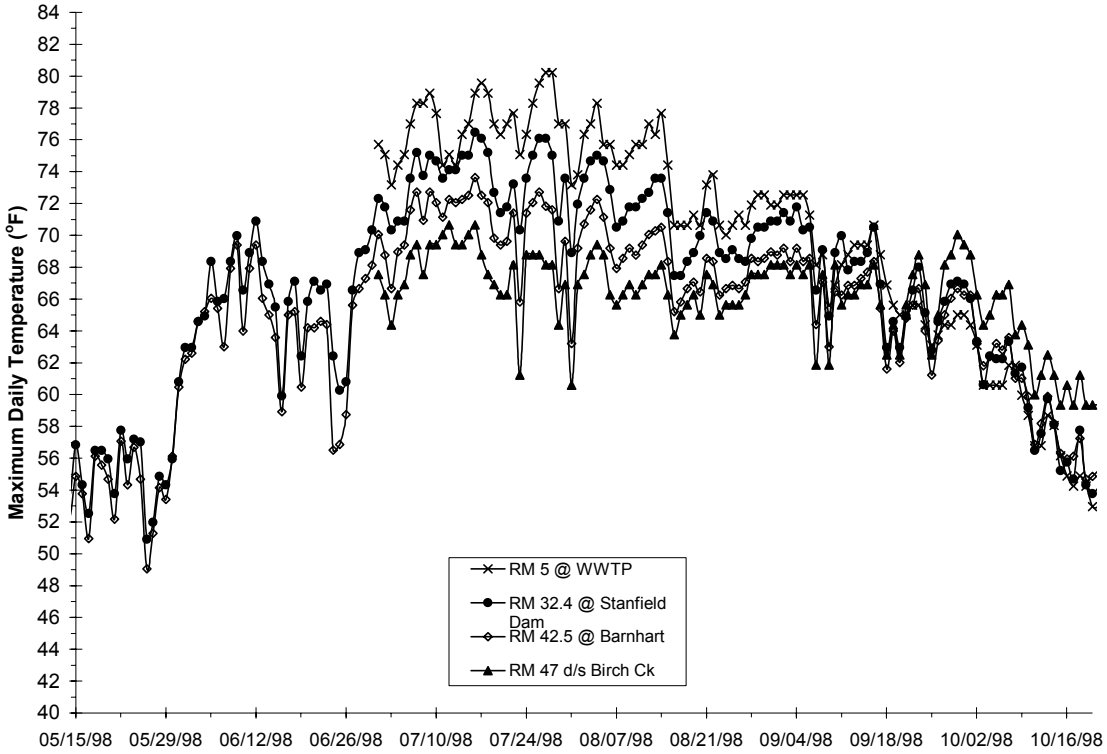

Forward Looking Infrared Radiometer (FLIR) Thermal Imagery

Forward looking infrared radiometer (FLIR) thermal imagery coupled with color videography and geographic positioning systems (GPS) produces spatially continuous temperature imagery. FLIR and color video images are collected with instruments mounted to a helicopter that can "fly" as much as 100+ miles of river/stream per day. The output data consists of GPS-tagged FLIR digital images that cover approximately 100 x 150 meters with less than 1 meter of spatial resolution and $\pm 0.5^{o}C$ accuracy. The spatial continuity of the FLIR data has made it possible to visually observe many of the thermodynamic processes associated with stream heating as they occur. Groundwater interactions with the stream column also register distinctly in the FLIR data imagery. Perhaps the greatest contribution of FLIR technology is the ability to display thermal habitat fragmentation of warmed reaches separated by isolated cool-water refugia. FLIR images were collected for the mainstem Umatilla River and Meacham Creek (below North Fork Meacham Creek) on August 10, 1998 (**Figure A-7**).

Figure A-7. Stream Segments with FLIR Thermal Imagery (1998)

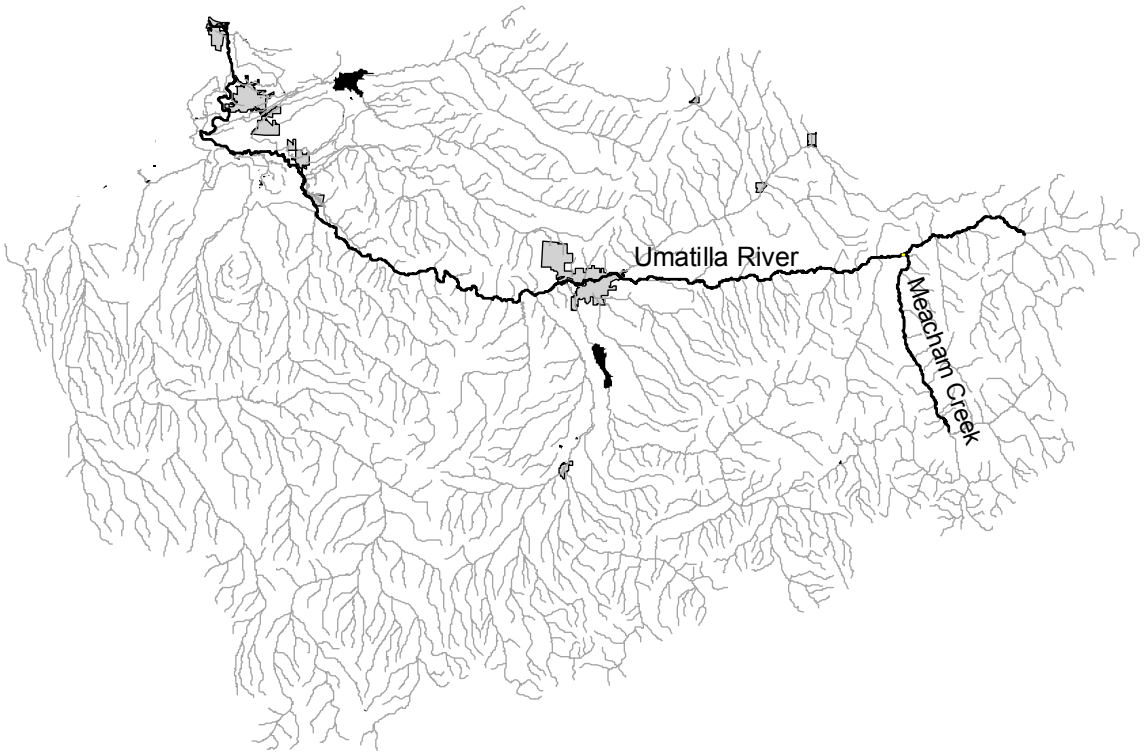

The mouth to Pendleton was flown on August 10, 1998 from 12:49 to 13:47. Pendleton to the North/South forks was flown on August 10, 1998 from 15:40 to 16:13. Meacham Creek was flown on August 10, 1998 from 16:20 to 16:33. Longitudinal FLIR temperature profiles for the lower Umatilla River, the upper Umatilla River, and Meacham Creek are presented in **Figure A-8**, **Figure A-9** and **Figure A-10**, respectively. Note that the river miles associated with the profiles are based upon the Oregon Water Resources Department (OWRD) map of the Umatilla drainage basin.

Figure A-8. Umatilla River Longitudinal FLIR Profile – Mouth to Upstream of Pendleton

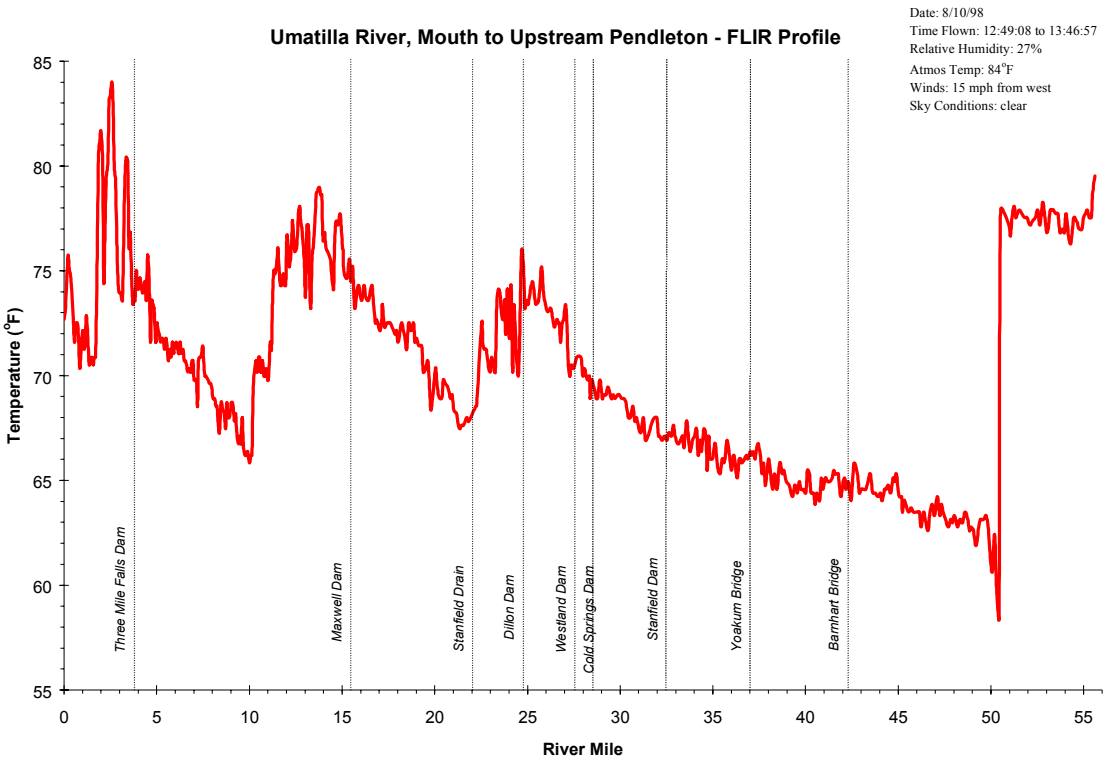

The longitudinal temperature profile from the mouth to above Pendleton is shown above in **Figure A-8**. It is important to note that there may be thermal stratification in the river behind dams. Interpretation of FLIR temperatures in these locations should be made with caution. Following are discussions of various parts of the FLIR profile:

The Umatilla Drain, RM 2.0: The FLIR imagery reveals a cool point source entering the Umatilla River from the east bank. This cool plume mixes rapidly, lowering the mainstem temperature nearly 10°F in the next quarter mile. Beyond that quarter mile reach, river temperatures begin to rise once again before entering the Columbia River.

Bedrock Channel, RM 2.5 to 3.0: This stretch of the Umatilla River flows through mostly bedrock channels. The river is multi-channeled in many areas and flows are relatively low (less than 5 cfs on August 10, 1998). Temperatures increase approximately 10°F in this region.

Three Mile Falls Dam, RM 3.7: Above the dam, the instream flow is approximately 50 cfs, most of which is diverted on August 10, 1998. Directly below the dam, approximately 2 cfs remains instream, and temperature spikes approximately 6°F.

Minnehaha Spring, RM 10.3: FLIR imagery shows a cool point source entering the Umatilla River from the east bank. Temperatures decrease approximately 5°F over the next quarter mile. Minnehaha Spring's effect can be seen in **Figure A-8**, just above river mile 10, where the temperature drops from 71°F to 66°F.

Maxwell Canal Seepage, RM 11-11.5: The Maxwell Canal lies parallel (within 50 meters) to the Umatilla River in this half-mile reach. FLIR imagery reveals cool seepage along the bank near the canal. Temperatures decrease nearly 6°F in this reach.

Echo Meadows, RM 20-25: A net decrease of approximately 8°F occurs within this five-mile reach. There are no point sources observed in the FLIR imagery, thus groundwater contributions are likely to be cooling the mainstem.

McKay Creek, RM 50.5: McKay Creek drastically reduces the Umatilla River temperature (in addition to augmenting flow). Downstream of the confluence, the Umatilla River is rapidly cooled by more than 15°F, before gradually heating once again.

Figure A-9. Umatilla River Longitudinal FLIR Profile– Upstream of Pendleton to the Forks

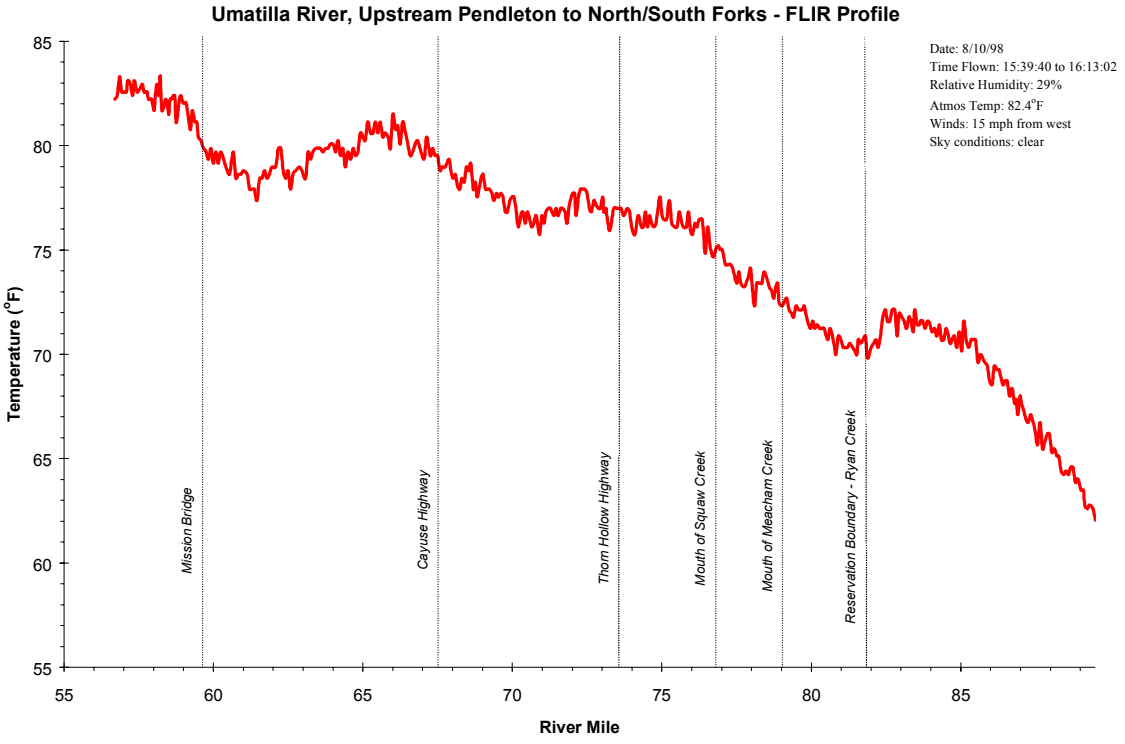

Temperatures in the upper portion of the Umatilla River were less dynamic than below Pendleton on August 10, 1998 (**Figure A-9**). The observed heating rate was 1.4°F per mile between river miles 89.5 and 83.0 and only 0.6°F between river miles 50 and 25. Less flow in the upper river is one factor related to the more rapid heating rate. No cool point sources or significant groundwater contributions are apparent in the FLIR imagery above Pendleton.

Figure A-10. Meacham Creek Longitudinal FLIR Profile – Mouth to North Meacham Creek

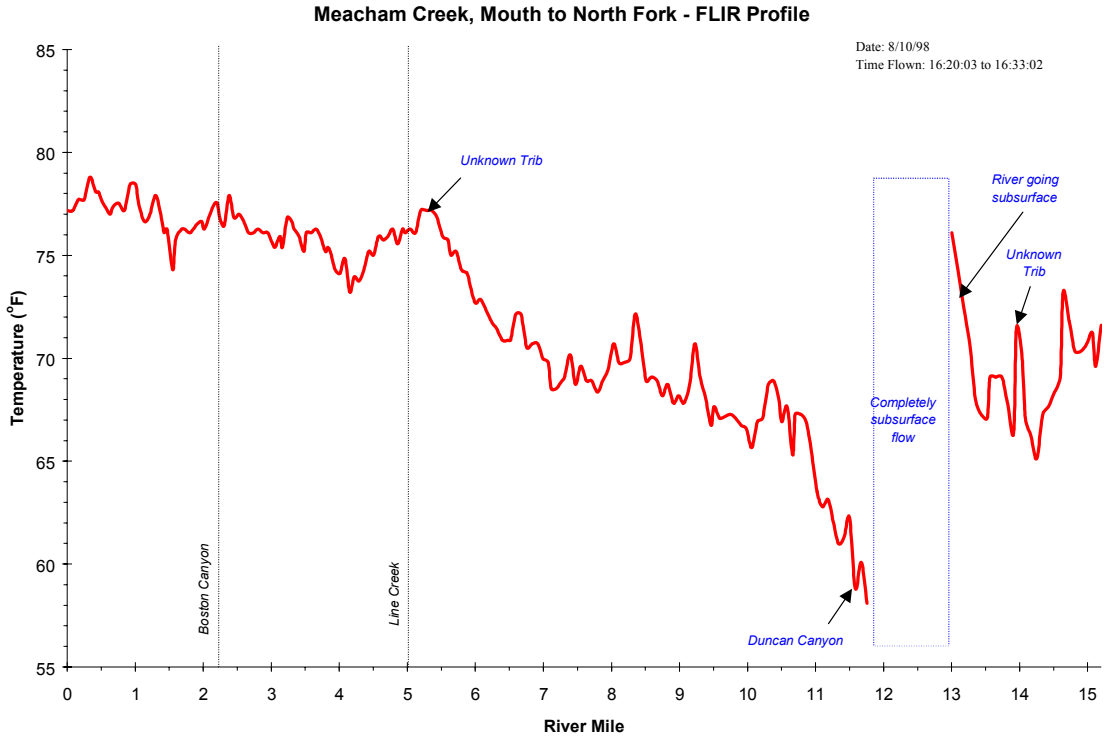

The most significant feature in the Meacham Creek FLIR profile is where the creek loses all surface flow between river miles 12 and 13 (**Figure A-10**). Before the creek goes subsurface, the temperatures rapidly increase to the mid-70°F range. A mile downstream, the creek re-surfaces, with temperatures below 60°F. The observed stream heating rate is approximately 3.3°F per mile between river miles 11.5 and 5.5. Meacham Creek temperatures are in the upper 70°F range by the time it reaches the Umatilla River.

The following FLIR images illustrate the temperature regime at several river confluences within the Umatilla Basin. **Image A-1** illustrates the confluence between the North and South Fork Umatilla River. Observed water temperatures in the North Fork are much lower than the South Fork Umatilla River. **Image A-2** illustrates the temperature regime between the Umatilla River and Meacham Creek. Observed Umatilla River temperatures were similar both upstream and downstream of Meacham Creek. **Image A-3** shows the confluence of McKay Creek with the Umatilla River. Nearly 200 cfs of cold bottom withdrawals from McKay Reservoir augment Umatilla River flow and lower its temperature about 15°F (see **Figure A-8**).

Image A-1. FLIR and Video Images of the North and South Fork Umatilla River Confluence[1]

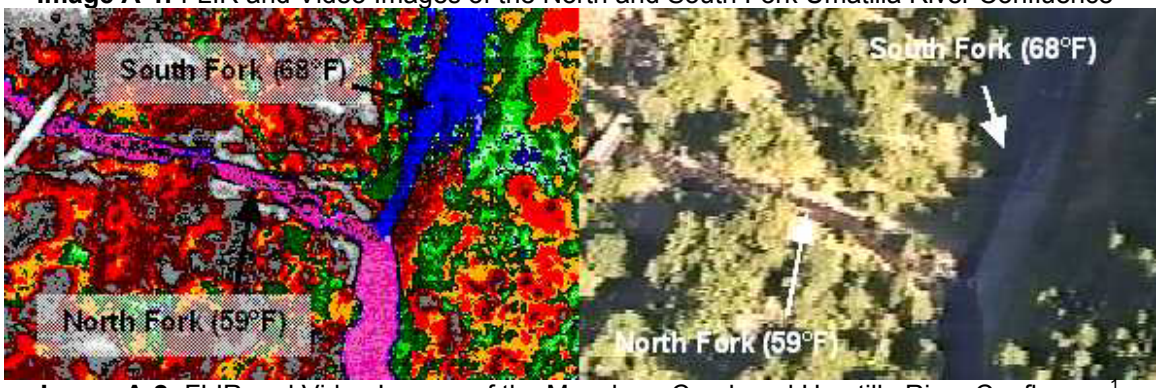

Image A-2. FLIR and Video Images of the Meacham Creek and Umatilla River Confluence[1]

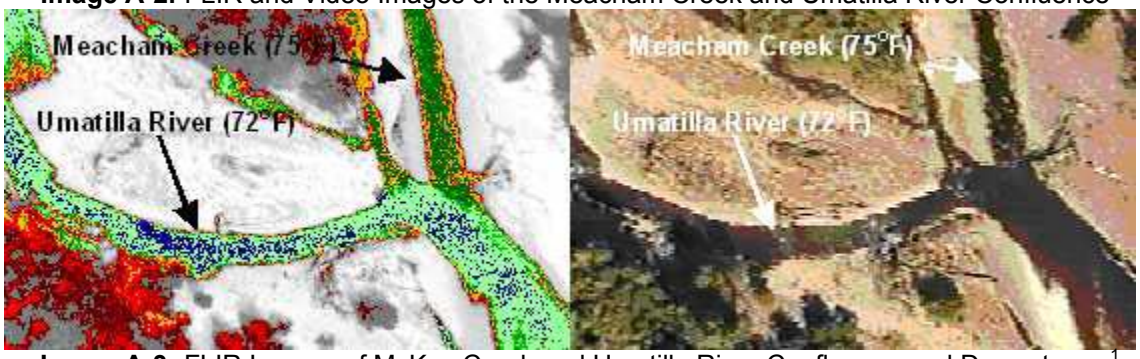

Image A-3. FLIR Images of McKay Creek and Umatilla River Confluence and Downstream[1]

(McKay Creek/Umatilla River confluence) (Mixing is "completed" at the bend 1/4 mile downstream)

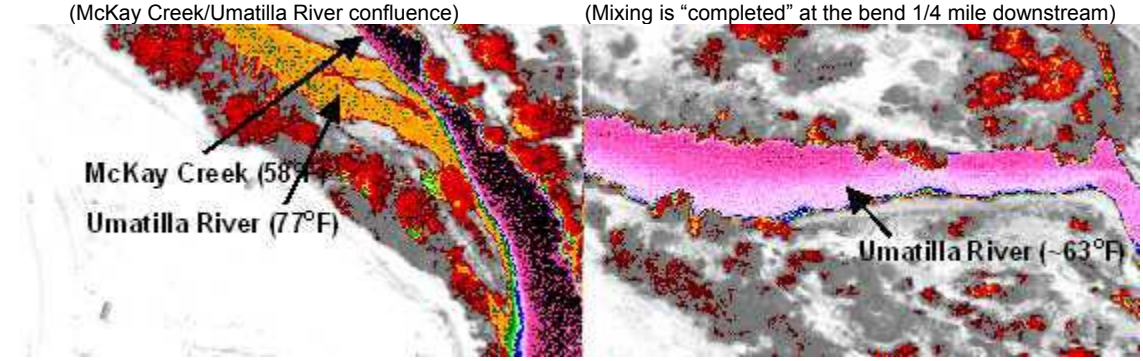

[1] **FLIR Image Temperature Scale (°F)**

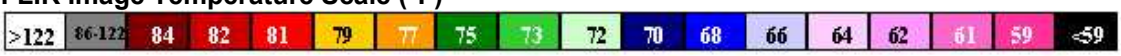

Effective Shade

During the summer of 1998, ODEQ measured effective shade at thirty-five sites in the Umatilla Basin using a Solar Pathfinder© (**Figure A-11**). Many of the monitoring sites were selected by stream accessibility considerations (i.e., public lands or public right of way) and efforts focused primarily on mainstem areas. Observed effective shade measurements along the Umatilla River were generally below 20%.

Figure A-11. Measured Effective Shade *(ODEQ data, 1998)*

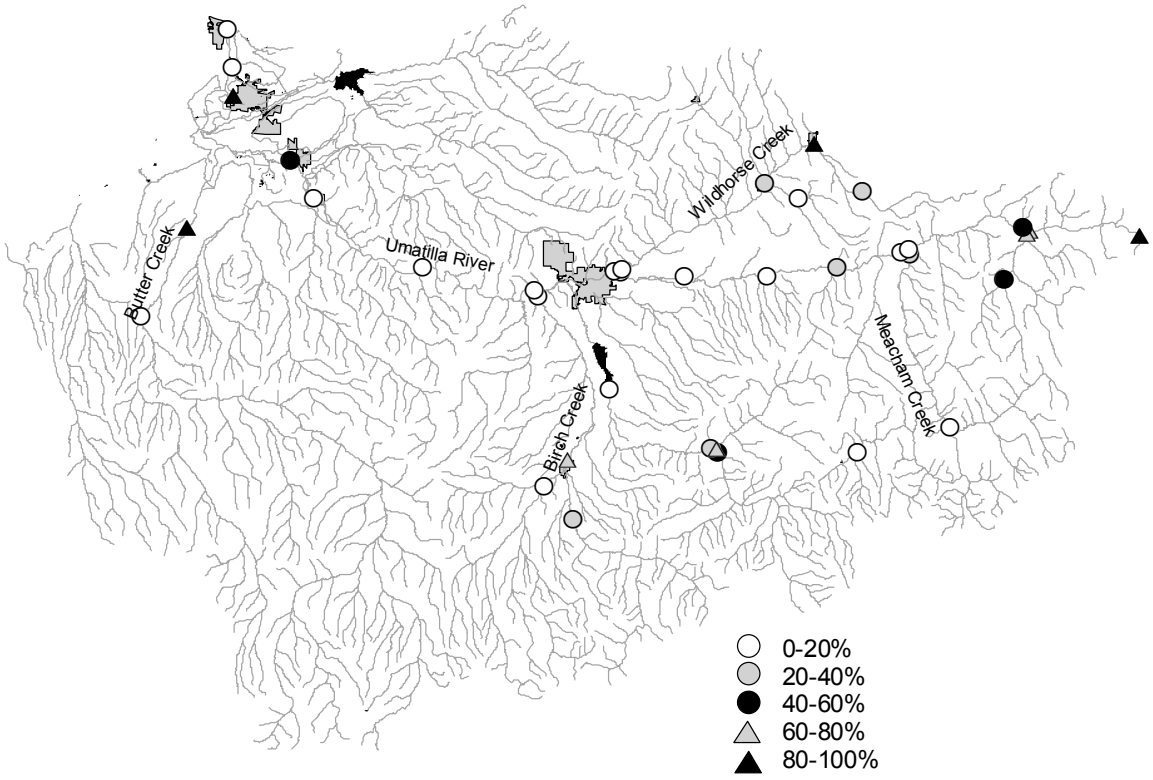

Current Riparian Conditions

The current condition of the riparian vegetation varies considerably in the Umatilla Basin. The majority of the upper tributary riparian vegetation is composed of narrow bands of hardwood and conifer species, including some National Forest lands. Galleries of large mature cottonwoods exist in some areas of CTUIR land. Lower mainstem and tributary reaches have riparian vegetation types primarily composed of shrubs and grasses, with some scattered hardwood trees (i.e., ash, cottonwood, and alder). In some cases where crop cultivation extends to the stream banks or where grazing pressure is high, woody or shade-producing riparian vegetation is sparce. Much of the lower mainstem is diked, and trees are actively prevented from growing on the dikes.

Undisturbed riparian areas in the Umatilla Basin generally progress towards late seral woody vegetation communities. Few, if any, riparian areas in the Umatilla Basin are unable to support either late seral woody vegetation or tall growing herbaceous vegetation.

A recent report regarding wildlife habitats in the Umatilla and Willow Creek Basins examines the differences between current and pre-settlement vegetation coverages (Kagan, 1999). The following quote from that report exemplifies the drastic changes that have occurred in the riparian landscape since European settlement:

> *"The most notable difference between the landscape in the study area now and in the 1850s is the conversion of native prairie to farmland. The large, forested riparian areas along the Umatilla River have largely disappeared. However, the most interesting change is the current lack of water in many areas where the original General Land Office (GLO) surveyors reported abundant springs and small creeks. These were recorded on a township basis and the differences are striking…"*
>
> *"The greatest percentage losses are in the riparian communities. These bottomland hardwood and willow communities show losses of 87%, and are clearly underestimated. Only the largest riparian bottomland areas were reported by the GLO surveyors* [are] *included in the map. Many thousands of acres dominated by willows with scattered alder and cottonwood were not reported, and therefore the 87% loss indication has been significantly underestimated. Actual losses are probably greater than 95%."*

Naturally Occurring Vegetation in the Umatilla River Basin

Recall that **Section 2.1.3.1** of the *Umatilla River Basin TMDL* describes the potential near stream vegetation, as determined by the Umatilla River Basin TMDL Technical Committee.

Flow

Low-Flow Statistics

Flow data has been collected in the Umatilla River Basin at 32 U.S. Geological Survey (USGS) gages. Daily stream flow measurements have been collected at several of these gages since 1903. Flow data was processed by DEQ staff to determine return periods for both high and low-flow conditions. Flow statistics were performed using the Log Pearson Type III distribution. Results from this analysis were presented in ODEQ Umatilla River Basin Data Review (1998). The 7Q10 flow represents the 7-day average flow that occurs on average once every 10 years. Therefore, the probability that this flow condition will occur during any year is 10%.

The summer low flow pattern in the Umatilla River mainstem reflects a highly managed flow condition. The Umatilla River upstream of Meacham Creek experiences a 7Q10 low flow of 36.2 cfs. This 7Q10 flow slightly increases to 37.7 cfs moving downstream to Cayuse. However, flow begins to decrease further downstream of this site (i.e., Pendleton 7Q10 = 21.6 cfs, upstream of McKay Creek 7Q10 = 16.2 cfs). The management of flow from McKay reservoir increases the flow in the Umatilla River downstream from McKay Creek confluence (i.e., Umatilla River at Yoakum 7Q10 = 24.0 cfs). Below Yoakum, Umatilla River flow volumes are severely reduced resulting in a 7Q10 of 0.1 cfs near the city of Umatilla.

Average monthly flow patterns for the Umatilla River illustrate a similar pattern, with mainstem summer flow levels increasing dramatically downstream of the McKay Creek confluence (i.e., Umatilla River at Yoakum, RM 37.0) (**Figure A-12**). It is important to point out that 1) monthly average river discharge rates decrease dramatically downstream of Yoakum, and 2) monthly average McKay Creek summer flows are generally equal or greater than mainstem flow conditions (**Figure A-12**).

Figure A-12. Longitudinal Trend of Average Monthly Flow Conditions in the Umatilla River.

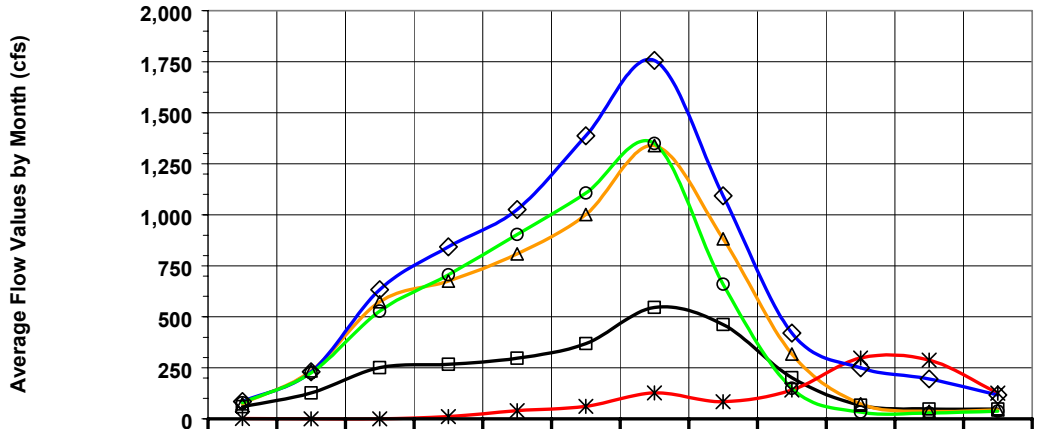

	Oct	Nov	Dec	Jan	Feb	Mar	Apr	May	Jun	Jul	Aug	Sep
UMA u/s Meacham Ck (RM 79)	59	128	251	267	297	369	546	462	202	67	48	48
UMA @ Pendleton (RM 56)	74	235	574	675	809	1,001	1,339	882	318	74	37	44
McKay Ck (near Pendleton)	2	0	0	12	40	62	128	84	141	299	288	126
UMA @ Yoakum (RM 37)	85	230	634	844	1,026	1,387	1,756	1,093	420	250	196	117
UMA near Umatilla (RM 2)	79	225	528	706	904	1,107	1,349	659	150	32	29	38

1998 Critical Period Discharge Measurements in the Umatilla Basin

Flows were measured throughout the Umatilla Basin over a four-day period during the summer of 1998. Observed flow conditions were below 10 cfs for all tributary streams. In addition, no flow (zero cfs) was observed at several tributary streams during this monitoring work. For example, portions of Meacham Creek became completely dry during the summer of 1998, especially downstream of North Fork Meacham Creek.

Observed flows *increased* dramatically downstream of the McKay Creek confluence, where nearly 200 cfs of McKay Reservoir water enters the Umatilla River (**Figure A-13**). Umatilla River flows then decreased dramatically between river mile 26.3 (Umatilla River at the City of Echo) and river mile 8.7 (Umatilla River at Westland Road) due to irrigation diversions. Below river mile 26.3, there are areas where Umatilla River flows increase as a result of irrigation drain and groundwater returns.

Figure A-13. Umatilla River Flow on August 10, 1998.

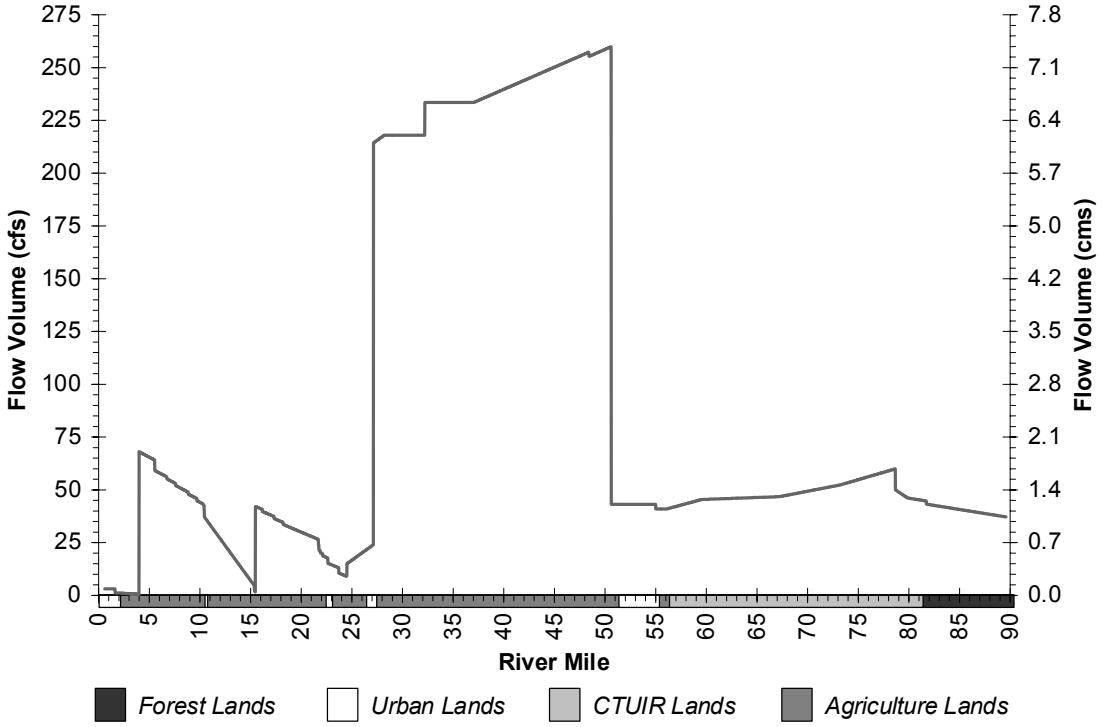

Channel Characterization Data

In 1998, members of the Umatilla TMDL technical committee used the Rosgen stream morphology classification system to describe several locations on the Umatilla River, as well as several tributaries. Level I Rosgen stream classifications break streams into groupings (letters A through G) that relate channel morphology to valley morphology, channel patterns, slope and shape. **Figure A-14** displays Rosgen Level I stream types. **Figure A-15** illustrates sample locations and the corresponding Rosgen Level I stream types. **Table A-2** presents the general parameter ranges associated with Rosgen Level I classification. Only Rosgen stream types that the TMDL technical committee identified for the Umatilla Basin are presented in **Table A-2**. Detailed descriptions of all Rosgen stream type classifications can be obtained from Rosgen (1994).

Figure A-14. Slope Ranges, Cross-Sections and Plan Views of Level I Rosgen Stream Types
(Image from Rosgen, 1996)

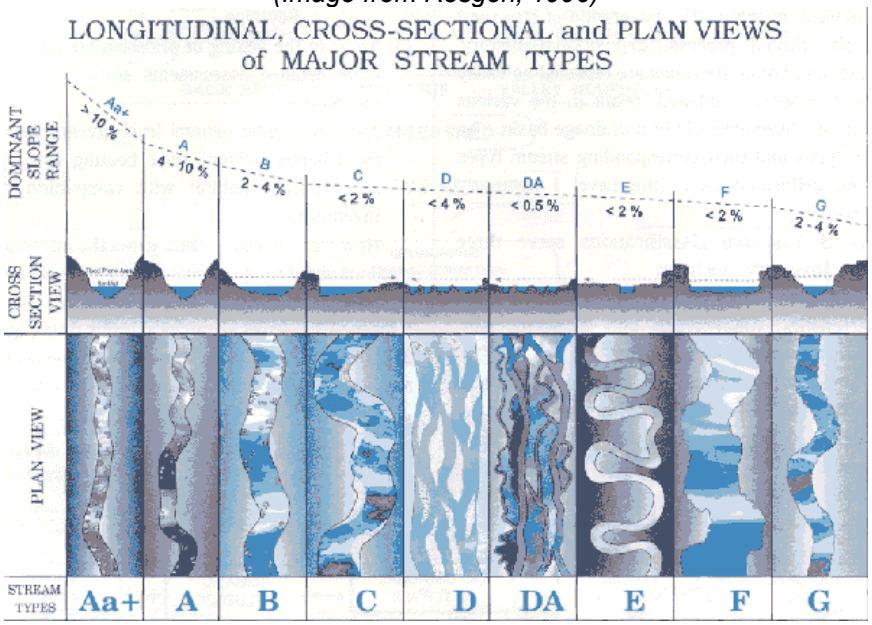

Table A-2. Generalized Parameter Ranges for Level I Rosgen Stream Types
(Data taken form Rosgen, 1996)

	Entrenchment	Sinuosity	Width to Depth	Stream Type
Single-Thread Channels	High (< 1.4)	Low (<1.2)	Low (<12)	A
		Moderate (>1.2)		G
			Moderate/High (>12)	F
	Moderate (1.4-2.2)		Moderate (>12)	B
	Low (>2.2)	Very High (>1.5)	Very Low (<12)	E
		High (>1.2)	Moderate/High (>12)	C
Multiple Channels		Low (<1.2)	Very High (>40)	D
		Low-High (1.2-1.5)	Low (<40)	D_A

Rosgen Level II morphologic classifications considers all of the Level I parameters as well as substrate particle size, entrenchment ratio, width to depth ratio and sinuosity. Level II classifications can provide insight as to reach-specific sediment supply, sensitivity to disturbance and the potential for natural recovery. Twenty-five Level II Rosgen classifications were performed for the Umatilla mainstem and selected tributaries during the summer of 1998.

Figure A-15. Umatilla Basin Morphologic Assessment – Rosgen Classifications

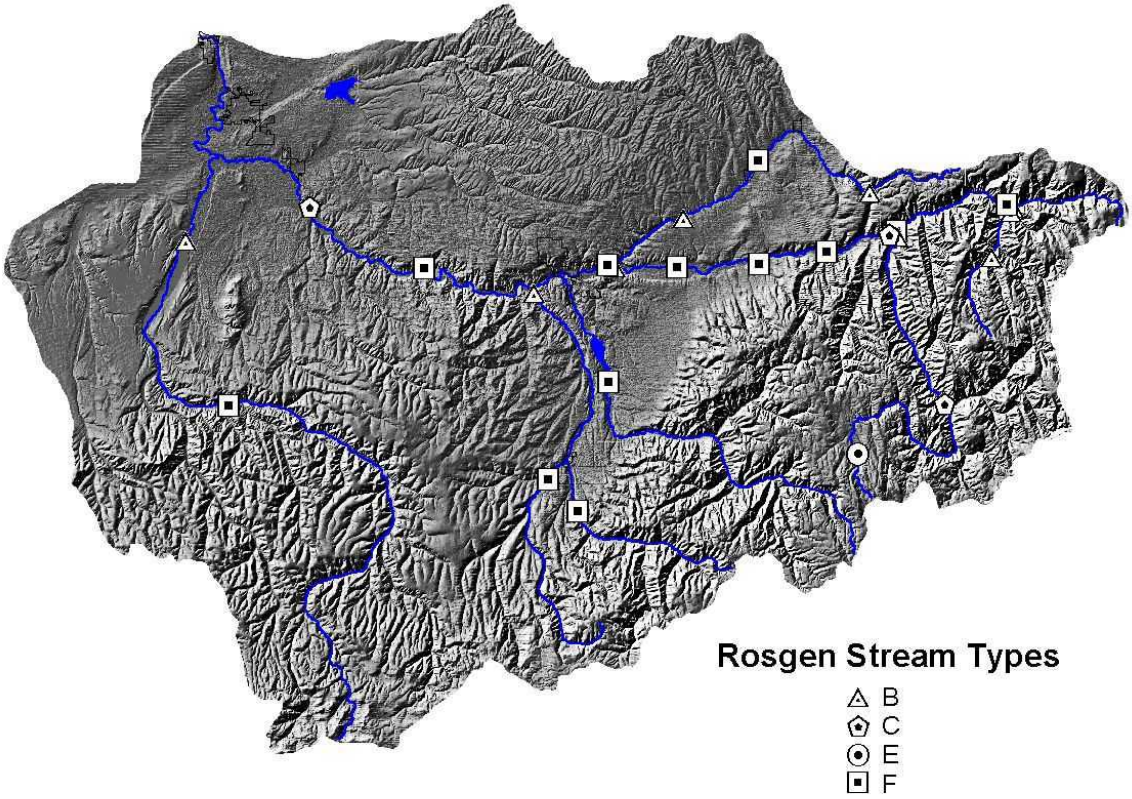

Generalized characteristics can be associated with each of the Level II Rosgen stream classes that relate channel morphology to sensitivity to disturbance, recovery potentials, sediment supply, streambank erosion potential and vegetation controlling influence. Rosgen (1994) presents these characteristics to provide guidance to riparian and sediment management.

Based on the Rosgen level II analysis, both the West Fork and East Fork of Birch Creek were classified as highly sensitive to disturbance, with high sediment supply and high streambank erosion potentials, and the natural recovery potentials are poor (F4 stream types). Lower Birch Creek was classified (at the gage) as a B4/F4 combination; a stream classification that has a moderate recovery potential. Most sites inventoried on the Umatilla River were classified as F4 stream types. However, the Echo and Gibbon sites were classified as C4 stream types, indicating that their recovery potentials are much higher than their F4 counterparts. Notably, the Highway 11 site was classified as a B1/B3 stream type, which is less sensitive to disturbances and has an excellent recovery potential. The North and South Forks of the Umatilla River both were classified as B types. This class is more resistant to disturbances and have a better recovery potential, compared to many sites sampled lower within the Basin. **Table A-3** summarizes stream classifications determined during Rosgen II efforts within the Umatilla Basin and the recovery potential associated with each classification.

Figures A-16 through **A-20** illustrate determined stream channel sensitivity to disturbance, stream channel recovery potential, stream channel sediment supply, streambank erosion potential, and stream channel controlling influence, respectively. All channel traits are based upon Rosgen level II classification results. It was determined that stream channels at most sites along the mainstem Umatilla River are highly sensitive to channel disturbance, have a high potential sediment supply, and a high streambank erosion potential. In addition, many tributary locations were also determined to be highly sensitive to channel disturbance. However, the

estimated recovery potential is highly variable throughout the Basin (**Figure A-17).** It was determined from Rosgen channel classification results that stream channel vegetation was only moderately influencing width/depth stability at many sites throughout the Umatilla Basin (**Figure A-20**).

Table A-3. Level II Rosgen Stream Types Generalized Characteristics

Sensitivity to Disturbance[1] *Vegetation Controlling Influence*[2] *Sediment Supply*[3] *Streambank Erosion Potential*			*Recovery Potential*[4]		
Very Low to Low	Moderate	High to Very High	Good to Excellent	Fair	Poor to Very Poor

Location	Level II Rosgen Stream Type	*Sensitivity to Disturbance*	*Vegetation Controlling Influence*	*Sediment Supply*	*Streambank Erosion Potential*	*Recovery Potential*
Birch Creek - Gage	B4c/F4					
East Fork	F4					
West Fork	F4					
Butter Creek - Madison	B6					
OWRD	F4					
McKay Creek - OWRD Gage	F4					
Meacham Creek - Gage	B4c					
Nibley	E6					
d/s North Fork	C4c					
N.F. Umatilla R. - Mouth	B3c					
S.F. Umatilla R. - Mouth	B3c					
Shimmiehorn	B4					
Umatilla R. - Cayuse	F4					
Corporation	F4					
Echo	C4					
Gibbon	C4					
Highway 11	B1c/B3c					
Mission	F1/F4					
Pendleton	F4					
Thorn Hollow	F4					
u/s Meacham	F4					
Yoakum Brdg.	F4					
Wildhorse Cr. - Gerking	F6/B6c					
Havanna	B6					
RM 26	B1/B4					

[1] Includes increases in streamflow magnitude and timing and/or sediment increases.
[2] Vegetation that influences width/depth ratio stability.
[3] Includes suspended and bedload from channel derived sources and/or from upstream adjacent slopes.
[4] Assumes natural recovery once the cause of instability is corrected.

Figure A-16. Stream Channel Sensitivity to Disturbance (Rosgen, 1994)

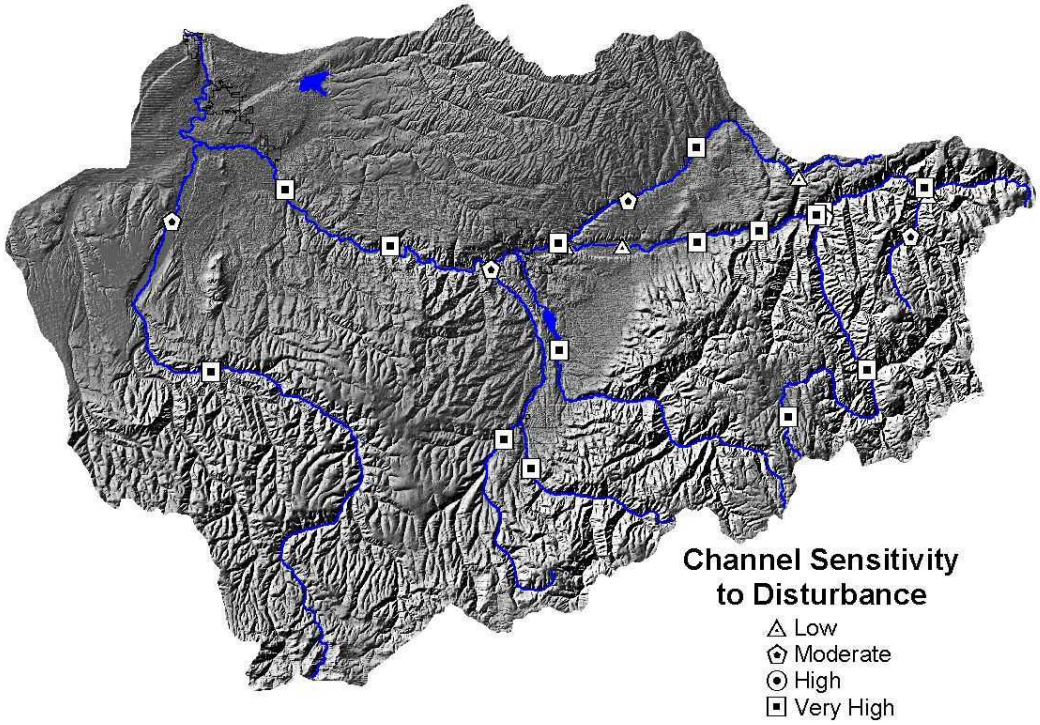

Figure A-17. Stream Channel Recovery Potential (Rosgen, 1994)

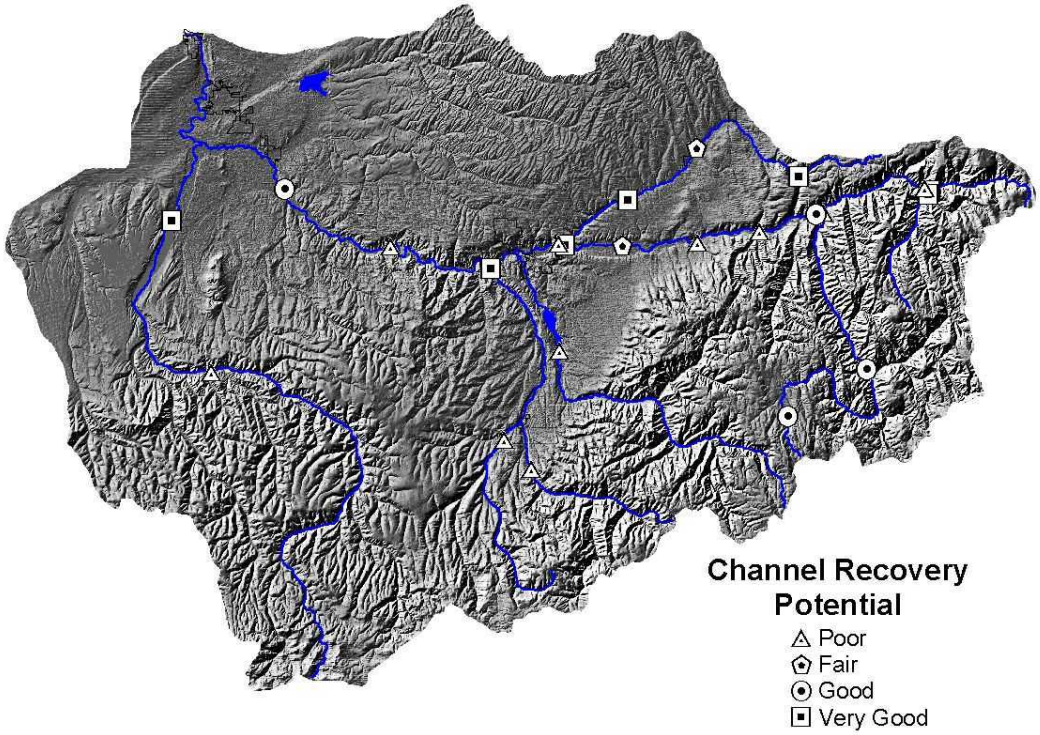

Figure A-18. Stream Channel Sediment Supply (Rosgen, 1994)

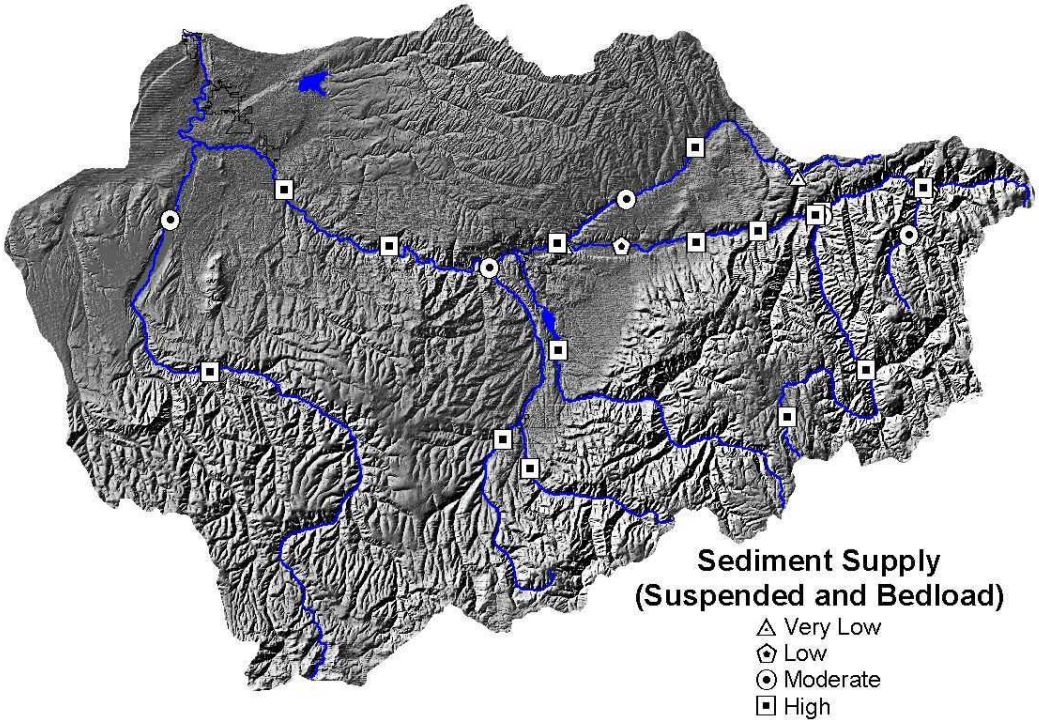

Figure A-19. Streambank Erosion Potential (Rosgen, 1994)

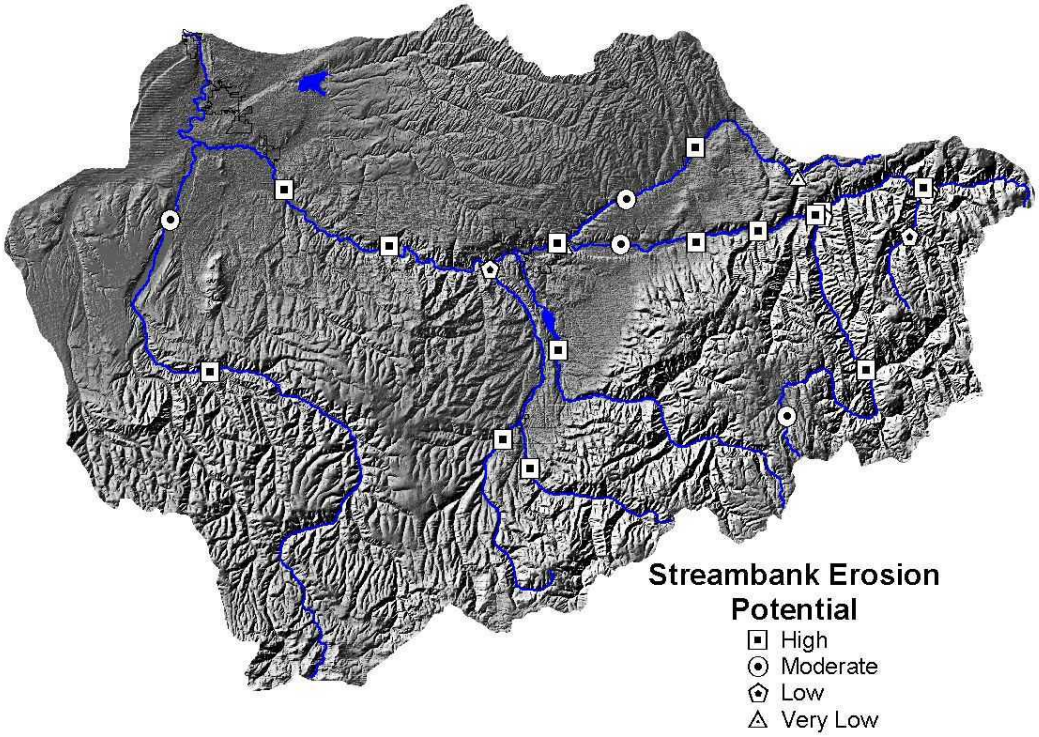

Figure A-20. Stream Channel Vegetation Controlling Influence (Rosgen, 1994)

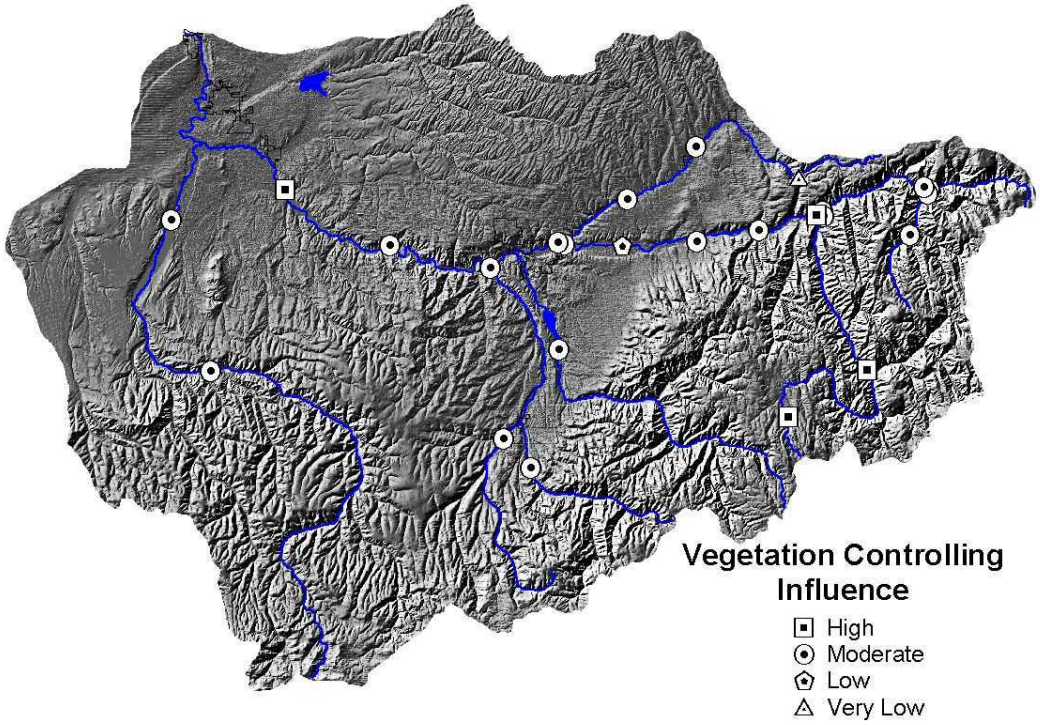

STREAM HEATING PROCESSES – BACKGROUND INFORMATION

Overview

Riparian vegetation, stream morphology, hydrology, climate, and geographic location influence stream temperature. While climate and geographic location are outside of human control, riparian condition, channel morphology and hydrology are affected by land use activities. Specifically, the elevated summertime stream temperatures attributed to anthropogenic sources in the Umatilla Basin result from the following:

- ✓ Riparian vegetation disturbance reduces stream surface shading via decreased riparian vegetation height, width and/or density, thus increasing the amount of solar radiation reaching the stream surface,
- ✓ Channel widening (increased width to depth ratios) increases the stream surface area exposed to energy processes, namely solar radiation,
- ✓ Near-Stream Disturbance Zone* (NSDZ) widening decreases potential shading effectiveness of shade-producing near-stream vegetation, and
- ✓ Reduced summertime base flows may result from instream withdrawals.

Human activities that contribute to degraded water quality conditions in the Umatilla Basin include timber harvest, as well as road, agriculture and rural and urban residential related riparian disturbances. The relationships between percent effective shade, channel morphology, hydrology and stream temperature are illustrated in **Figure A-21**.

Figure A-21. Stream Heating Processes in the Umatilla Basin

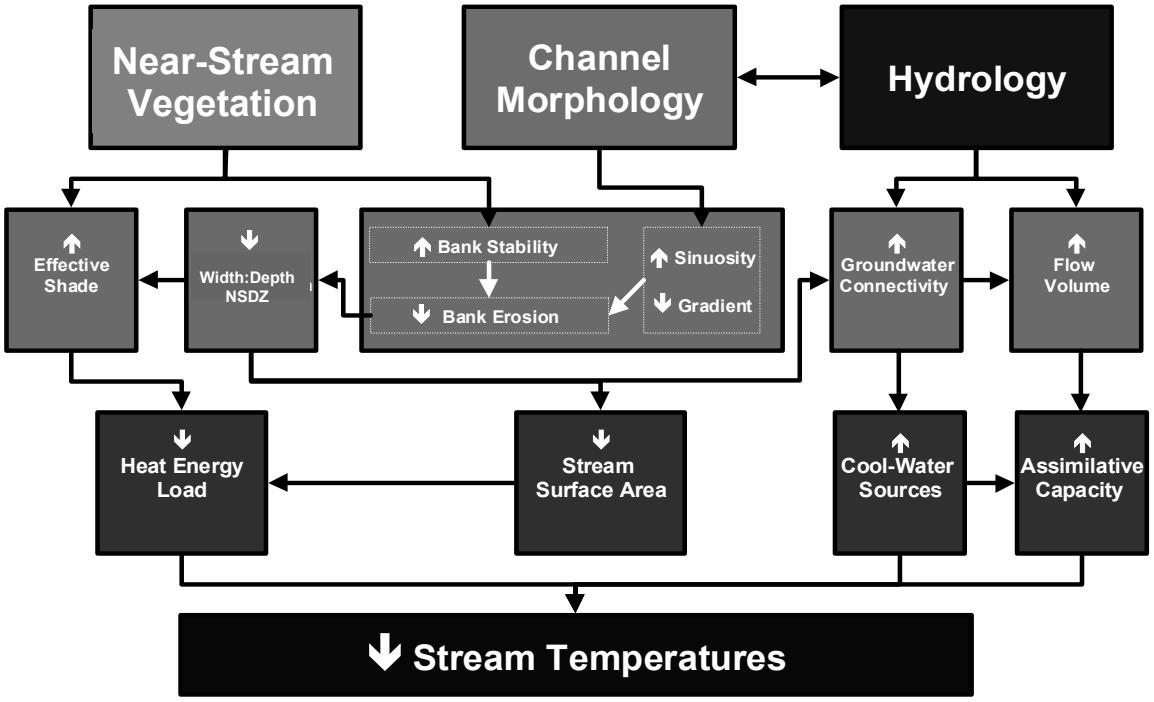

* The term "near-stream disturbance zone" is define on page 9 of the Umatilla Basin TMDL.

The Dynamics of Shade

Stream surface shade is a function of several landscape and stream geometric relationships. Some of the factors that influence shade are listed in **Table A-4**. Geometric relationships important for understanding the mechanics of shade are displayed in **Figure A-22**. In the Northern Hemisphere, the earth tilts on its axis toward the sun during summertime months allowing longer day length and higher solar altitude, both of which are functions of solar declination (i.e., a measure of the earth's tilt toward the sun). Geographic position (i.e., latitude and longitude) fixes the stream to a position on the globe, while aspect provides the stream/riparian orientation. Riparian height, width and density describe the physical barriers between the stream and sun that can attenuate and scatter incoming solar radiation (i.e., produce shade). The solar position has a vertical component (i.e., altitude) and a horizontal component (i.e., azimuth) that are both functions of time/date (i.e., solar declination) and the earth's rotation (i.e., hour angle). While the interaction of these shade variables may seem complex, the math that describes them is relatively straightforward geometry, much of which was developed decades ago by the solar energy industry.

Table A-4. Factors that Influence Stream Surface Shade

Description	*Measure*
Season/Time	Date/Time
Stream Characteristics	Aspect, Near-Stream Disturbance Zone Width
Geographic Position	Latitude, Longitude
Vegetative Characteristics	Buffer Height, Buffer Width, Buffer Density
Solar Position	Solar Altitude, Solar Azimuth

Percent effective shade is perhaps the most straightforward stream parameter to monitor/calculate and is easily translated into quantifiable water quality management and recovery objectives. **Figure 23** demonstrates how effective shade is monitored/calculated. Using solar tables or mathematical simulations, the *potential daily solar load* can be quantified. The *measured solar load* at the stream surface can easily be measured with a Solar Pathfinder© or estimated using mathematical shade simulation computer programs (Boyd, 1996 and Park, 1993).

Figure A-22. Effective Shade - Defined

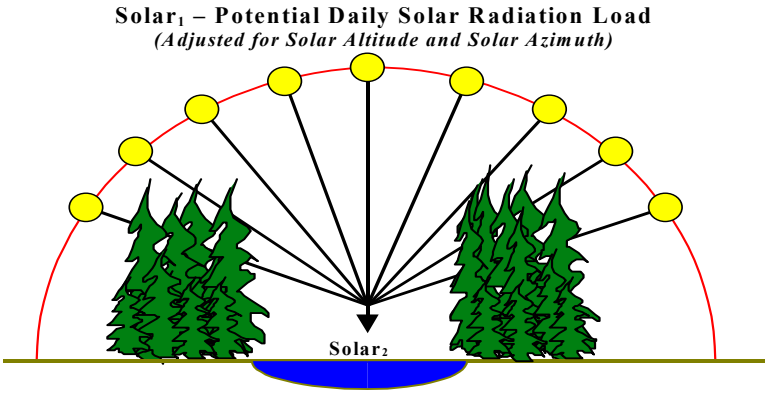

Effective Shade Defined:

$$\text{Effective Shade} = \frac{(\text{Solar}_1 - \text{Solar}_2)}{\text{Solar}_1}$$

Where,

$Solar_1$: Potential Daily Solar Radiation Load

$Solar_2$: Measured Daily Solar Radiation Load at Stream Surface

Figure A-23. Geometric Relationships that Affect Stream Surface Shade

Solar Altitude and **Solar Azimuth** are two basic measurements of the sun's position. When a stream's orientation, geographic position, riparian condition and solar position are known, shading characteristics can be simulated.

Solar Altitude measures the vertical component of the sun's position
Solar Azimuth measures the horizontal component of the sun's position

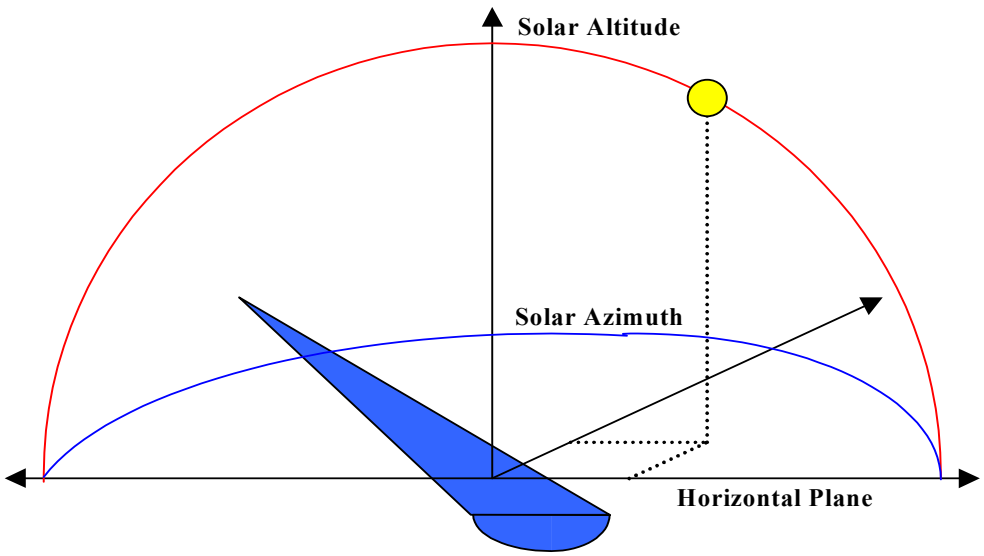

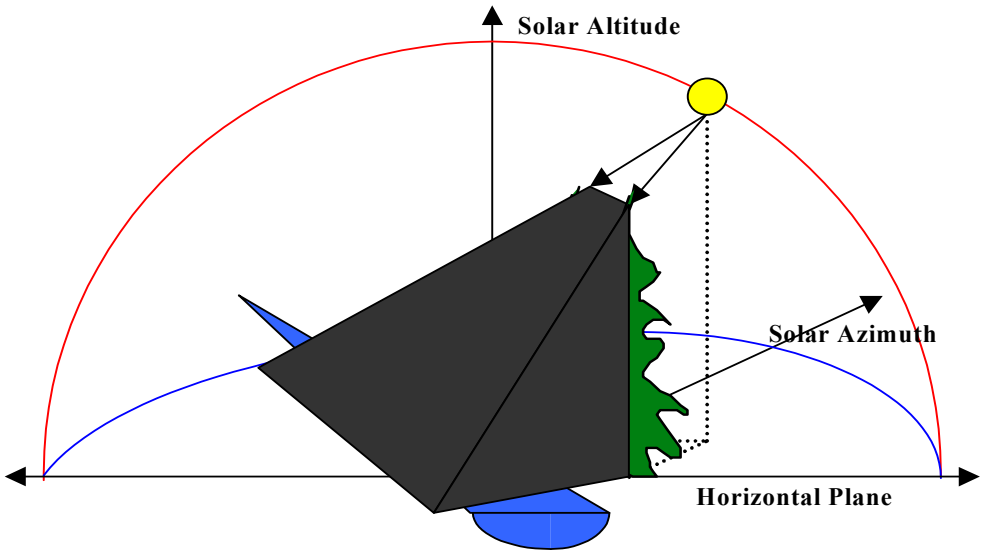

FLIR Thermal Imagery

FLIR thermal imagery facilitates visual observation of the effects that riparian vegetation has upon the stream and surrounding environment. It may be helpful to remind the reader that this image measures only surface temperatures of the ground, stream or riparian vegetation. In essence, FLIR thermal imagery measures the temperature of the outermost portions of the bodies/objects in the image (i.e., ground, riparian vegetation, stream). The bodies of interest are opaque to longer wavelengths and there is little, if any, penetration of the bodies.

For example, **Image A-4** displays FLIR thermal imagery collected in eastern Oregon. The outer surfaces of the trees are depicted along with ground and stream temperature. Contained in the thermal image (**Image A-4**) are trees that are casting shadows. The cultivated ground temperature is greater than the calibrated sensitivity of the FLIR instrumentation (greater than 86°F). An individual tree can be seen on the left bank of the stream in the middle of the frame and two trees are visible on the right bank in the upper and lower regions of the frame. The outer surfaces of the trees are warm (≈86°F). The ground temperatures are markedly cooler in the shadows cast by these three trees. In the case of ground temperature, there is greater than 20°F difference between the cultivated ground surfaces inside and outside of cast shadow. It is apparent that the thermal environment differs significantly between the shaded and non-shaded conditions.

Within this section, FLIR thermal imagery is used to sample the longitudinal stream temperatures. Further analysis can then associate the effects that riparian vegetation, channel morphology, and hydrology have upon these stream temperatures. It may be helpful to remind the reader that these images measure only surface temperatures of the ground, stream or riparian vegetation.

Image A-4. Cooling Effect of Shade on Ground Surfaces[5]

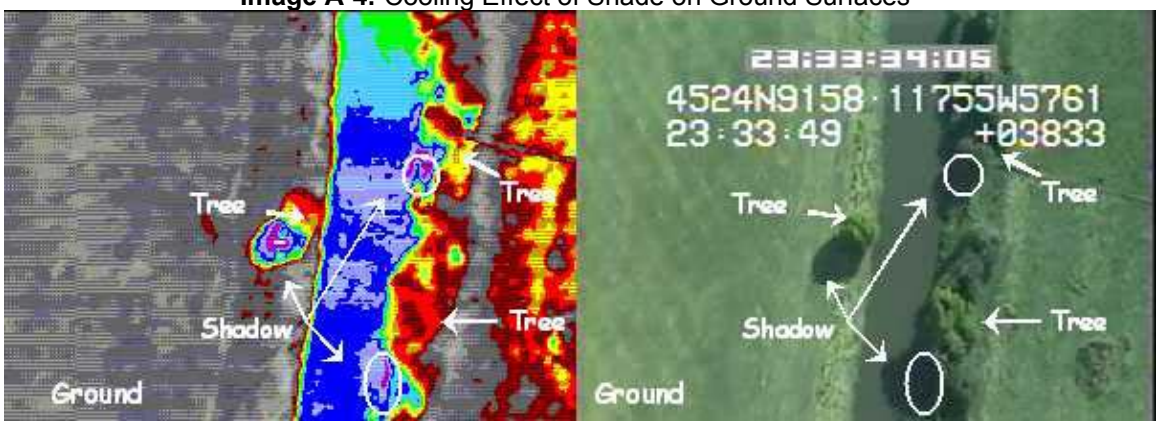

[5] **FLIR Thermal Image Temperature Scale (°F)**

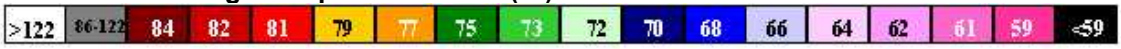

Temperature Related to Channel Morphology

Changes in channel morphology, namely channel widening, impact stream temperatures. As a stream widens, the surface area exposed to radiant sources and ambient air temperature increases, resulting in increased energy exchange between the stream and its environment (Boyd, 1996). Further, wide channels are likely to have decreased levels of shade due to simple geometric relationships between riparian height and channel width. Conversely, narrow channels are more likely to experience higher levels of shade. An additional benefit inherent to narrower/deeper channel morphology is a higher frequency of pools that contribute to aquatic habitat or cold water refugia.

Channel Width

The width to depth ratio is a fundamental measure of channel morphology. High width to depth ratios (greater than 10.0) imply wide shallow channels, while low width to depth ratios (less than 10.0) suggest that the channel is narrow and deep. The PACFISH target for width:depth is 10.0 (USFS, 1995). In terms of reducing stream surface exposure to radiant energy sources, it is generally favorable for stream channels to be narrow and deep (low width to depth ratios).

Factors that Affect Stream Width

Channel widening is often related to degraded riparian conditions that allow increased stream bank erosion and sedimentation of the streambed. Both active stream bank erosion and sedimentation correlate strongly with riparian vegetation type and age. Riparian vegetation contributes to rooting strength and flood plain/stream bank roughness that dissipates erosive energies associated with flowing water. Established/Mature woody riparian vegetation adds the highest rooting strengths and flood plain/stream bank roughness. Annual (grassy) riparian vegetation communities offer less rooting strength and flood plain/stream bank roughness. It is expected that width to depth ratios would be lower (narrower and deeper channels) when established/mature woody vegetation is present. Annual (grassy) riparian communities may allow channels to widen and become shallower.

Further, channel morphology, namely wetted width:depth values, are not solely dependent on riparian conditions. Sedimentation can deposit material in the channel and agrade the streambed, reducing channel depth and increasing channel width. Flow events play a major role in shaping the stream channel. Channel modification usually occurs during high flow events. Naturally, land uses that affect the magnitude and timing of high flow events may negatively impact channel width and depth.

However, riparian vegetation conditions will affect the resilience of the stream banks/flood plain during periods of sediment introduction and high flow. Linking width to depth ratios to riparian vegetation is fundamental. Disturbance processes may have drastically differing results depending on the ability of riparian vegetation to shape and protect channels. Desirable low width to depth ratios (less than 10.0 (PACFISH/INFISH target)) are thus related to riparian vegetation community composition and condition by:

- ✓ ***Building stream banks:*** *Trap suspended sediments, encourage deposition of sediment in the flood plain and reduce incoming sources of sediment.*
- ✓ ***Maintaining stable stream banks:*** *High rooting strength and high stream bank and flood plain roughness prevent stream bank erosion.*
- ✓ ***Reducing flow velocity (erosive kinetic energy):*** *Supplying large woody debris to the active channel, high pool:riffle ratios and adding channel complexity that reduces shear stress exposure to stream bank soil particles.*

Stream Bank Erosion

Stream bank erosion results from detachment, entrainment and removal of bank material as individual grains or aggregates via fluvial processes. *Stream bank failure* indicates a gravity-related collapse of the stream bank by mass movement. Both *stream bank erosion* and *stream bank failure* result in *stream bank retreat*, which is a net loss of stream bank material and a corresponding widening of the stream channel.

Stream bank stability reflects the condition of riparian vegetation contributing to rooting strength in stream bank soils and flood plain roughness. Riparian vegetation rooting structure serves to strengthen the stream bank and resist the erosive energy exerted on the stream bank during high flow conditions. Flood plain roughness reflects the ability of the flood plain to dissipate erosive flow energy during high flow events that over-top stream banks and inundate the flood plain. Riparian vegetation disturbance often has a compounding effect of increased stream bank erosion, increased kinetic energy exposure, decreased bank rooting strength, loss of soil cohesion and loss of flood plain roughness.

Stream Bank Protection and Riparian Vegetation

A stream bank erosion recovery process requires the concurrent occurrence of two elements that induce stream bank building: protect stream banks from kinetic energy (bank particle cohesion) and reduce kinetic energy (stream bank/flood plain roughness). High levels of stream bank cohesion tend to protect the stream bank from erosive kinetic energy associated with flowing water. Stream bank erosion reflects looseness of bank soil, rock and organic particles. The opposite condition is cohesion of stream bank soil, rock and organic particles. Vegetation strengthens particle cohesion by increasing rooting strength that helps bind soil and add structure to the stream bank. Different riparian vegetation communities (annual, perennial, deciduous, mixed and conifer dominated) offer a variety of rooting strengths to stream banks. It is a general observation that healthy/intact indigenous riparian vegetation communities will add preferable stream bank cohesion over bare soil/ground conditions.

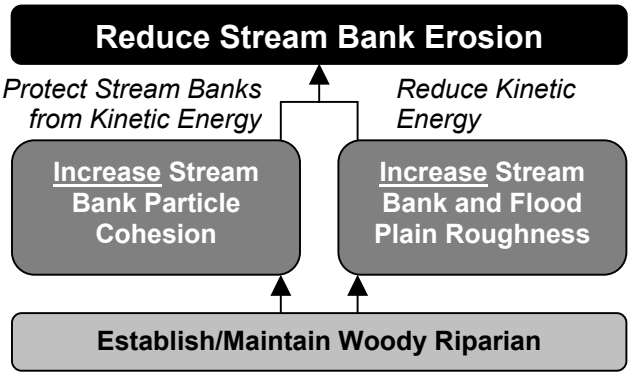

Physical relationships that relate to decreasing/preventing stream bank erosion can be summarized as:

- ✓ *Rough surfaces decrease local flow velocity,*
- ✓ *Reduced local velocity lowers shear stress acting on the stream bank,*
- ✓ *Lower shear stress acting on the stream bank will be less likely to detach and entrain stream bank particles.*

In an effort to control stream bank erosion processes, the focus then becomes to retain high stream bank and flood plain roughness via riparian vegetation. The species composition and condition of the riparian vegetation determines natural stream bank roughness. Values of roughness (Manning's n) correspond to various riparian conditions (**Figure A-24**).

Figure A-24. Manning's n (Roughness Coefficient) Related to Riparian Vegetation

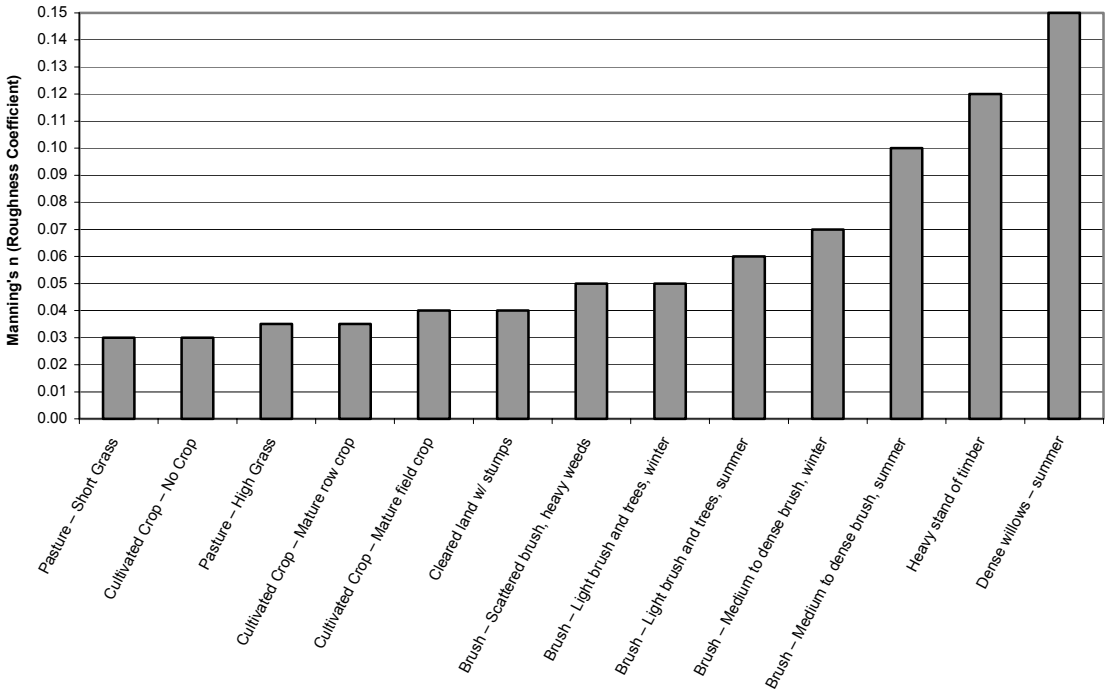

In essence, the roughness coefficients help explain the relationship between riparian vegetation types and active stream bank erosion:

- ✓ *Highest stream bank erosion rates correspond with annual/perennial riparian vegetation types that have a low Manning's n (roughness coefficient).*

- ✓ *Low stream bank erosion rates correspond with woody riparian vegetation types that have a high Manning's n (roughness coefficient).*

Higher values imply increasing roughness that reduces stream bank erosion, reduces local shear stress and slows local flow velocity (Chow, 1959).

Sedimentation

Streambed material classification defines *fines* as sand, silt and organic material that have a grain size of 6.4 mm or less. Sediments may affect the spawning success of salmonids. Sedimentation of spawning gravel has been shown to significantly impair the success of juvenile emergence from gravel *redds*. Sedimentation may affect survival through entombment of juvenile or through reduction of intergravel dissolved oxygen delivery.

Studies have shown that fry emergence is seriously compromised as fine sediments are introduced into spawning gravel (**Figure A-25,** from Tappel and Bjornn, 1993). When fine grain sized substrate cover spawning gravel (*redds*) anadromous *sac-fry* (larval fish) may emerge prematurely. *Sac-fry* are often forced out of gravel before they have absorbed their yolk sacs as a fine sediments fill the interstitial pore spaces of the *redd*, resulting in a lack of oxygen (Tappel and Bjornn, 1993). Low survival rates accompany *sac-fry* that have been forced to prematurely emerge from the *redd*.

Figure A-25. Percentage Sac Fry Emergence in Gravel/Sand Mixtures
[Fine sediment was granitic sand with particles less than 6.4 mm]

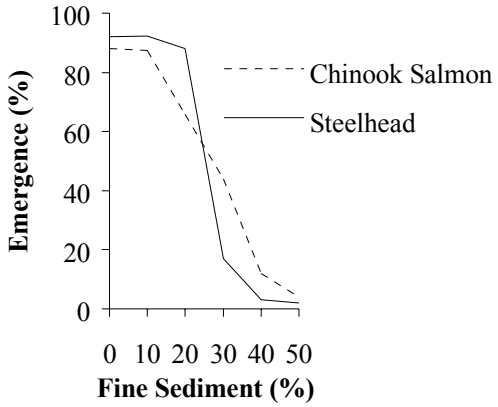

Everest et al. (1987) observed that stable channels containing stored sediments and large woody debris are more productive at every trophic level than either degraded channels devoid of sediment or channels that are agraded and unstable. Stowell et al. (1983) reported that increased fine sediment in spawning gravel has been shown to decrease survival of juvenile salmon emerging from the *redd.* Researchers have presented similar relationships (Waters, 1995; Irving and Bjornn, 1984; and Tappel, 1981). Deposition and embeddedness can influence embryo survival, emergence from the gravel and juvenile or adult use of the habitat. Harvey (1993) found no functional predictors that would quantify the effects of sedimentation on the survival or rearing of salmonids, but recommended that any incremental increase in embeddedness should be avoided.

Increases in bed sediments, affected by landscape and bank mass failures, are often accompanied by channel widening and braiding resulting in increased bank erosion and decreased pool riffle amplitude. Reduced channel complexity may be associated with reduced habitat complexity for aquatic species (salmonids and food sources such as macroinvertebrate communities).

Beschta et al. (1981) concluded that bedload processes are extremely important in shaping the character of quality of stream habitats. Sedimentation of the stream substrate, particularly the gravel used for spawning, produces significant detrimental effects on salmonid resources (Iwamoto et al., 1978). Everest et al (1987) observed that watershed characteristics, as well as the erosion and bedload processes, will affect the level of risk to salmonids by accelerated sedimentation. Fine sediments can act directly on the fish by (Newcombe and McDonald 1991):

- ✓ *Killing salmonids or reducing growth or reducing disease resistance,*
- ✓ *Interfering with the development of eggs and larvae,*
- ✓ *Modifying natural movements and migration of salmonids, or*
- ✓ *Reducing the abundance of food organisms.*

Sediment sources, both upslope and instream, are elevated in some portions of the Umatilla Basin. Before lasting improvements in channel substrate can take place, these sources must be reduced, in some cases, dramatically. Further, if the stream channel, riparian zone and/or upslope landscape is in a degraded state, the same high flow events that transport sediments out of the stream channel can introduce large quantities of fine sediment.

Sediment, once introduced into the stream channel, either becomes deposited in the bed substrate, deposits along banks or remains suspended in the water column (i.e., transported downstream). Fine sediment deposited in the stream bed material must be re-suspended during high flow events and transported downstream or deposited in the flood plain/stream bank areas bordering the stream channel. These processes occur during hydrologic events that are relatively infrequent. Major sediment moving events have return periods measured in decades.

In conclusion, the condition of the stream channel and upslope landscape will create drastically different consequences in terms of sedimentation during high flow events:

> ***Resilient/Healthy System:*** *Prevent large introductions of fine sediment from upslope or riparian areas, maintain stream bank stability, encourage deposition in the flood plain and bank building processes, introduce disturbed riparian vegetation (large woody debris into the active channel) and allow the resuspension and transportation of existing stream bed fine substrate in the downstream direction.*
>
> ***Degrading/Impaired System:*** *Allow large introductions of fine sediment from upslope or riparian areas, experience moderate to high rates of active stream bank erosion, allow erosion in the flood plain and bank retreating processes, is unable to introduce disturbed riparian vegetation (large woody debris into the active channel) and resuspended/transported stream bed fine substrate is replaced by incoming fine sediment sources.*

Temperature Related to Hydrology

Groundwater Mixing

Groundwater inflow has a cooling effect on summertime stream temperatures. Subsurface water is insulated from surface heating processes and most often groundwater temperatures fluctuate little and are cool (45^{o}F to 55^{o}F). Many land use activities that disturb riparian vegetation and associated flood plain areas affect the connectivity of the Umatilla River and its tributaries to groundwater sources. Groundwater inflow not only cools summertime stream temperatures, but also augments summertime flows. Reductions or elimination of groundwater inflow will have a compounding warming effect on the Umatilla River and its tributaries.

FLIR thermal imagery detects groundwater contributions as cooler plumes within the instream temperatures. **Image A-5** shows distinct seeps that deliver groundwater. Areas of cooler soils saturated with groundwater are marked with circles. (Cooler surface temperatures resulting from riparian shading are present on this image and is marked by an arrow.) The mere presence of saturated riparian soils is easily determined with FLIR thermal imagery.

The ability of riparian soils to capture, store and slowly release groundwater is largely a function of the level of riparian disturbance. Human land use can reduce the storage capacity of riparian soils. Riparian disturbance can also separate the connectivity of the flood plain and the stream.

Flood Plain Connectivity

Flood plain disruption can occur when a permeability barrier prevents normal flood plain functions, such as connecting saturated riparian soils with the Umatilla River and tributaries. **Image A-6** illustrates a condition in the Lower Umatilla River in which flood plain connectivity with the river is extremely limited. Any cooling effect from the riparian zone on the left bank can not effect river temperatures.

Surrounding Thermal Environment

Ground temperatures can be a source of heat energy to the stream. When the ground is warmer than the stream, heat will transfer from the stream bank to the water column. In fact, ground surfaces can conduct heat to the stream hundreds of times faster than that of the air column surrounding the stream. Solids (ground surfaces) have higher conductivity than gases (air). Conductivities of soils are on the order of 500 to 3,500 times greater than that of air (Halliday and Resnick, 1988).

Degraded riparian areas that allow excessive stream bank warming will introduce heat into the stream faster than cooler, highly vegetated stream banks. Once again, riparian condition is implicated as a controlling factor in stream temperature dynamics because ground/soil temperatures are a function of the shading.

Air affects stream temperatures at a slower *rate.* Nevertheless, this should not be interpretted to mean that air temperatures do not affect stream temperature. Air can deliver heat to a stream via the convection/conduction pathway, which is the slowest of the water energy transfer processes (Bowen, 1926; Beschta and Weatherred, 1984; Boyd, 1996; Chen, 1996). However, prolonged exposure to air temperatures warmer than the stream can induce gradual stream heating. Because the rate of energy transfer is slow, air temperature related stream column heating cannot explain the rapid daily heating and cooling cycles that streams experience.

Flow Volume

Stream temperature is generally inversely related to flow volume. As flows decrease, stream temperature tends to increase, if energy processes remain unchanged (Boyd, 1996). Runoff in the Umatilla Basin is primarily derived from snowmelt, with peaks typically occurring in the spring. Late summer low flows are common for many streams in the Umatilla Basin due to low summer precipitation combined with extensive irrigation withdrawals. Low flows are of particular concern along the Umatilla mainstem, with many streams over-appropriated, or have insufficient flow to support anadromous and resident fish stocks, meet water quality standards or provide for recreational opportunities (ODEQ, 1995).

Very low water volumes are present in areas of the mainstem Umatilla River (**Image A-8**). Flow within this illustrated section of the river is confined within a channel in the bedrock. No effective riparian shading is available for this portion of channelized Umatilla River, and bedrock temperatures are extremely elevated. Accordingly, water temperatures within this channel are 81-84^{o}F. **Image A-7** illustrates the temperature and flow regime within the Umatilla River less than one mile upstream of Three Mile Falls Water temperatures are approximately 5-13^{o}F cooler and water volumes are much greater at this upstream location.

Image A-5. Umatilla River at River Mile 11 on August 10, 1998[6]

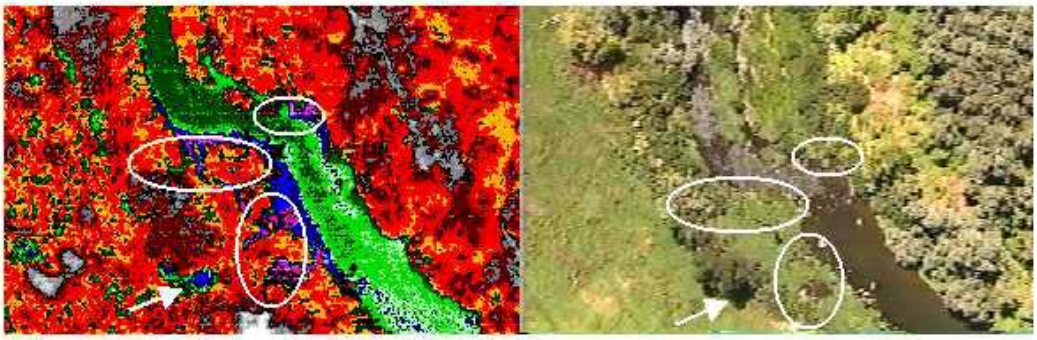

Image A-6. Umatilla River at River Mile 2 on August 10, 1998

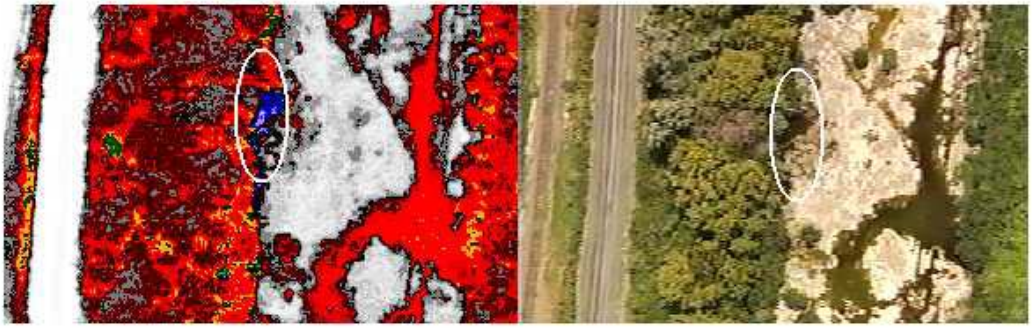

Image A-7. Umatilla River Directly above Three Mile Falls Dam and
Image A-8. Umatilla River Directly below Three Mile Falls Dam (August 10, 1998)

Directly Above Three Mile Falls Dam Diversion

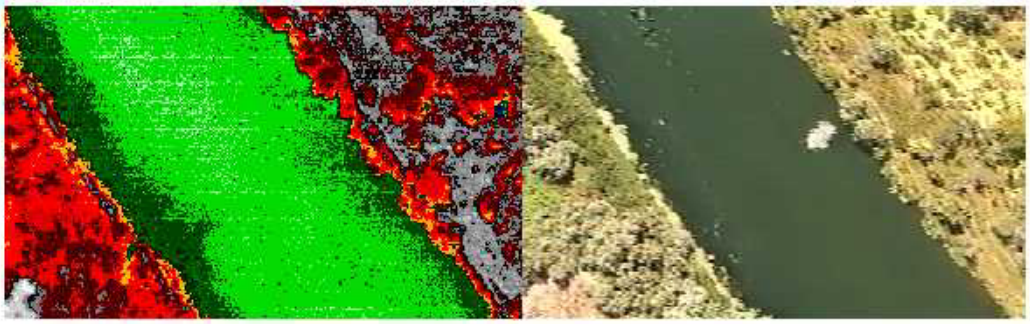

Directly Below Three Mile Falls Dam Diversion

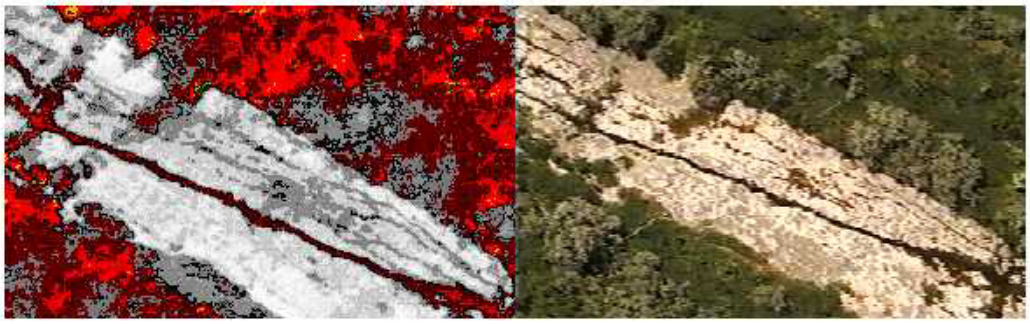

[6] **FLIR Thermal Image Temperature Scale (°F)**

MODEL DEVELOPMENT

Conceptual Model

At any particular instant of time, a defined stream reach is capable of sustaining a particular water column temperature. Stream temperature change that results within a defined reach is explained rather simply. The temperature of a parcel of water traversing a stream/river reach enters the reach with a given temperature. If that temperature is greater than the energy balance is capable of supporting, the temperature will decrease. If that temperature is less than energy balance is capable of supporting, the temperature will increase. Stream temperature change within a defined reach, is induced by the energy balance between the parcel of water and the surrounding environment and transport of the parcel through the reach. The general progression of the model is outlined in the model flow chart, **Figure A-26**.

Figure A-26. Temperature Model Flow Chart

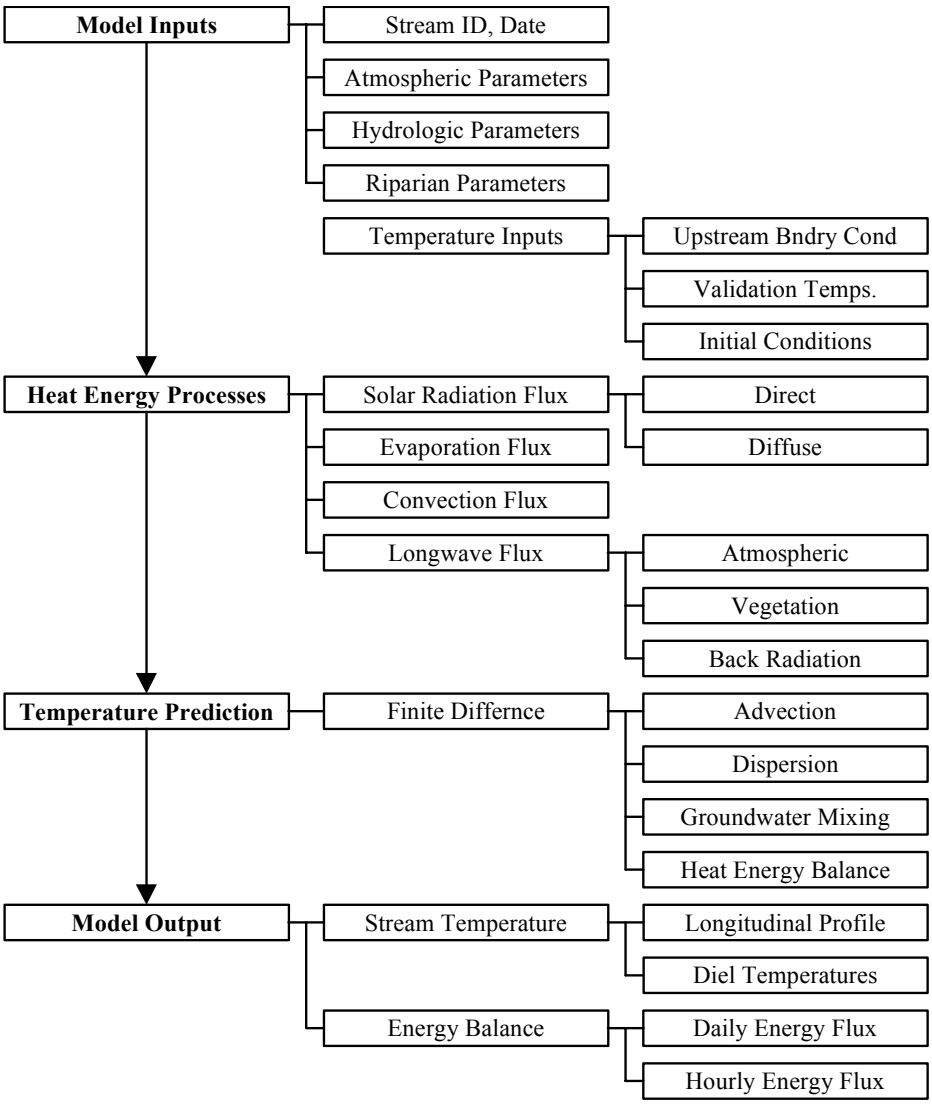

It takes time for the water parcel to traverse the longitudinal distance of the defined reach, during which the energy processes drive stream temperature change. At any particular instant of time, water that enters the upstream portion of the reach is never exactly the temperature that is supported by the defined reach. And, as the water is transferred downstream, heat energy and hydraulic process that are variable with time and space interact with the water parcel and induce water temperature change. The described modeling scenario is a simplification, however, understanding the basic processes in which stream temperatures change occurs over the course of a defined reach and period of time is essential.

Governing Equations

Heat Energy Processes

Water temperature change is a function of the total heat energy contained in a discrete volume and may be described in terms of energy per unit volume. It follows that large volume streams are less responsive to temperature change, and conversely, low flow streams will exhibit greater temperature sensitivity.

Equation A-1. Heat Energy per Unit Volume Temperature Change,

$$\Delta T_w = \frac{E_i}{V_i \cdot \rho \cdot c_p}$$

Which can be rearranged as,

$$\frac{E_i}{V_i} = \Delta T_w \cdot \rho \cdot c_p = \frac{\text{energy}}{\text{volume}} = \frac{\text{cal}}{m^3}$$

Where,

c_p:	Specific heat capacity of water (1000 cal $kg^{-1} \cdot K^{-1}$)
E_i:	Heat energy (cal)
ρ:	Water density (1000 kg m^{-3})
ΔT_w:	Water temperature Change (^oC)
V_i:	Unit volume (m^3)

Water has a relatively high heat capacity ($c_w = 10^3$ cal kg^{-1} K^{-1}) (Satterlund and Adams 1992). Conceptually, water is a heat sink. Heat energy that is gained by the stream is retained and only slowly released back to the surrounding environment, represented by the cooling flux ($\Phi_{cooling}$). Heating periods occur when the net energy flux (Φ_{total}) is positive: ($\Phi_{heating} > \Phi_{cooling}$).

Equation A-2. Heat Energy Continuity,

$$\Phi_{total} = \Phi_{heating} - \Phi_{cooling}$$

In general, the net energy flux experienced by all stream/river systems follows two cycles: a seasonal cycle and a diurnal cycle. In the Pacific Northwest, the seasonal net energy cycle experiences a maximum positive flux during summer months (July and August), while the minimum seasonal flux occurs in winter months (December and January). The diurnal net energy cycle experiences a daily maximum flux that occurs at or near the sun's zenith angle, while the daily minimum flux often occurs during the late night or the early morning. It should be noted, however, that meteorological conditions are variable. Cloud cover and precipitation seriously alter the energy relationship between the stream and its environment.

The net heat energy flux (Φ_{total}) consists of several individual thermodynamic energy flux components, as depicted in **Figure A-27**, namely: solar radiation (Φ_{solar}), long-wave radiation ($\Phi_{longwave}$), conduction ($\Phi_{conduction}$), groundwater exchange ($\Phi_{groundwater}$) and evaporation ($\Phi_{evaporation}$).

Equation A-3. Net Heat Energy Continuity,

$$\Phi_{total} = \Phi_{solar} + \Phi_{longwave} + \Phi_{convection} + \Phi_{evaporation} + \Phi_{streambed} + \Phi_{groundwater}$$

Figure A-27. Heat Energy Processes

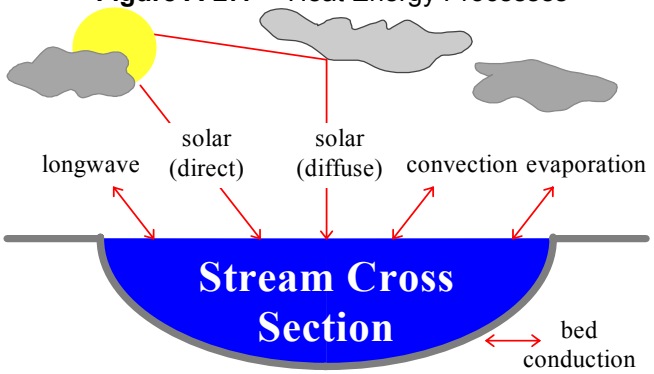

Stream temperature is an expression of heat energy per unit volume, which in turn is an indication of the rate of heat exchange between a stream and its environment. The heat transfer processes that control stream temperature include solar radiation, longwave radiation, convection, evaporation and bed conduction (Wunderlich, 1972; Jobson and Keefer, 1979; Beschta and Weatherred, 1984; Sinokrot and Stefan, 1993; Boyd, 1996). With the exception of solar radiation, which only delivers heat energy, these processes are capable of both introducing and removing heat from a stream. **Figure A-27** displays heat energy processes that solely control heat energy transfer to/from a stream.

When a stream surface is exposed to midday solar radiation, large quantities of heat will be delivered to the stream system (Brown 1969, Beschta et al. 1987). Some of the incoming solar radiation will reflect off the stream surface, depending on the elevation of the sun. All solar radiation outside the visible spectrum (0.36μ to 0.76μ) is absorbed in the first meter below the stream surface and only visible light penetrates to greater depths (Wunderlich, 1972). Sellers (1965) reported that 50% of solar energy passing through the stream surface is absorbed in the first 10 cm of the water column. Removal of riparian vegetation, and the shade it provides, contributes to elevated stream temperatures (Rishel et al., 1982; Brown, 1983; Beschta et al., 1987). The principal source of heat energy delivered to the water column is solar energy striking the stream surface directly (Brown 1970). Exposure to direct solar radiation will often cause a dramatic increase in stream temperatures. The ability of riparian vegetation to shade the stream throughout the day depends on vegetation height, width, density and position relative to the stream, as well as stream aspect.

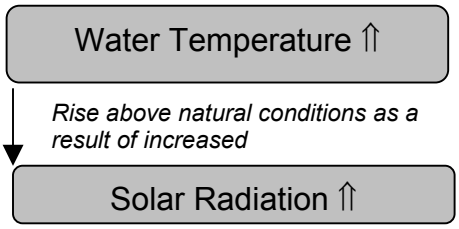

Both the atmosphere and vegetation along stream banks emit longwave radiation that can heat the stream surface. Water is nearly opaque to longwave radiation and complete absorption of all wavelengths greater than 1.2μ occurs in the first 5 cm below the surface (Wunderlich, 1972). Longwave radiation has a cooling influence when emitted from the stream surface. The net

transfer of heat via longwave radiation usually balances so that the amount of heat entering is similar to the rate of heat leaving the stream (Beschta and Weatherred, 1984; Boyd, 1996).

Evaporation occurs in response to internal energy of the stream (molecular motion) that randomly expels water molecules into the overlying air mass. Evaporation is the most effective method of dissipating heat from water (Parker and Krenkel, 1969). As stream temperatures increase, so does the rate of evaporation. Air movement (wind) and low vapor pressures increase the rate of evaporation and accelerate stream cooling (Harbeck and Meyers, 1970).

Convection transfers heat between the stream and the air via molecular and turbulent conduction (Beschta and Weatherred, 1984). Heat is transferred in the direction of warmer to cooler. Air can have a warming influence on the stream when the stream is cooler. The opposite is also true. The amount of convective heat transfer between the stream and air is low (Parker and Krenkel, 1969; Brown, 1983). Nevertheless, this should not be interpretted to mean that air temperatures do not affect stream temperature.

Depending on streambed composition, shallow streams (less than 20 cm) may allow solar radiation to warm the streambed (Brown, 1969). Large cobble (> 25 cm diameter) dominated streambeds in shallow streams may store and conduct heat as long as the bed is warmer than the stream. Bed conduction may cause maximum stream temperatures to occur later in the day, possibly into the evening hours.

The instantaneous heat transfer rate experienced by the stream is the summation of the individual processes:

$$\Phi_{Total} = \Phi_{Solar} + \Phi_{Longwave} + \Phi_{Evaporation} + \Phi_{Convection} + \Phi_{Conduction}.$$

Solar Radiation (Φ_{Solar}) is a function of the solar angle, solar azimuth, atmosphere, topography, location and riparian vegetation. Simulation is based on methodologies developed by Ibqal (1983) and Beschta and Weatherred (1984). *Longwave Radiation* ($\Phi_{Longwave}$) is derived by the Stefan-Boltzmann Law and is a function of the emissivity of the body, the Stefan-Boltzmann constant and the temperature of the body (Wunderlich, 1972). *Evaporation* ($\Phi_{Evaporation}$) relies on a Dalton-type equation that utilizes an exchange coefficient, the latent heat of vaporization, wind speed, saturation vapor pressure and vapor pressure (Wunderlich, 1972). *Convection* ($\Phi_{Convection}$) is a function of the Bowen Ratio and terms include atmospheric pressure, and water and air temperatures. *Bed Conduction* ($\Phi_{Conduction}$) simulates the theoretical relationship ($\Phi_{Conduction} = K \cdot dT_b / dz$), where calculations are a function of thermal conductivity of the bed (K) and the temperature gradient of the bed (dT_b/dz) (Sinokrot and Stefan, 1993). Bed conduction is solved with empirical equations developed by Beschta and Weatherred (1984).

The ultimate source of heat energy is solar radiation both diffuse and direct. Secondary sources of heat energy include long-wave radiation, from the atmosphere and streamside vegetation, streambed conduction and in some cases, groundwater exchange at the water-stream bed interface. Several processes dissipate heat energy at the air-water interface, namely: evaporation, convection and back radiation. Heat energy is acquired by the stream system when the flux of heat energy entering the stream is greater than the flux of heat energy leaving. The net energy flux provides the rate at which energy is gained or lost per unit area and is represented as the instantaneous summation of all heat energy components.

Non-Uniform Heat Energy Transfer Equation

The rate change in stream temperature is driven by the heat energy flux (Φ_i). It is easily shown that a defined volume of water will attain a predictable rate change in temperature, provided an

accurate prediction of the heat energy flux. The rate change in stream temperature (T) is calculated as shown in **Equation A-4**.

Equation A-4. Rate Change in Temperature Caused by Heat Energy Thermodynamics,

$$\frac{\partial T}{\partial t} = \left(\frac{Ax_i \cdot \Phi_i}{\rho \cdot c_p \cdot V_i} \right),$$

Which reduces to,

$$\frac{\partial T}{\partial t} = \left(\frac{\Phi_i}{\rho \cdot c_p \cdot D_i} \right).$$

Where,

Ax_i:	cross-sectional area (m^2)
C_p:	specific heat of water (cal $kg^{-1} \cdot {}^oC^{-1}$)
D_i:	average stream depth (m)
t:	time (s)
T:	Temperature (^oC)
V_i:	volume (m^3)
Φ_i:	total heat energy flux (cal $m^{-2} \cdot s^{-1}$)
ρ:	density of water (kg/m^3)

Advection (U_x) redistributes heat energy in the positive longitudinal direction. No heat energy is lost or gained by the system during advection, and instead, heat energy is transferred downstream as a function of flow velocity. In the case where flow is uniform, the rate change in temperature due to advection is expressed in the first order partial differential equation below.

Equation A-5. Rate Change in Temperature Caused by Advection,

$$\frac{\partial T}{\partial t} = -U_x \cdot \frac{\partial T}{\partial x}$$

Dispersion processes occur in both the upstream and downstream direction along the longitudinal axis. Heat energy contained in the system is conserved throughout dispersion, and similar to advection, heat energy is simply moved throughout the system. The rate change in temperature due to dispersion is expressed in the second order partial differential equation below.

Equation A-6. Rate Change in Temperature Caused by Dispersion,

$$\frac{\partial T}{\partial t} = D_L \cdot \frac{\partial^2 T}{\partial x^2}$$

The dispersion coefficient (D_L) may be calculated by stream dimensions, roughness and flow. In streams that exhibit high flow velocities and low longitudinal temperature gradients, it may be assumed that the system is advection dominated and the dispersion coefficient may be set to zero (Sinokrot and Stefan 1993). In the event that dispersion effects are considered significant, the appropriate value for the dispersion coefficient can be estimated with a practical approach developed and employed in the QUAL 2e model (Brown and Barnwell 1987). An advantage to this approach is that each parameter is easily measured, or in the case of Manning's coefficient (n) and the dispersion constant (K_d), estimated.

Equation A-7. Physical Dispersion Coefficient,

$$D_L = C \cdot K_d \cdot n \cdot U_x \cdot D^{\frac{5}{6}}$$

Where,

C:	Unit conversion C = 3.82 for English units C = 1.00 for Metric units
D:	Average stream depth (m)
D_L:	Dispersion coefficient (m^2/s)
K_d:	Dispersion constant
n:	Manning's coefficient
U_x:	Average flow velocity (m/s)

The simultaneous non-uniform one-dimensional transfer of heat energy is the summation of the rate change in temperature due to heat energy thermodynamics, advection and dispersion. Given that the stream is subject to steady flow conditions and is well mixed, transverse temperature gradients are negligible (Sinokrot and Stefan 1993). An assumption of non-uniform flow implies that cross-sectional area and flow velocity vary with respect to longitudinal position. The following second ordered parabolic partial differential equation describes the rate change in temperature for non-uniform flow.

Equation A-8. Non-Uniform One-dimensional Heat Energy Transfer,

$$\frac{\partial T}{\partial t} = -U_x \cdot \frac{\partial T}{\partial x} + D_L \cdot \frac{\partial^2 T}{\partial x^2} + \frac{\Phi}{c_p \cdot \rho \cdot D_i}$$

$$\text{Steady Flow: } \frac{\partial U_x}{\partial t} = 0$$

$$\text{Non-Uniform Flow: } \frac{\partial U_x}{\partial x} \neq 0$$

The solution to the *one-dimensional heat energy transfer equation* is essentially the summation of thermodynamic heat energy exchange between the stream system and the surrounding environment and physical processes that redistribute heat energy within the stream system. It is important to note that all heat energy introduced into the stream is conserved, with the net heat energy value reflected as stream temperature magnitude. Further, heat energy is transient within the stream system, due to longitudinal transfer of heat energy (i.e., advection and dispersion). The net heat energy flux (□) is calculated at every distance step and time step based on physical and empirical formulations developed for each significant energy component. The dispersion coefficient (D_L) is assumed to equal zero.

Boundary Conditions and Initial Values

The temperatures at the upstream boundary (i_o) for all time steps (t_o ,t_1,..., t_{M-1}, t_M) are supplied by the upstream temperature inputs. At the downstream boundary temperature at longitudinal position i_{n+1} is assumed to equals that of i_n with respect to time t. Initial values of the temperatures at each distance node (i_o ,i_1,..., i_{N-1}, i_N) occurring at the starting time (t_o) can be input by the model user or assumed to equal the boundary condition at time t_o.

Spatial and Temporal Scale

The lengths of the defined reaches are 100 feet. The temperature model is designed to analyze and predict stream temperature for one day and is primarily concerned with daily prediction of the diurnal energy flux and resulting temperatures on August 10, 1998. Prediction time steps are limited by stability considerations for the finite difference solution method.

ANALYTICAL FRAMEWORK

Overview

Data collected during this TMDL effort has allowed the development of temperature simulation methodology that is both spatially continuous and spans full day lengths (diurnal). Detailed spatial data sets have been developed for the following parameters (from the forks to the mouth):

- ✓ River and Tributary Mapping at 1:5,000 scale,
- ✓ Riparian Vegetation Species, Size and Density Mapping at 1:5,000 scale,
- ✓ Near-Stream Disturbance Zone Width Measurement at 1:2,500 scale,
- ✓ West, East and South Topographic Shade Angles calculations at 1:5,000 scale,
- ✓ Stream Elevation and Gradient at 1:5,000 scale,
- ✓ Hydrology Developed from Field Data - Spatially Continuos Flow, Wetted Width, Velocity and Depth Profiles.

All input data is longitudinally referenced in the model allowing spatial and/or continuous inputs to apply to certain zones or specific river segments. This section contains several figures that longitudinally display the input parameters used to calibrate the temperature model (**Figures A-36** through **A-46**).

Spatial Input Parameters

Longitudinal Distance (meters): Defines the modeled reaches for which spatial input parameters reference. Model reaches are 30 meters each, are derived from DOQ 1:5000 river layer digitized from Digital Orthophoto Quads (DOQs), and are measured in the downstream direction (**Figure A-28**).

Elevation (meters): Sampled for each model reach from a Digital Elevation Model (DEM).

Gradient (%): Is the difference between the upstream and downstream elevations divided by the reach length.

Bedrock (%): The percent of streambed material that has a diameter of 25 cm or greater. Values are derived from stream survey data or assumed where data is limited.

Aspect (decimal degrees from North): Measured from DOQ 1:5,000 rivers layer and represents the direction of stream flow.

Flow Volume (cubic meters per second): Measured by DEQ with standard USGS protocols with interpolation between flow measurement sites. Irrigation diversion and return flows for 15-minute intervals measured by Bureau of Reclamation and Water Resources Department.

Flow Velocity (meters per second): Derived from Manning's equation and Leopold power functions calibrated to measured flow velocity data.

Wetted Width (meters): Derived from Manning's equation and Leopold power functions calibrated to measured wetted width data.

Average Depth (meters): Derived from Manning's equation and Leopold power functions calibrated to measured average depth data. Calculated based on assuming rectangular channel.

Near-Stream Disturbance Zone Width (meters): Measured from 1:5,000 DOQs (**Figure A-30**).

Channel Incision (meters): Depth of the active channel below riparian terrace or floodplain. Measured by the Confederated Tribes of the Umatilla Indian Reservation (CTUIR).

Riparian Height (meters): Obtained from Landsat thermal satellite imagery and aerial photo interpretation (see "Data Source Descriptions" for details) (**Figure A-29**).

Canopy Density (%): Obtained from Landsat thermal satellite imagery and aerial photograph interpretation (see "Data Source Descriptions" for details) (**Figure A-29**).

Riparian Overhang (meters): Distance of riparian vegetation intrusion over Near-Stream Disturbance Zone. Assumed to be zero for entire simulation distance due to lack of data.

Topographic Shade Angle (decimal degrees): The angle made between the stream surface and the highest topographic features to the west, east and south as calculated from DEM at each stream reach (**Figure A-31**).

Continuous Input Parameters

Wind Speed (meters per second): Hourly values measured at Pendleton Airport via the National Weather Service (**Figure A-33**).

Relative Humidity (%): Hourly values measured by DEQ (**Figure A-32**).

Air Temperature (^{o}C): Hourly values measured by DEQ (**Figure A-34**).

Stream Temperature (^{o}C): Hourly values measured by DEQ.

Tributary Temperature (^{o}C): Hourly values measured by DEQ (**Figure A-35**).

Tributary/Irrigation Return Flow Volume (cubic meters per second): Measured or estimated flow volumes for all major tributaries/irrigation returns.

Data Source Descriptions

Existing Vegetation: Landsat thermal satellite imagery (1997) that has been delineated into polygons according to vegetation species, size, and canopy density. The pixel size of this data is 25 meters. Tree sizes were presented as diameter at breast height (DBH) ranges. The mid-range DBH was used to calculate approximate heights for each species. All coverage was verified using Digital Orthophoto Quarter Quads (DOQQs) or Digital Orthophoto Quads (DOQs).

Digital Elevation Models (DEM): 30-meter DEMs are available for the entire state of Oregon through the State Service Center for Geographic Information Systems (SSCGIS).

Digital Orthophoto Quarter Quads (DOQQs): DOQQs for the Umatilla Basin are available from the United States Geologic Survey (the aerial photos were taken in 1997). (DOQs are typically available for areas where DOQQs are not.) USGS DOQQs correspond to the topographic map quarter quadrants.

Digital Orthophoto Quads (DOQs): DOQs for the Umatilla Basin are available through the State Service Center for Geographic Information Systems (SSCGIS). (DOQQs are typically available for areas where DOQs are not.)

Figure A-28. Model Methodolgy - Stream Digitization from DOQs (1:3000)

Figure A-29. Model Methodology - LandSat Data Overlaying DOQs for Visual Inspection (1:3000)

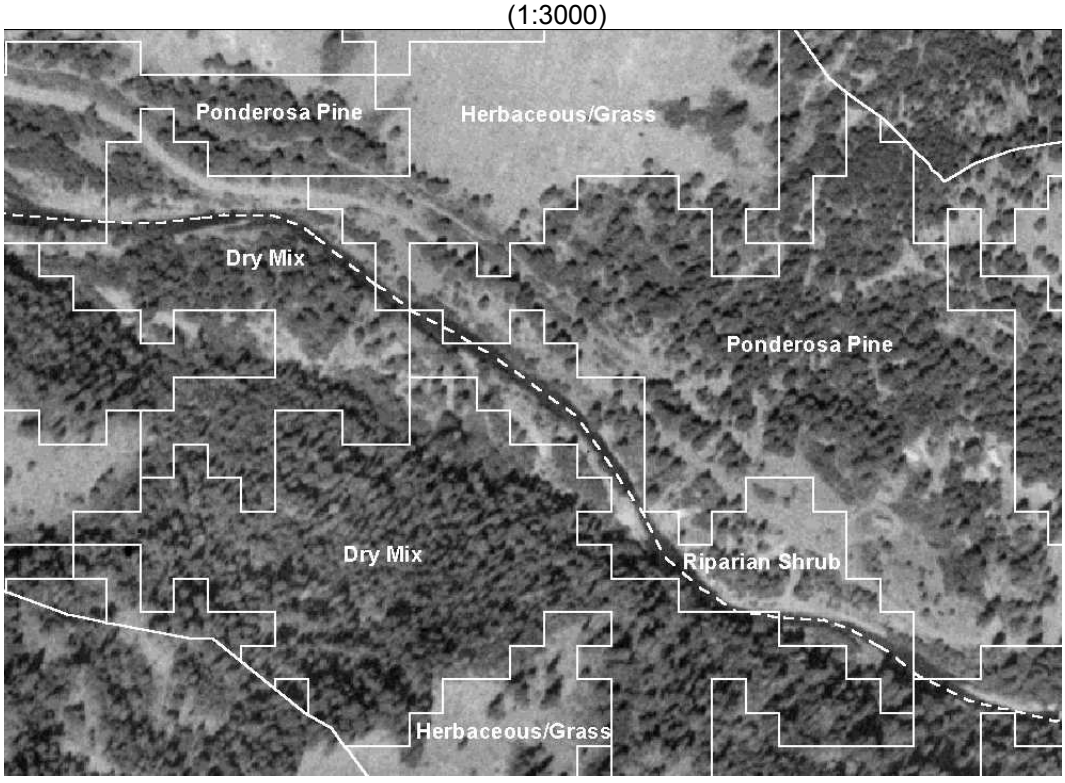

Figure A-30. Model Methodology – Near-Stream Disturbance Zone Measured from DOQs (1:1500)

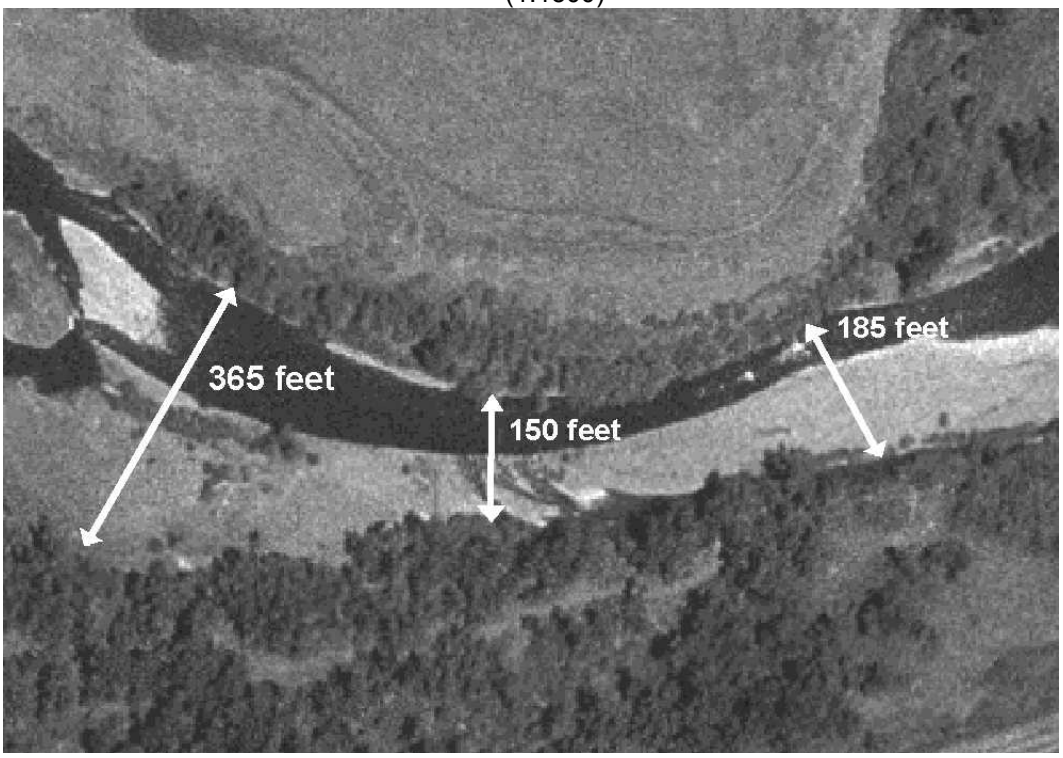

Figure A-31. Model Methodology - Calculation of Topographic Shade from the DEM

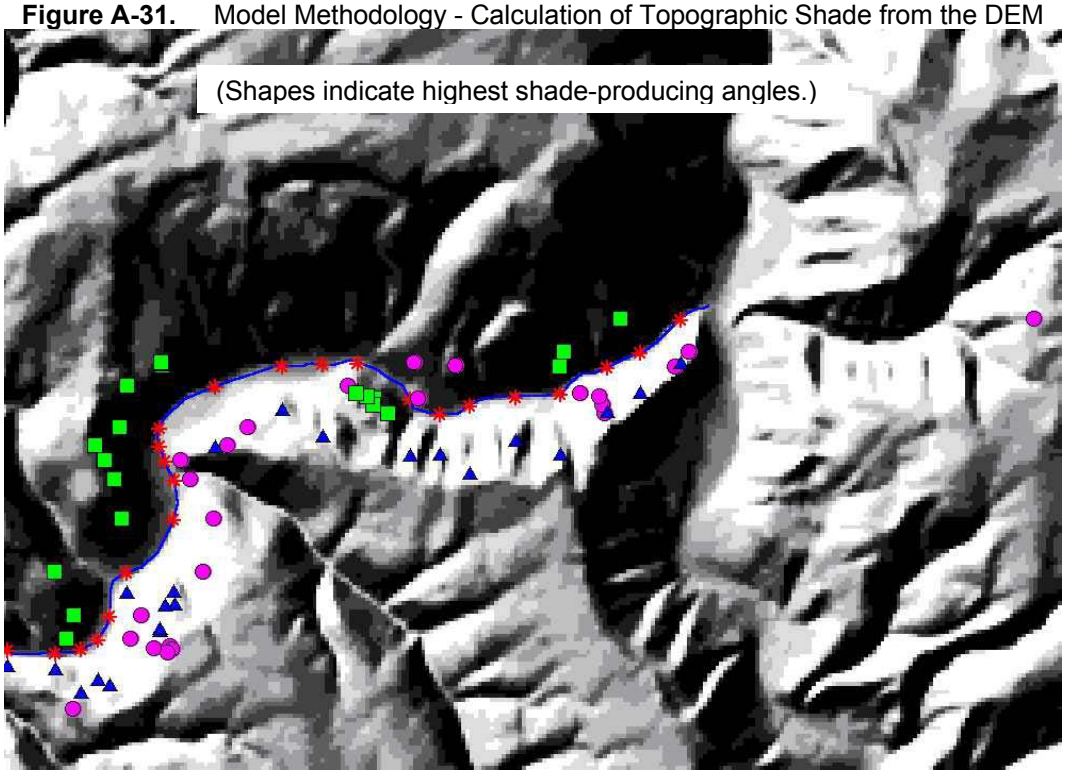

Figure A-32. Model Input Data - Relative Humidity

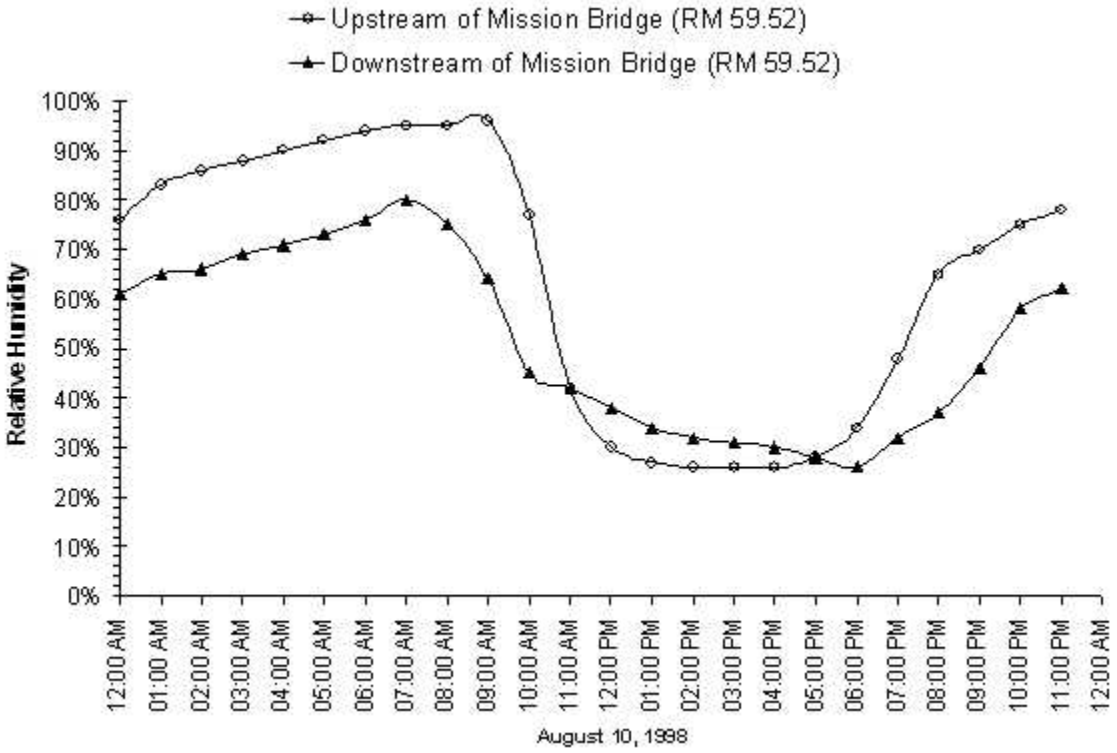

Figure A-33. Model Input Data - Wind Speed

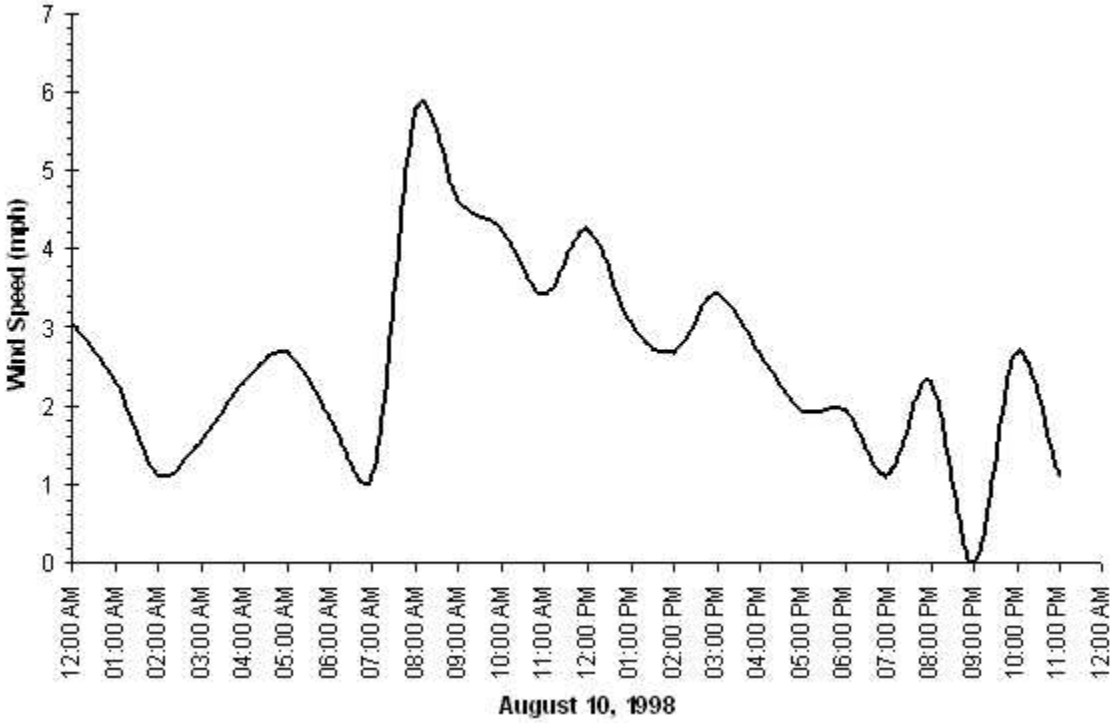

Figure A-34. Model Input - Air Temperature

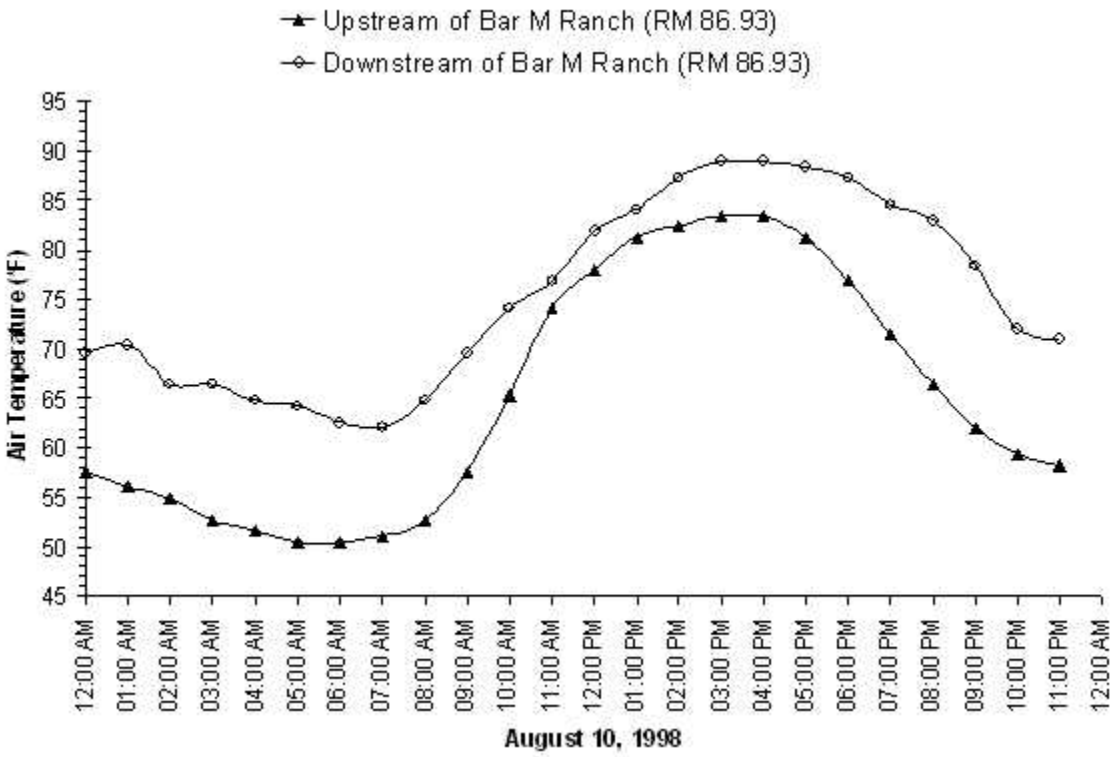

Figure A-35. Model Input - Tributary Temperatures

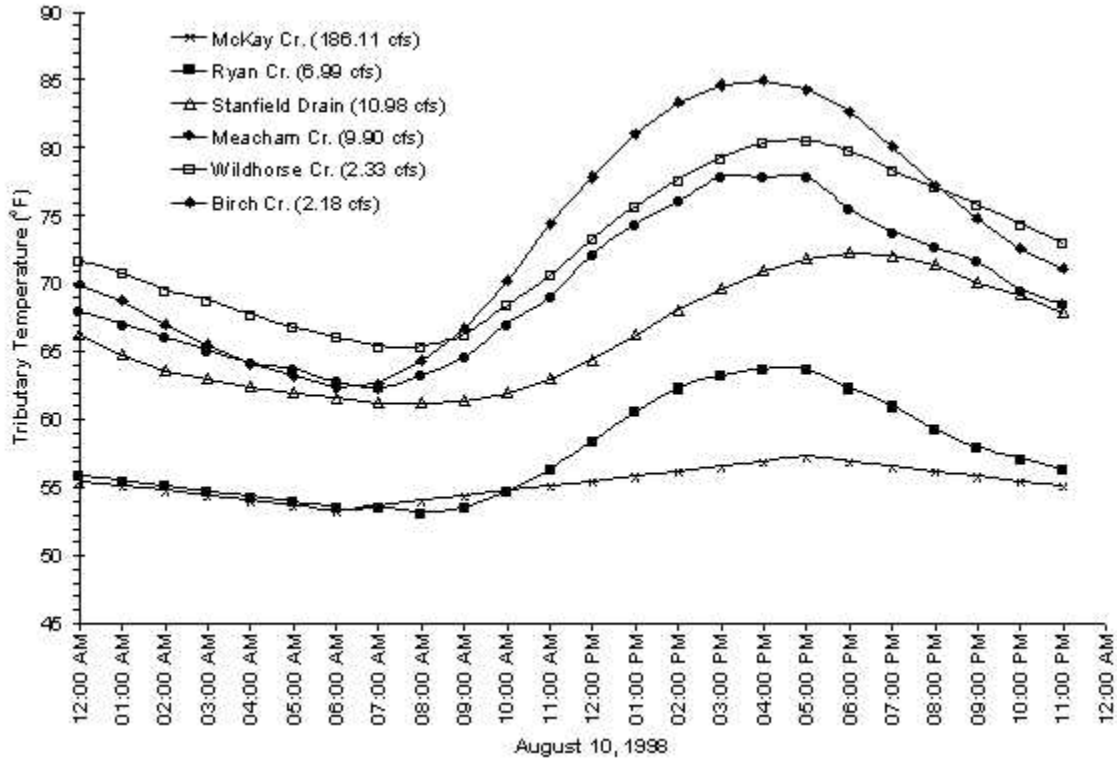

Figure A-36. Model Input Data – Current Riparian Vegetation Width

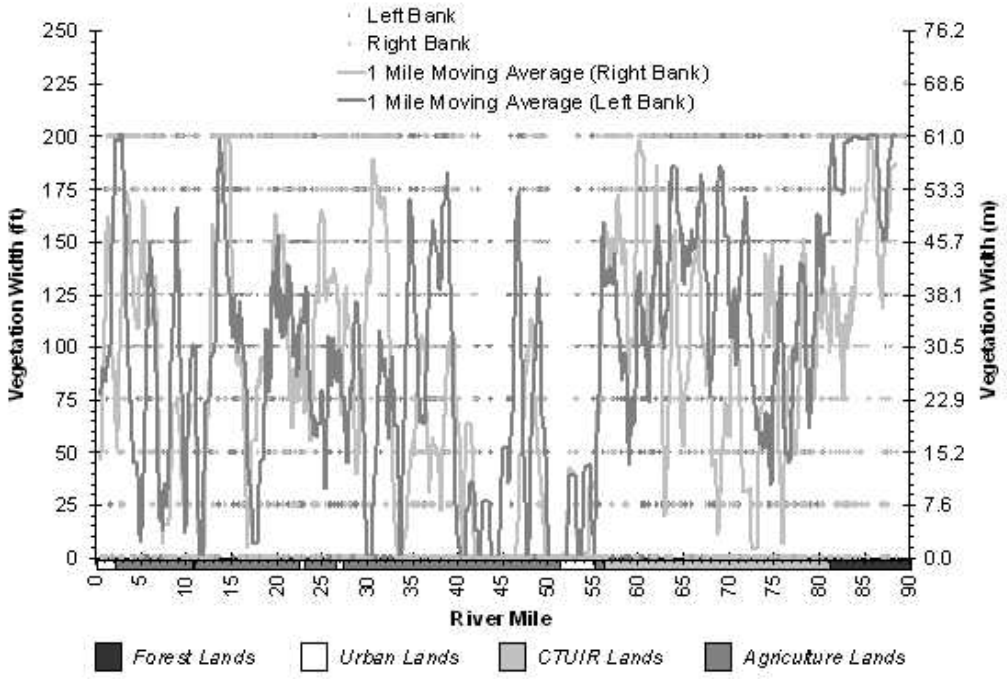

Figure A-37. Model Input Data – Current Riparian Vegetation Density

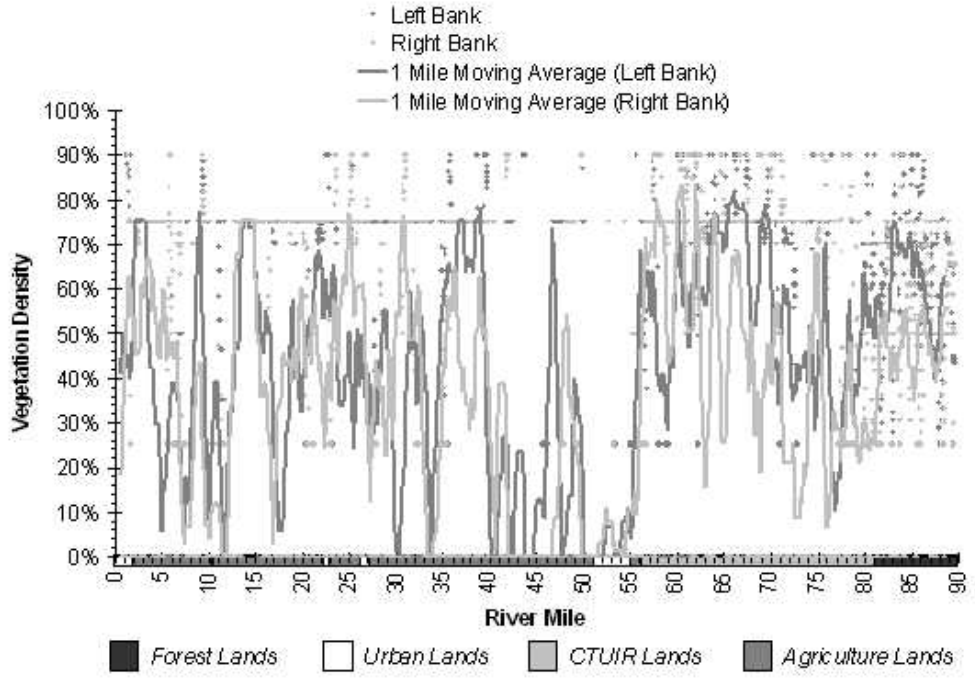

Figure A-38. Model Input Data – Current Riparian Vegetation Height
*(Also see **Figures 15** through **18** of the Umatilla Basin TMDL)*

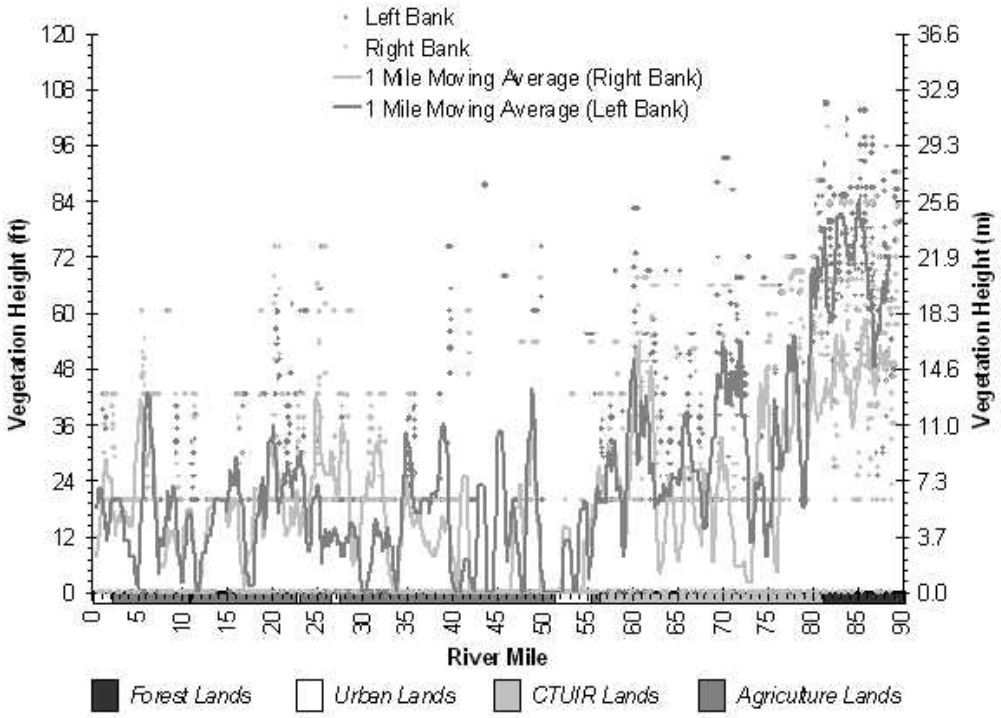

Figure A-39. Model Input Data - Topographic Shade

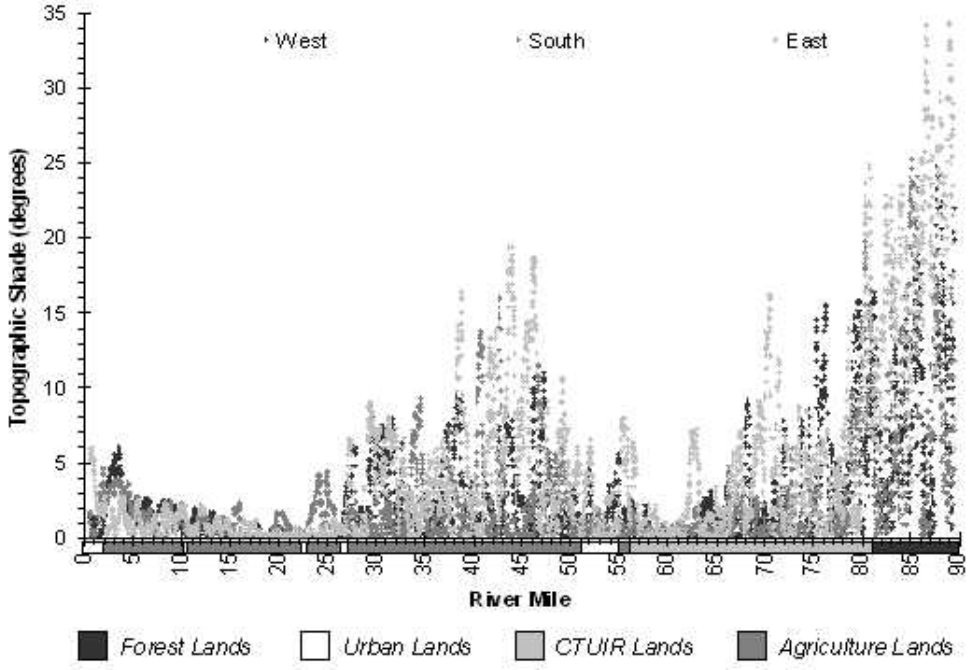

Figure A-40. Model Input Data - Stream Aspect (Downstream Direction)

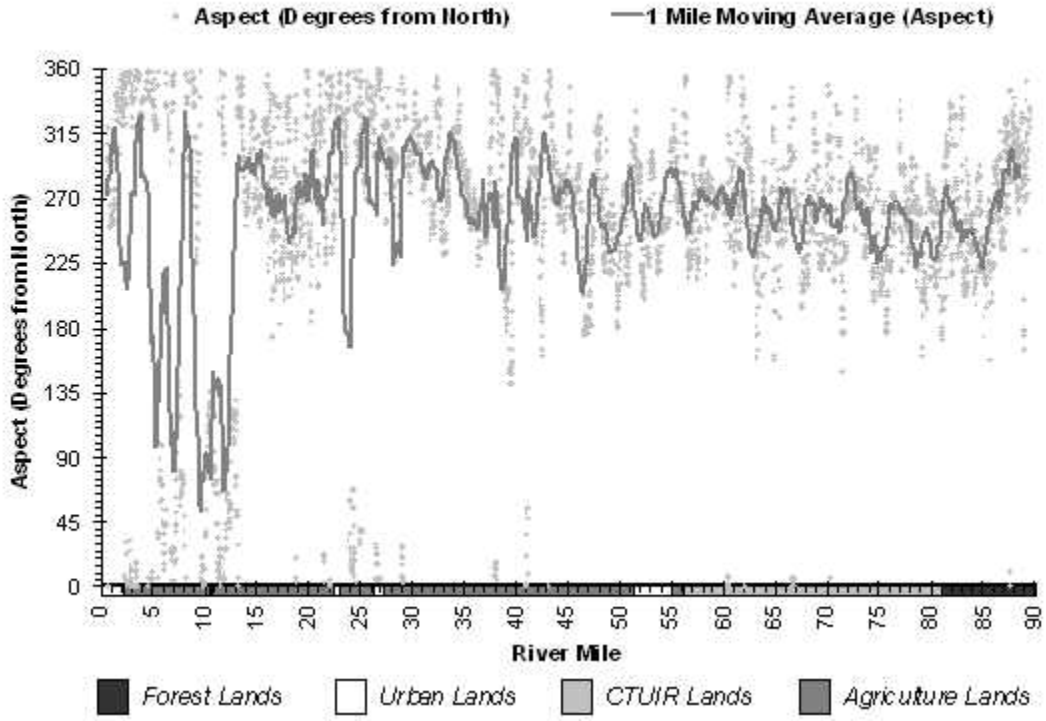

Figure A-41. Model Input Data - Flow Velocity

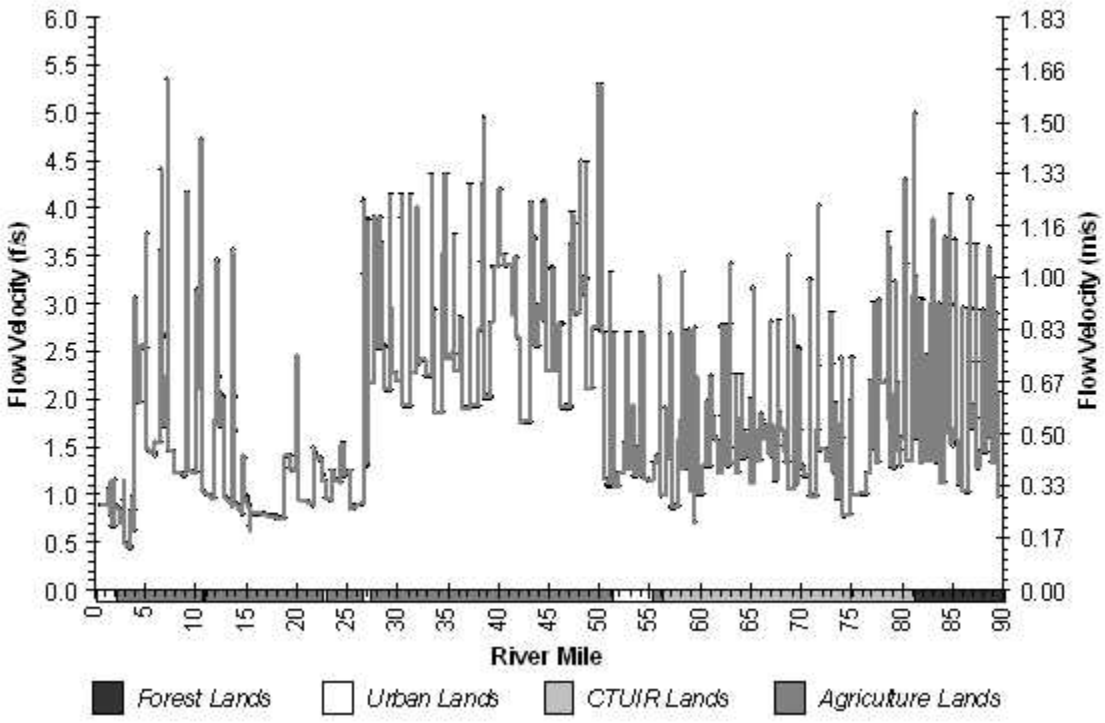

Figure A-42. Model Input Data - Flow Volume

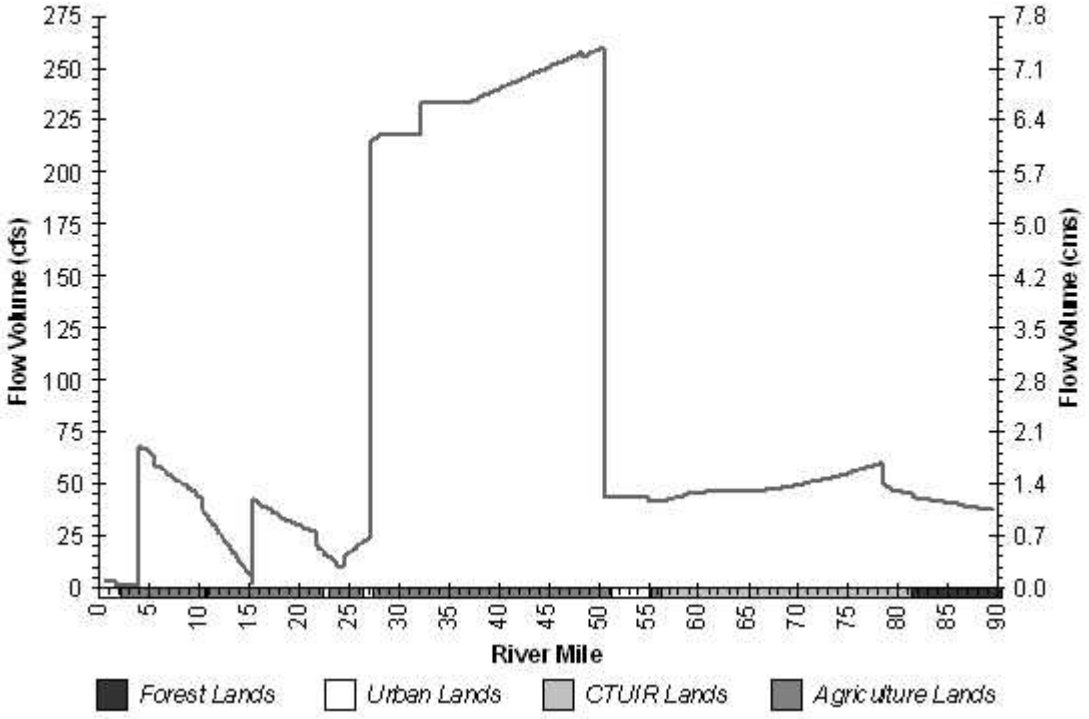

Figure A-43. Model Input Data - Sinuosity

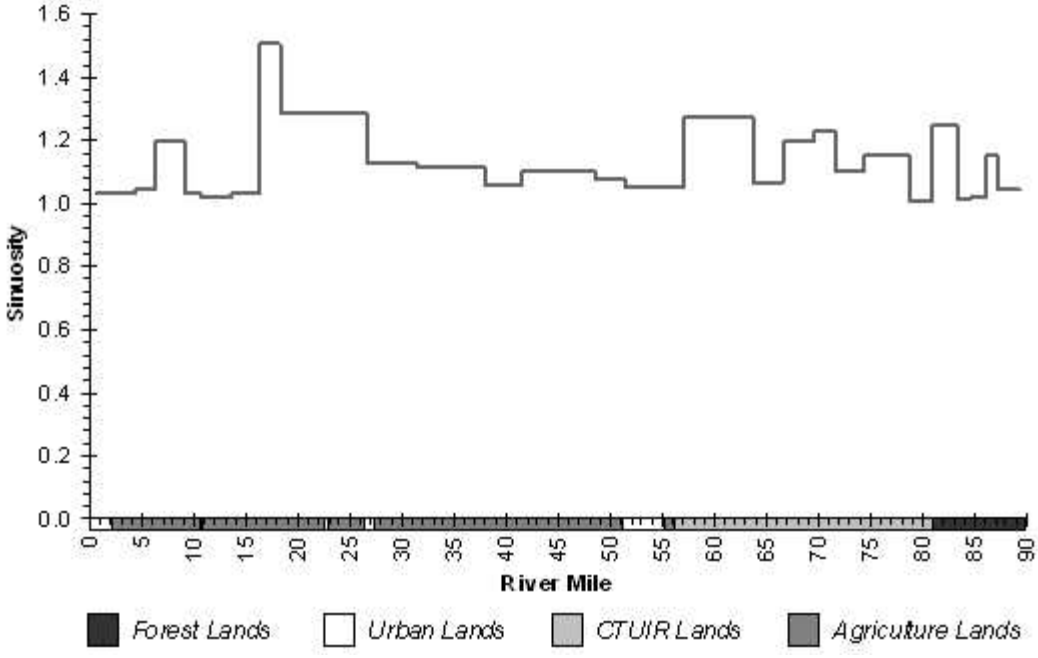

Figure A-44. Model Input Data - Stream Depth

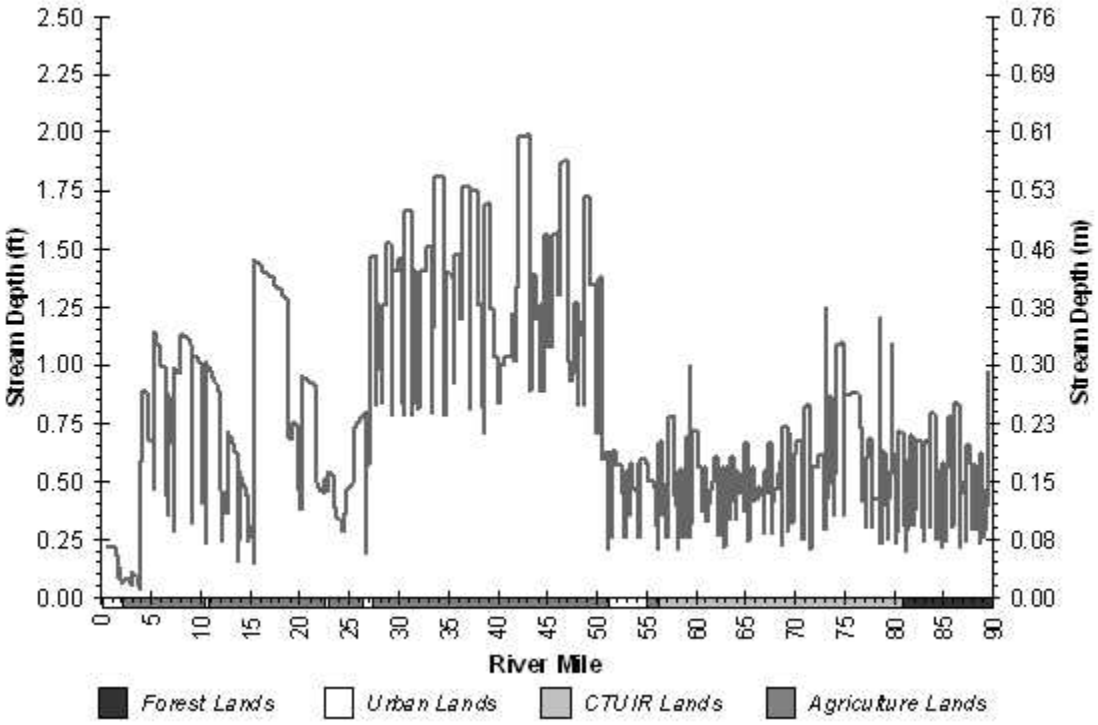

Figure A-45. Model Input Data - Near-Stream Disturbance Zone Width and Wetted Width

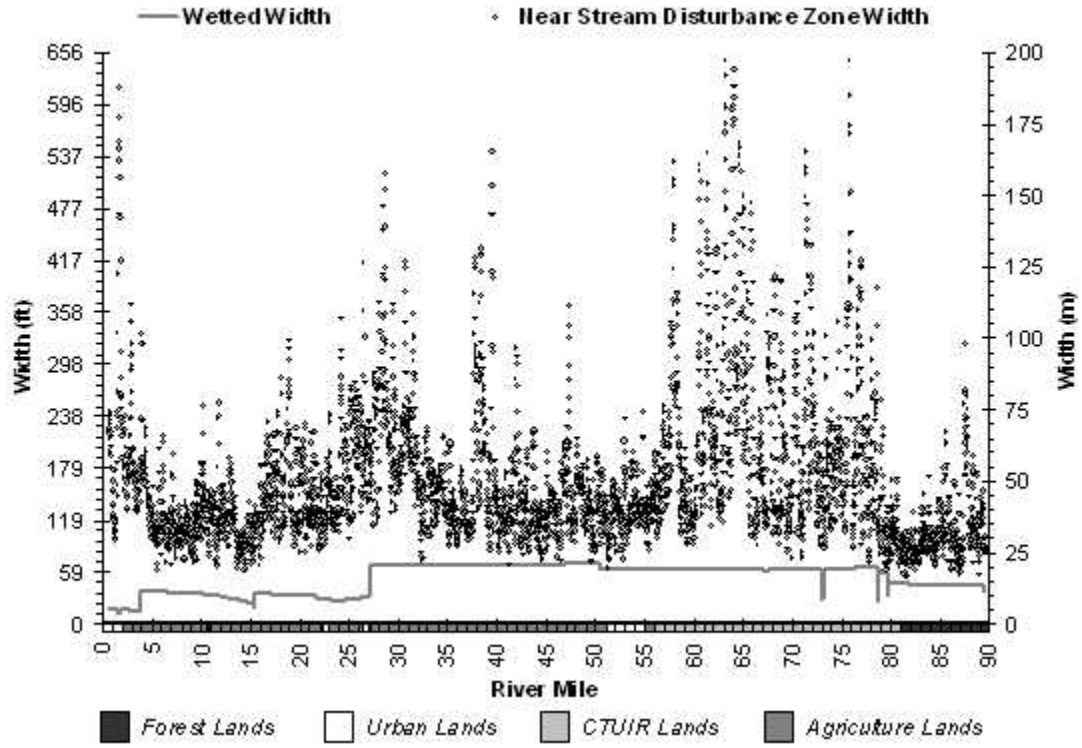

Figure A-46. Model Input Data - Stream Elevation and Gradient

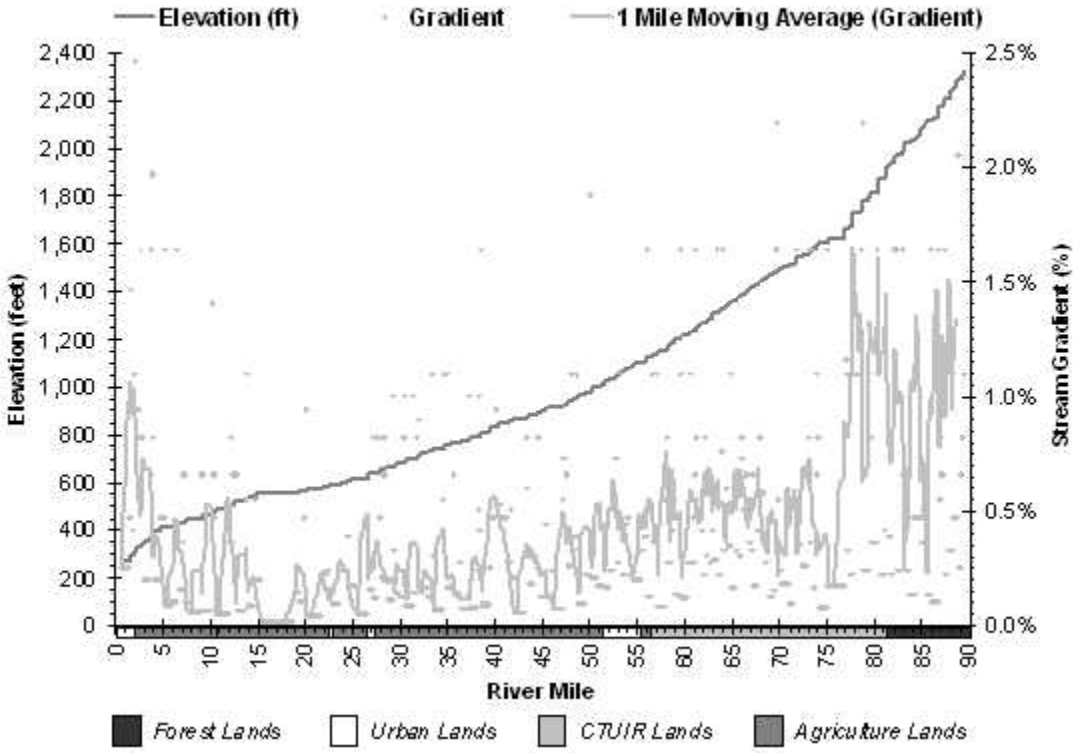

Results

Validation

Statistical analyses were performed to compare the actual (FLIR) and predicted stream temperatures (spatial data validation). Similarly, statistical analyses were performed to compare the actual and the predicted diel stream temperatures at ten hourly monitoring locations (continuous data validation). The statistical validation results are summarized below.

Spatial Data Validation	*Continuous Data Validation*
n = 4700	n = 240
R^2 = 0.82	R^2 = 0.96
Average Standard Error = 2.34°F	Average Standard Error = 0.85°F
Average Deviation = 1.66°F	Average Deviation = 1.76°F

Spatial Data Validation

The standard errors, average deviations, and correlation coefficients for the spatial data are presented in **Figure A-47**. The lowest correlation coefficient occurs in the lower half of the Umatilla River, where numerous irrigation withdrawals and returns create a highly variable flow regime, thus resulting in a more difficult model calibration. For the entire 89.6 miles of modeled river, the standard error is 2.34°F.

Figure A-47. Spatial Data Validation

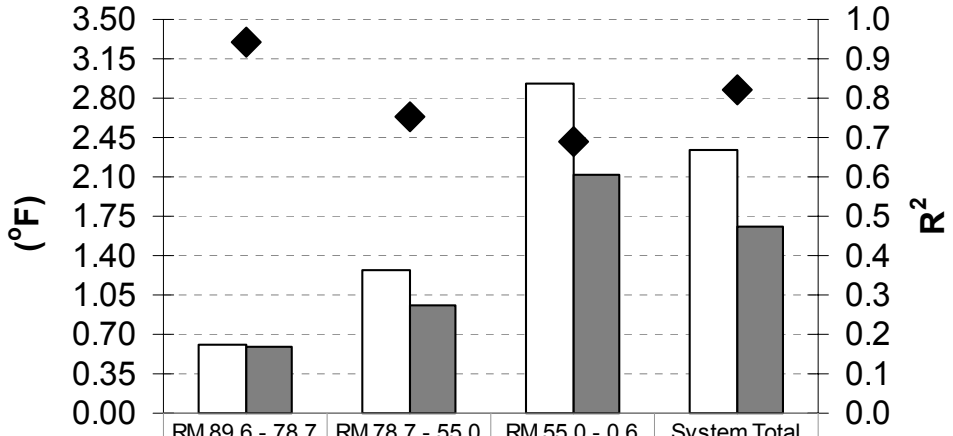

	RM 89.6 - 78.7	RM 78.7 - 55.0	RM 55.0 - 0.6	System Total
□ Standard Error	0.61	1.27	2.92	2.34
■ Average Deviation	0.59	0.96	2.11	1.66
◆ Correlation Coefficient	0.94	0.75	0.69	0.82

The calibrated model predictions are shown in **Figure A-48**. Recall from earlier discussion, that the Umatilla River was flown for FLIR in two trips; the lower half around 2:00 pm on August 10, 1998 and the upper half around 4:00 pm on the same day. The solid lines in the figure below are the calibrated model current condition predictions. Continuous temperature monitoring sites (Vemcos) are symbolized by large diamonds. Recall that FLIR gives outer surface temperatures only. The Vemcos were anchored at the bottom of the river channel, where they recorded hourly water temperatures. The correlation between the FLIR temperatures and the Vemco temperatures indicates that the stream is completely mixed throughout the majority of the system. However, there may be some stratification in the backwater behind dams.

Figure A-48. Calibrated Model Output – Model Validation

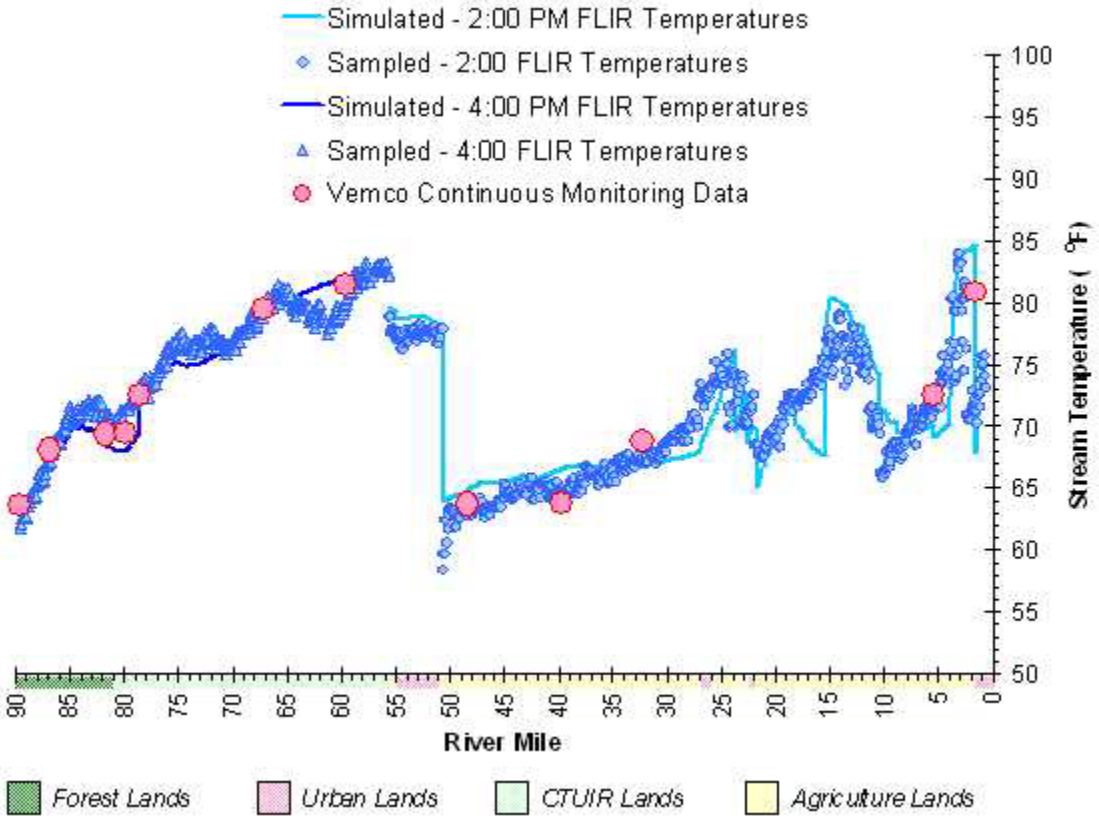

Continuous Data Validation

Statistical analysis results of the continuous temperature data are shown in **Figure A-49**. Correlation coefficients were typically near or above 0.90. The actual and predicted diel temperature profiles for each of the ten sites are shown in **Figure A-50**.

Figure A-49. Continuous Data Validation

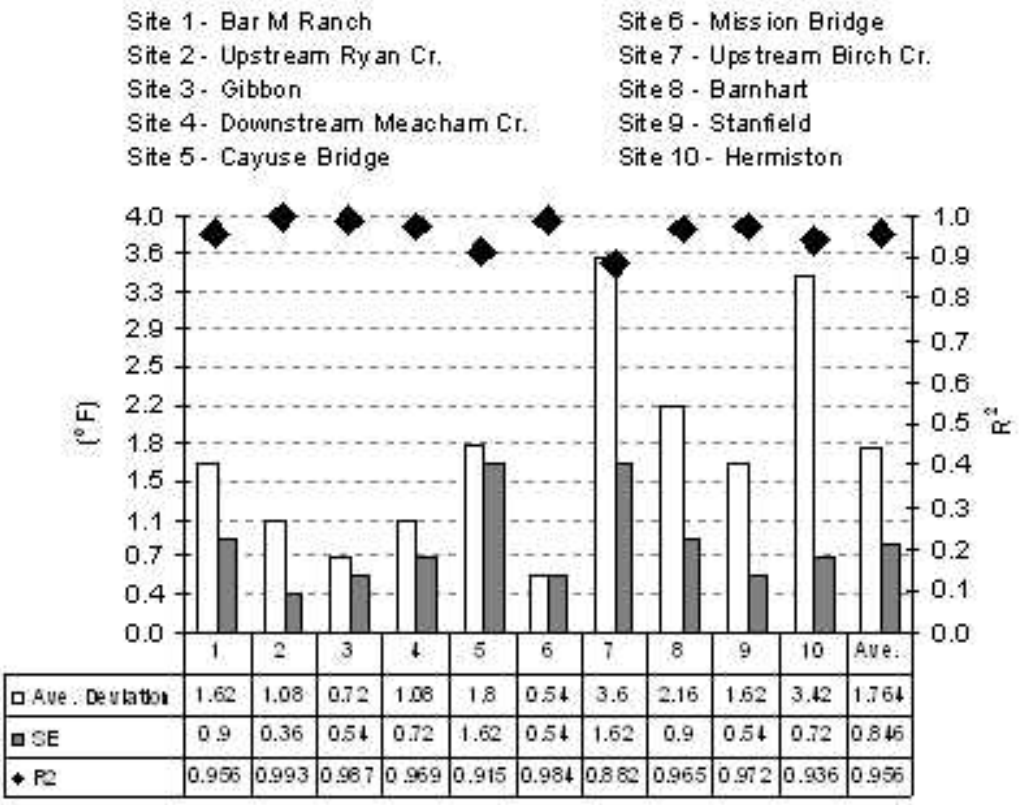

	1	2	3	4	5	6	7	8	9	10	Ave.
Ave. Deviation	1.62	1.08	0.72	1.08	1.8	0.54	3.6	2.16	1.62	3.42	1.764
SE	0.9	0.36	0.54	0.72	1.62	0.54	1.62	0.9	0.54	0.72	0.846
R2	0.956	0.993	0.987	0.969	0.915	0.984	0.882	0.965	0.972	0.936	0.956

Figure A-50. Diurnal Temperature Profiles - Measured and Simulated

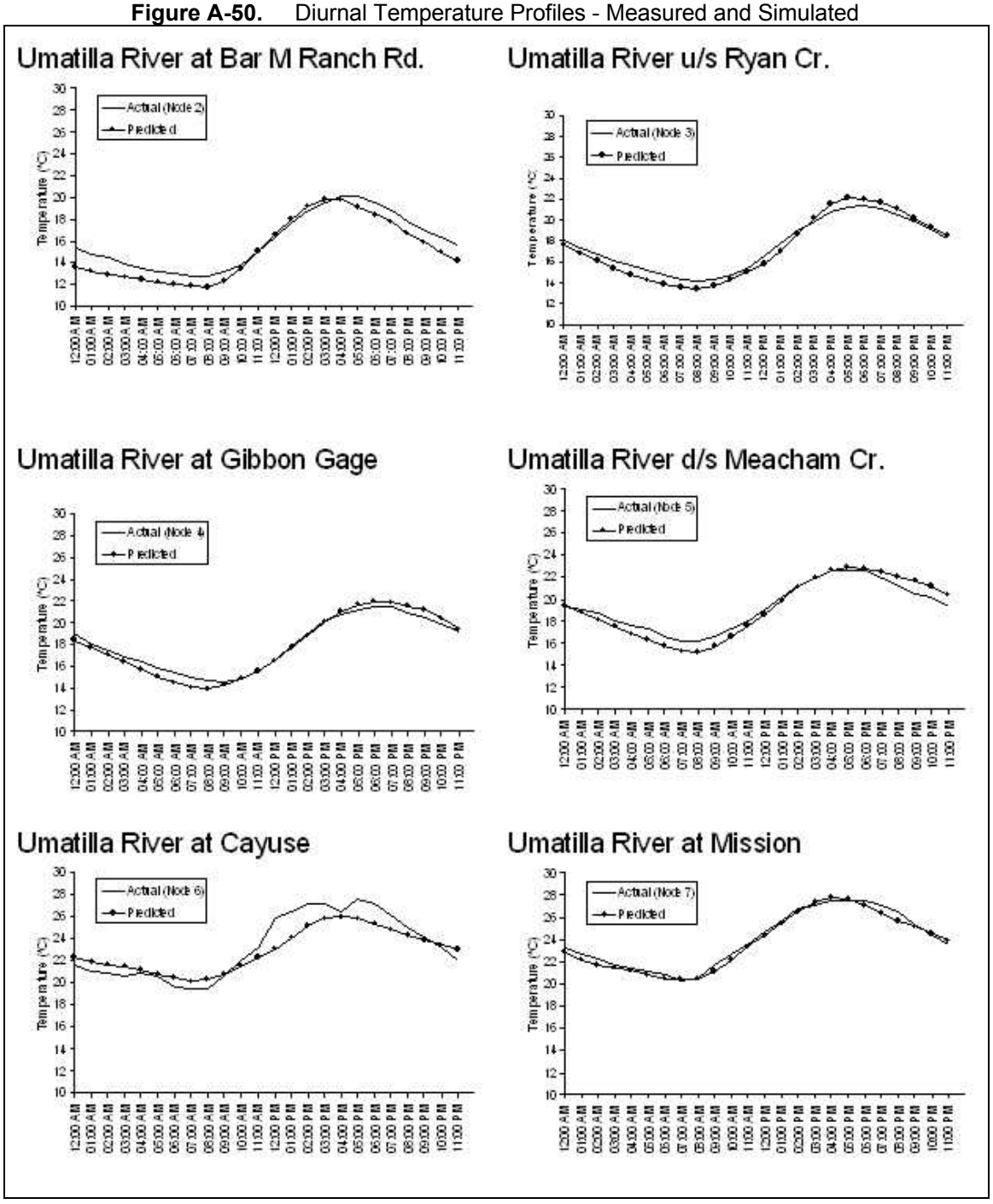

Figure A-50 (continued). Diurnal Temperature Profiles - Measured and Simulated

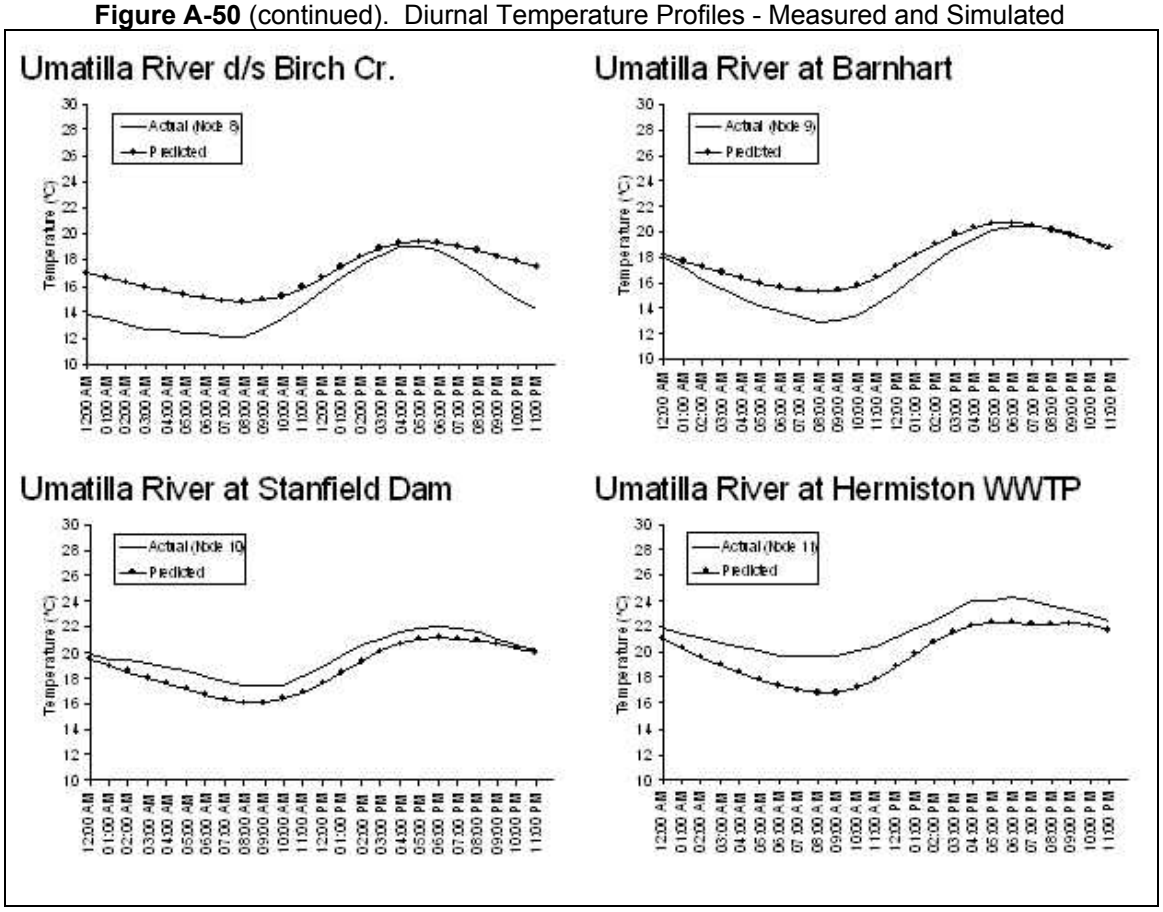

Individual Parameter Sensitivities

Once the model was calibrated to the current conditions, sensitivity analyses were performed by varying a single input parameter while all other parameters remained at current conditions. **Table A-5** describes the various parameters that were tested for sensitivity.

Table A-5. Single Parameter Scenarios

Parameter	*Scenario Name*	*Description*
Flow Volume	Natural Flow	Assumed flows that would exist without mainstem withdrawals. No surface irrigation return flows via drains.
	Flow Augmentation	Assumed flows that would exist without mainstem withdrawals. Augmentation from McKay Reservoir exists.
Near-Stream Disturbance Zone (NSDZ)	Potential NSDZ	Assumed Near Stream Disturbance Zone widths were at the potential widths, as determined by the Umatilla River Basin TMDL Technical Committee.
Near-Stream Vegetation	Potential Vegetation	Assumed near stream vegetation at potential height, width and density, as determined by the Umatilla River Basin TMDL Technical Committee.

Near-Stream Disturbance Zone

The near-stream disturbance zone width correlates to the distance that the near-stream vegetation is from the water. By reducing near-stream disturbance zone widths, vegetation will be closer to the water and the chances of a shadow being cast on the water surface is increased.

Shown in **Figure A-51**, are system potential NSDZ widths. For the NSDZ scenario, existing near-stream disturbance zone widths that that are greater than the target were reduced. Current widths that are less than the target, remained unchanged.

The longitudinal profiles comparing the current near-stream disturbance zone widths with the targets are shown in **Figure A-52**. This parameter alone has little effect on stream temperatures largely due to the fact that there is inadequate existing vegetation to shade the river.

Figure A-51. Longitudinal Profiles of Near-Stream Disturbance Zone Widths

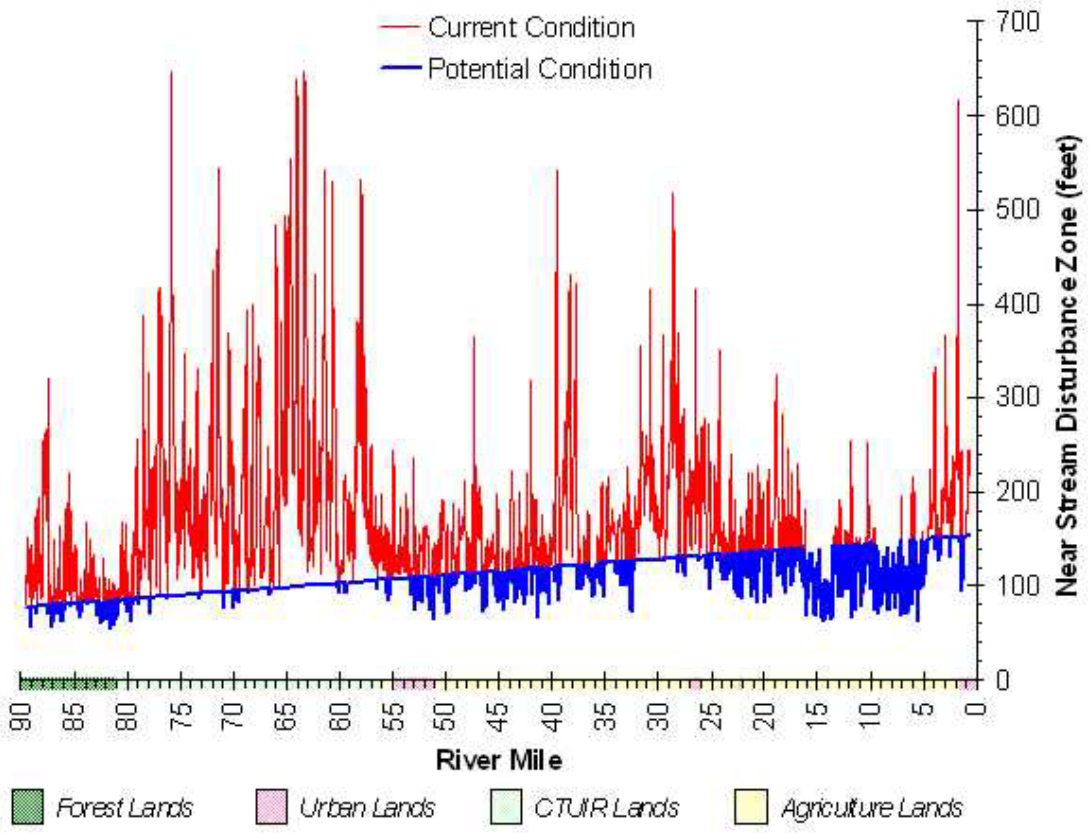

Figure A-52. Near-Stream Zone of Disturbance Scenario

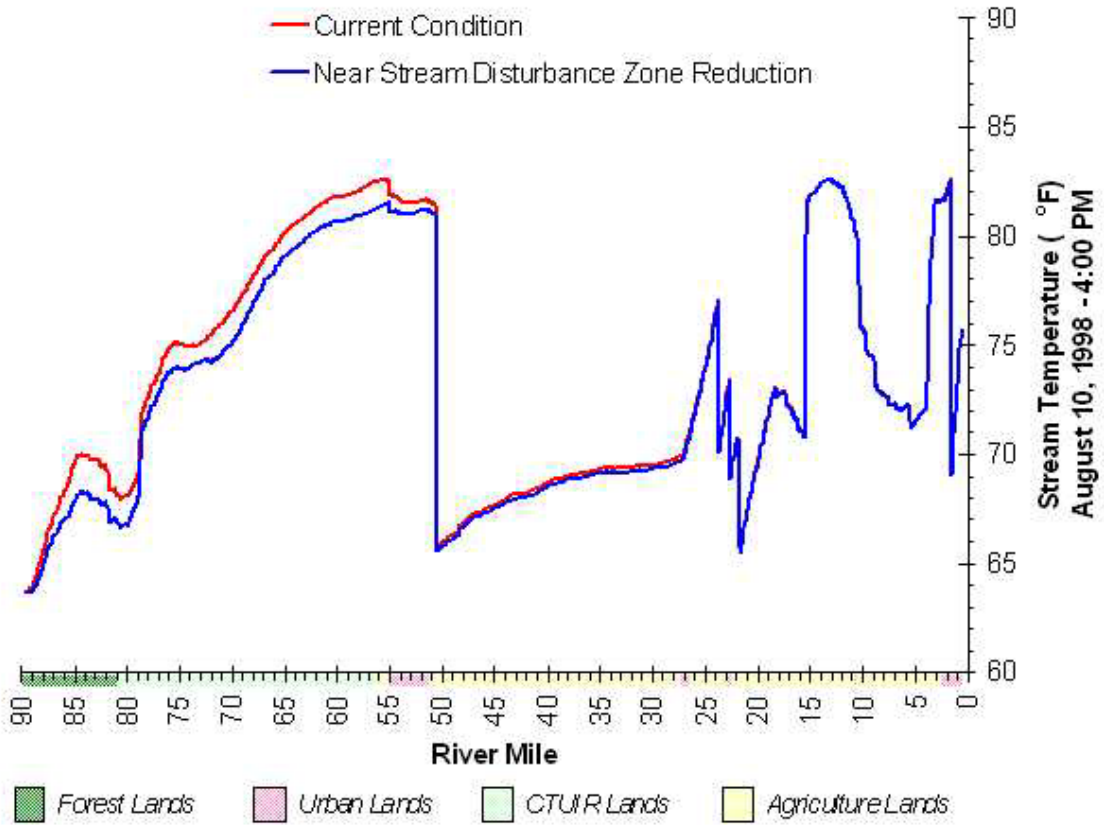

Flow

Two flow scenarios were modeled. The flow inputs for each are shown in **Figure A-53**.

"Natural flow" condition is defined as the flow regime that would likely occur assuming that there were no anthropogenic impacts on the Umatilla River (i.e., no dams, no irrigation withdrawals or returns, no McKay reservoir releases). In **Figure A-54**, the most prominent stream temperature deviation from current conditions occurs below river mile 25, as a result of flow being maintained within the river.

The "flow augmentation" scenario is essentially the same as the "natural flow" scenario; however, McKay Reservoir flow augmentation is occurring. **Figure A-54** reveals the significant temperature reduction resulting from about 200 cfs of cool McKay Reservoir hypolimnion water. Below McKay Creek, flow is maintained in the stream, and relatively little heating occurs.

Figure A-53. Flow Scenario Longitudinal Inputs

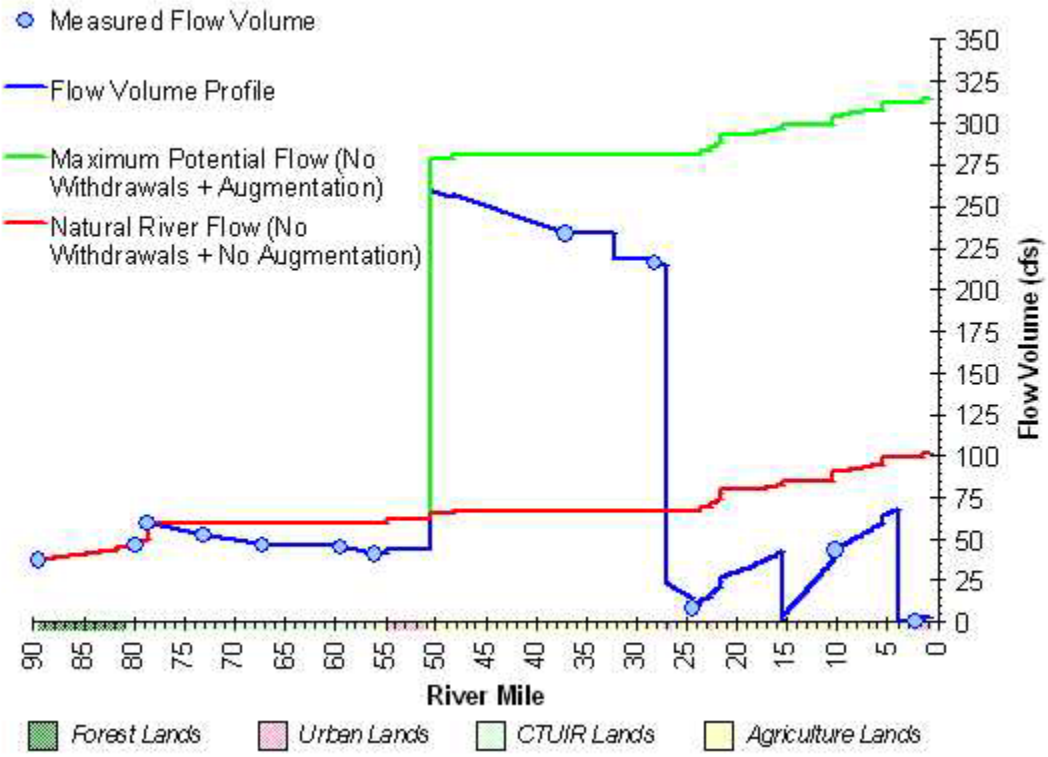

Figure A-54. Flow Scenarios

Natural Flow: No withdrawals return flows or augmentation from McKay

Flow Augmentation: No withdrawals or return flows with augmentation from McKay

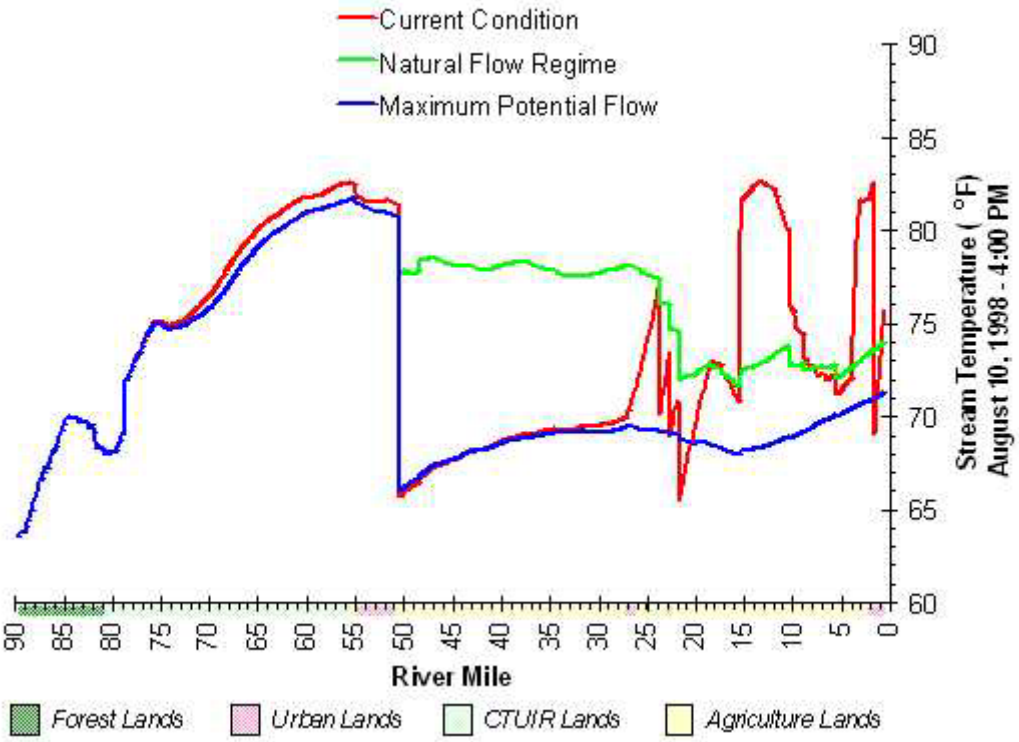

Near-Stream Vegetation Scenarios

Potential vegetation was simulated, as described in **Section 2.1.3.1, Table 8** of the TMDL**.**

Current near-stream woody vegetation is sparse or non-existent along much of the Umatilla River. The temperature responses seen in **Figure A-55** indicate that vegetation enhancements alone will not significantly reduce Umatilla River temperatures. Shade levels produced in the potential vegetation scenario are still rather low due to the extremely wide existing near-stream disturbance zone.

Figure A-55. Near-Stream Vegetation Scenarios

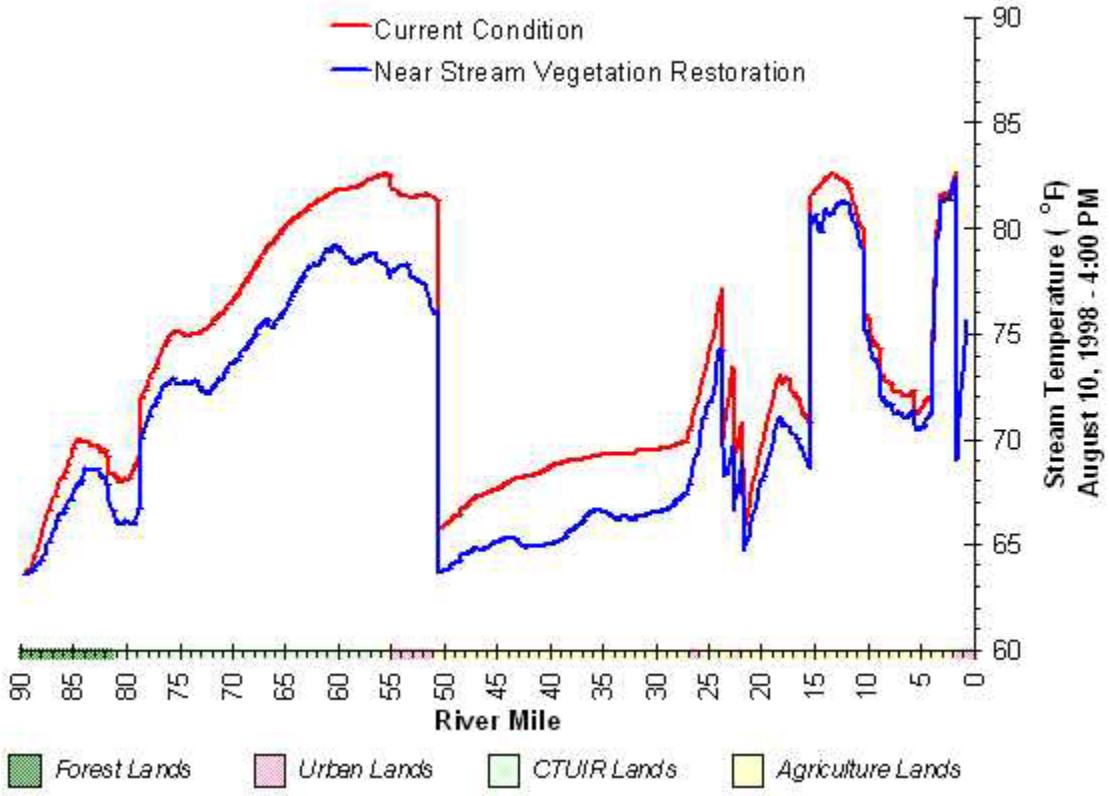

System Potential Scenarios

As indicated by the single-parameter sensitivity analyses, stream temperature reductions are best achieved by improving a combination of channel, bank, and vegetation parameters. Combining multiple parameters into one scenario may be representative of the Umatilla River system potential. **Table A-6** lists the three system potential scenarios that were run using the calibrated model. Note that the only difference between the three combination scenarios is the flow regime. Each combination scenario factors in late seral near-stream vegetative communities, improved tributary water quality, reduced near-stream disturbance zone widths, and targeted width to depth ratios.

Table A-6. Combination Parameter Scenarios

Parameter	*Scenario Name*	*Description*
System Potential Scenarios	Combination 1	• Tributaries < 64°F • Potential Vegetation • Potential Near-Stream Disturbance Zone Widths • Targeted W:D ratios • Existing Flow Condition
	Combination 2	• Combination 1, except for • Natural Flow Scenario
	Combination 3	• Combination 1, except for • Flow Augmentation Scenario

The following three figures display the system potential stream temperatures.

In **Figure A-56**, significant temperature reductions are apparent throughout the system under the existing flow regime. In the lower portion of the river, temperatures still spike to near lethal levels in locations where the flow is reduced to only a few cubic feet per second (i.e., below Three Mile Falls Dam).

The second combination scenario (**Figure A-57**) reveals the stream temperature patterns that may occur under natural flow conditions. Notably, the Umatilla River maintains near-70°F temperatures below Pendleton.

Umatilla River temperatures below Pendleton can potentially be maintained in the mid 60°F range under a natural flow condition with augmentation from McKay Reservoir (**Figure A-58**).

Figure A-56. Combination 1 Scenario – System Potential with Current Flow Regime

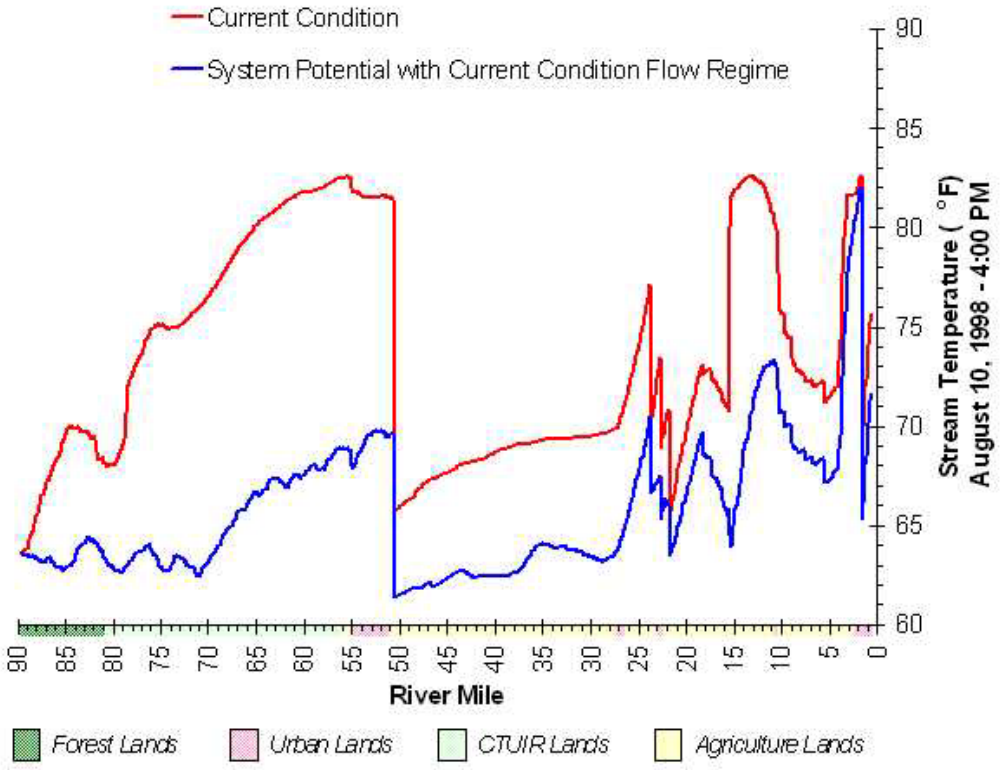

Figure A-57. Combination 2 Scenario – System Potential with Natural Flow Regime

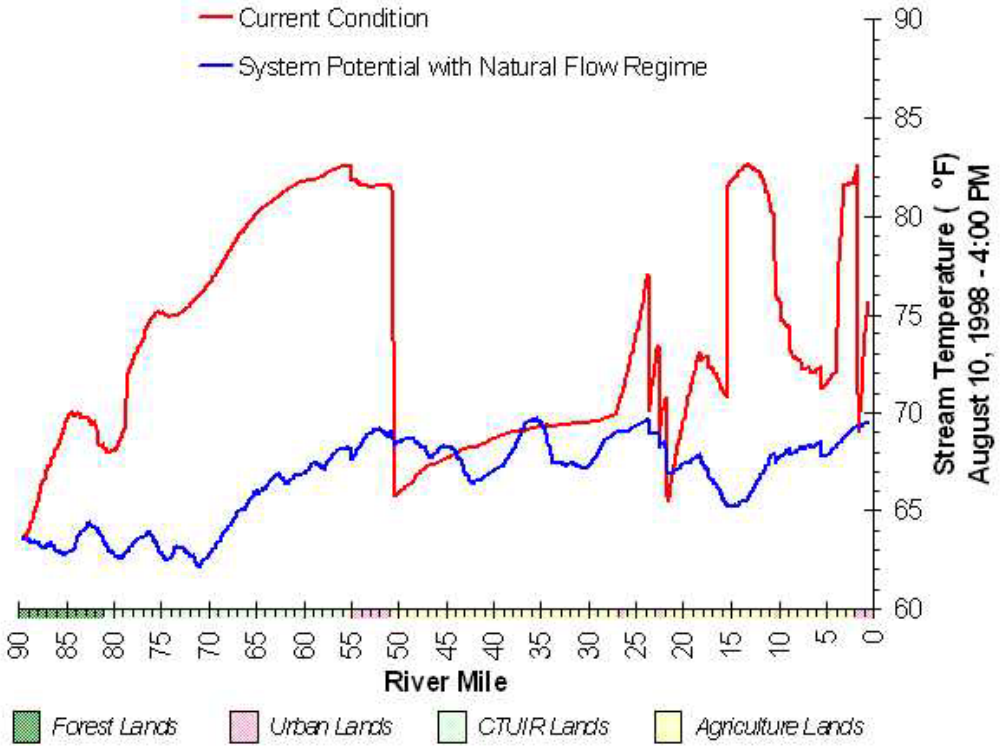

Figure A-58. Combination 3 Scenario – System Potential with Flow Augmentation

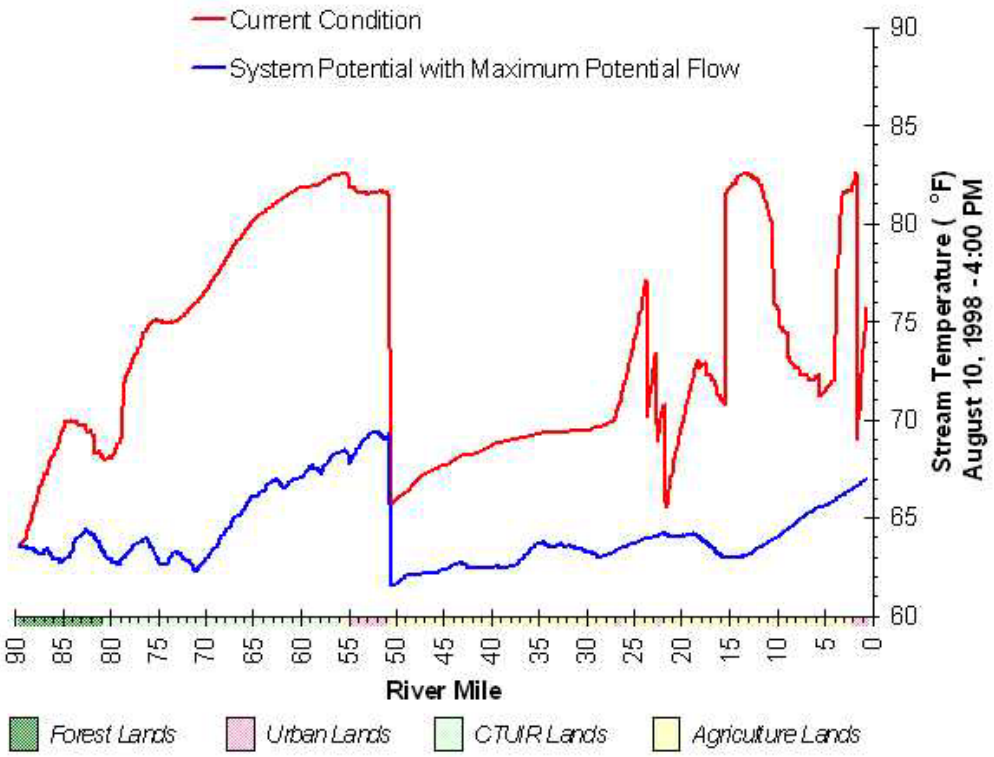

Spatial Distributions of Temperature

Under current conditions, 80% of the Umatilla River exceeds 68.5°F and about 43% of the river is greater than 73°F (**Figure A-59**). Very little thermal refugia currently exists for salmonids. Combination 1 (System Potential with Current Flow Regime) increases the thermal refugia significantly, with only about 4% of the Umatilla River exceeding 73°F. Combination 2 (System Potential with Maximum Potential Flows) achieves the lowest potential temperatures, with none exceeding 73°F. Note that Combination 3 (System Potential with Maximum Potential Flows) results in fewer river miles below 68.5°F, simply due to the fact that there is no McKay Reservoir flow augmentation to further cool the lower river.

Figure A-59. Spatial Distributions of Temperature Ranges as a Percentage of the Umatilla Mainstem for the Current Condition and System Potential Scenarios

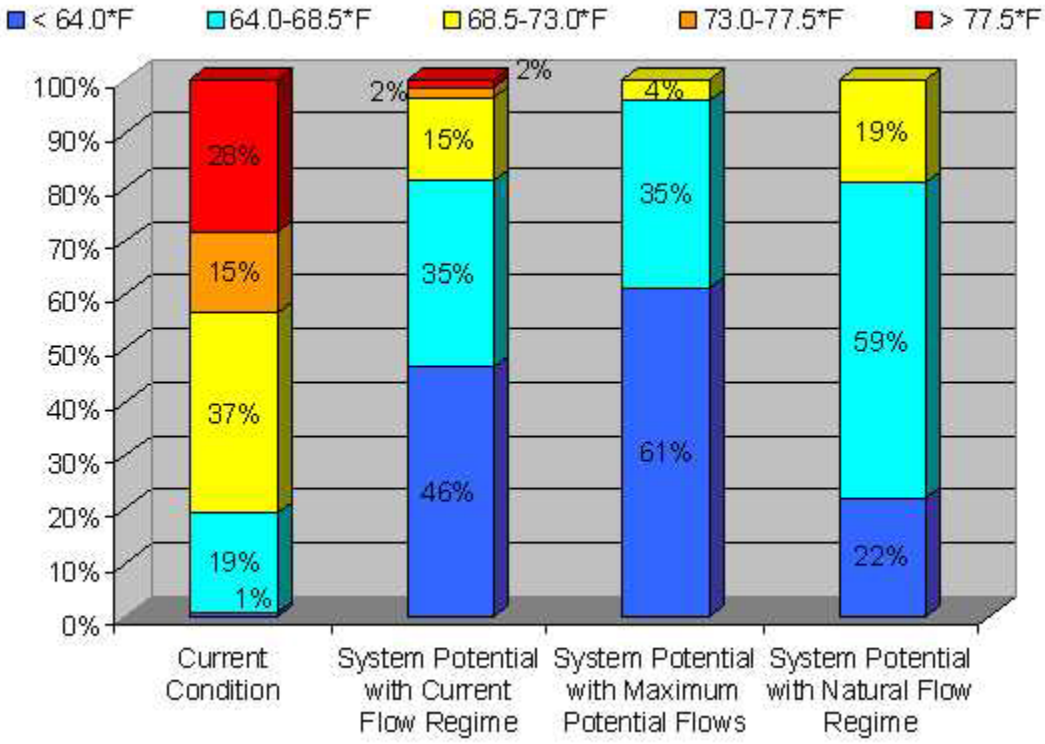

Radiant Energy Loading

Current and system potential radiant energy loading are displayed in **Figure A-60**. Radiant energy loading (left axis) can be directly translated into percent effective shade (right axis). Much of the Umatilla River system is currently at the maximum possible radiant energy loading (has no shade), due to the lack of adequate near-stream vegetation and extremely wide near-stream disturbance zones. Radiant energy loading and percent effective shade are identical for all three combinations because the only parameter that differs between the combinations is flow. All shade-determining parameters (i.e., vegetation and NSDZ width) are the same in all three combinations. Thus, all of the combination scenarios result in the same loading capacities; however, predicted stream temperatures vary between combinations due to flow differences.

Figure A-60. Radiant Energy Loading and Effective Shade for Current Condition and System Potential (Combinations 1-3)

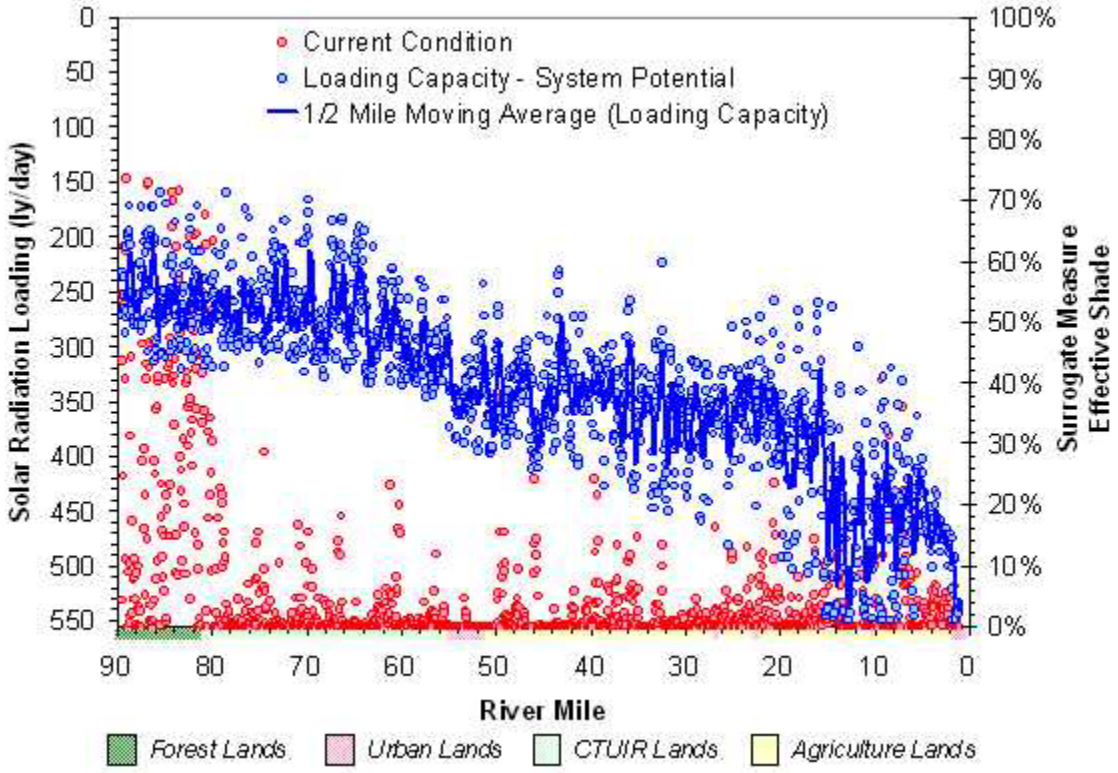

Figure A-61 displays the current and system potential radiant energy loading that must occur to meet the loading capacity.

Figure A-61. Radiant Energy Loading Reductions for Current Condition and System Potential (Combinations 1-3)

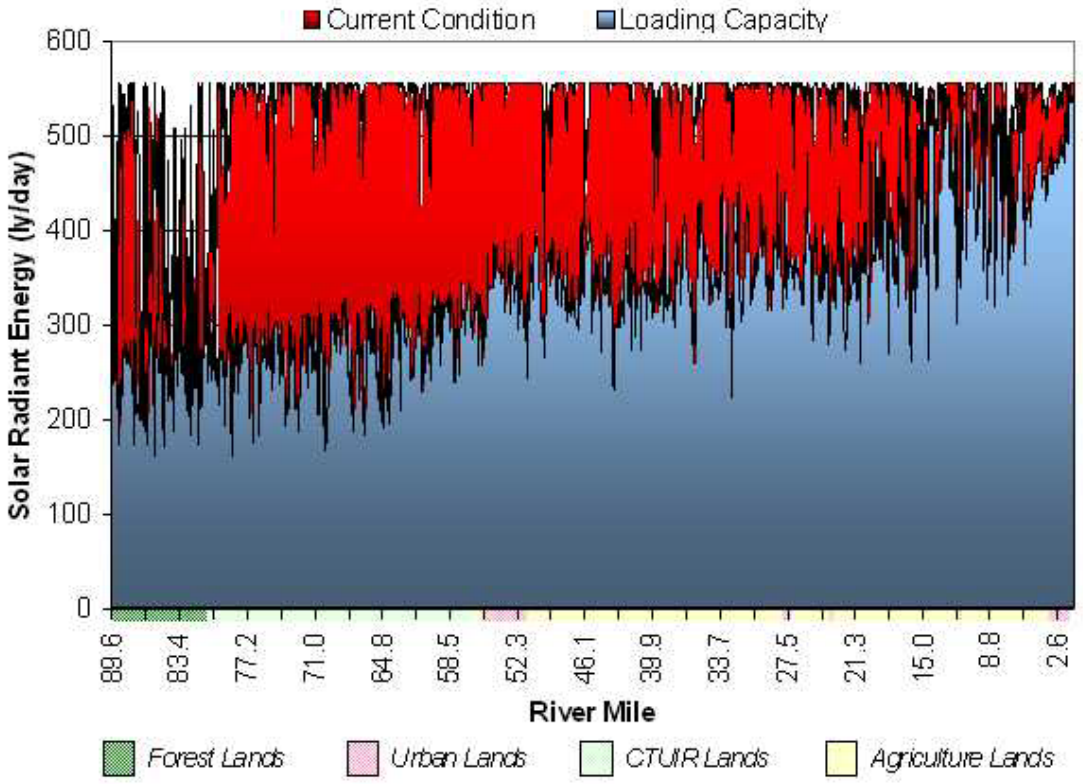

System Sensitivity Analysis

Figures A-62 through **A-64** summarize the stream temperature deviation between the current condition and the single-parameter scenarios. Average deviations are presented for five sites along the Umatilla River. Once again, it is apparent that the individual parameters have little affect on Umatilla River temperatures. Of particular interest is the 9.2°F increase below McKay Creek in the natural flow scenario. Recall that the natural flow scenario has no flow augmentation from McKay Creek.

Figure A-62. Flow Sensitivity

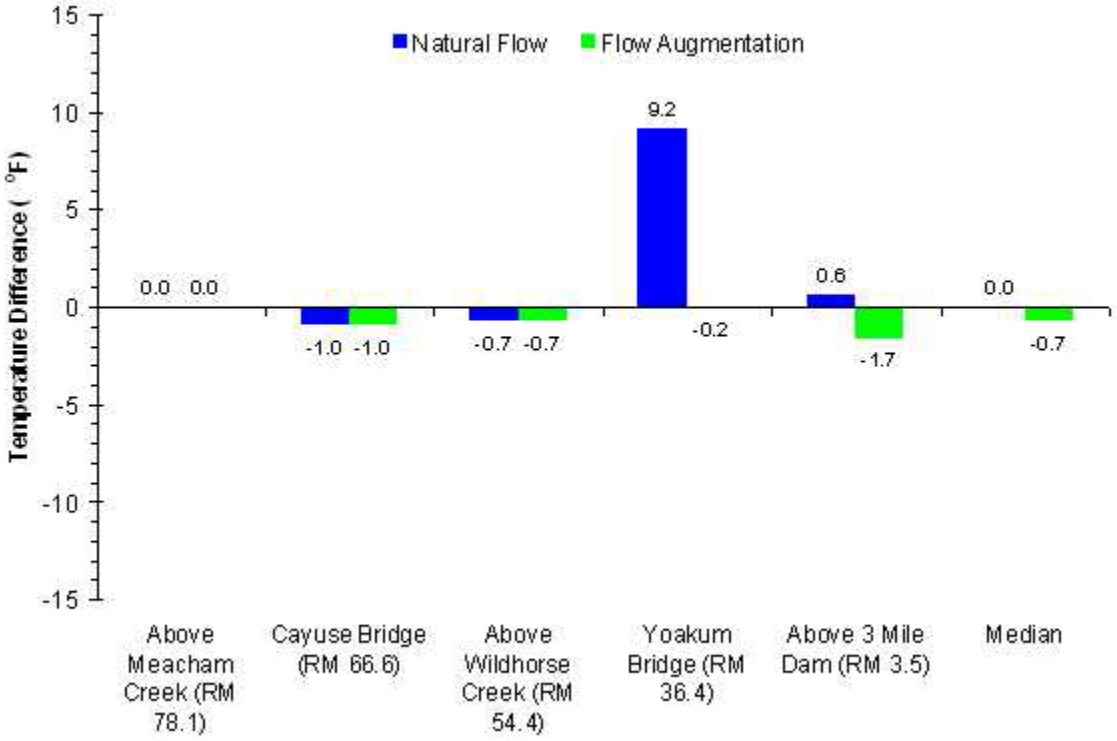

Figure A-63. Near-Stream Zones of Disturbance Sensitivity

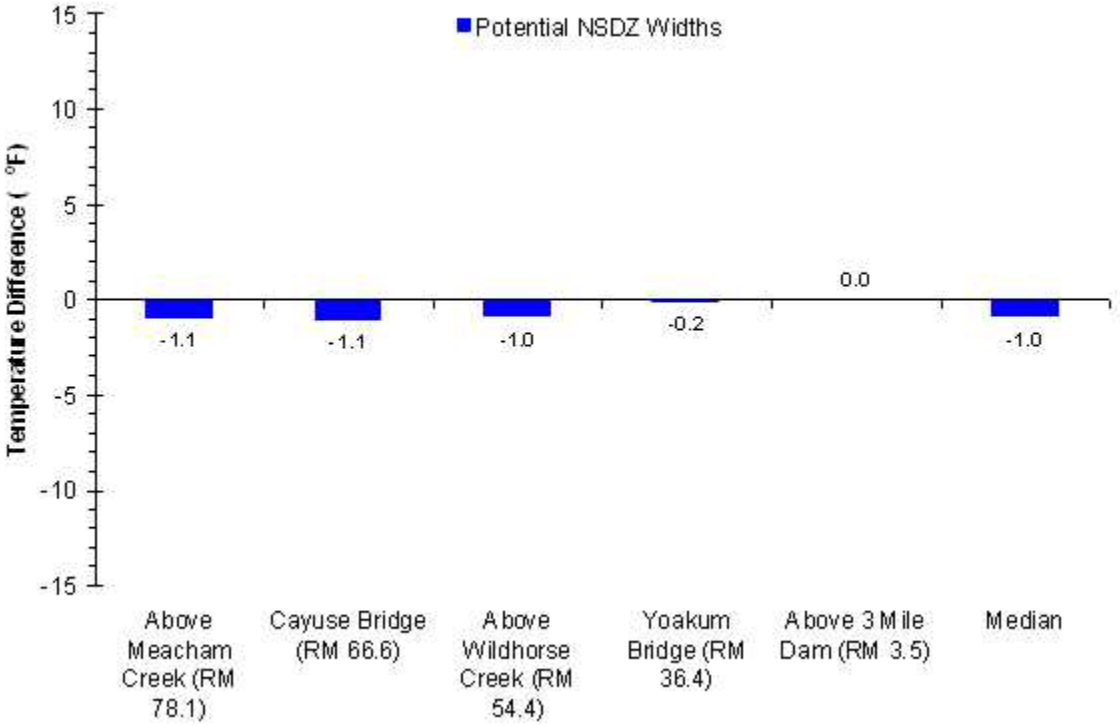

Figure A-64. Vegetation Height Sensitivity

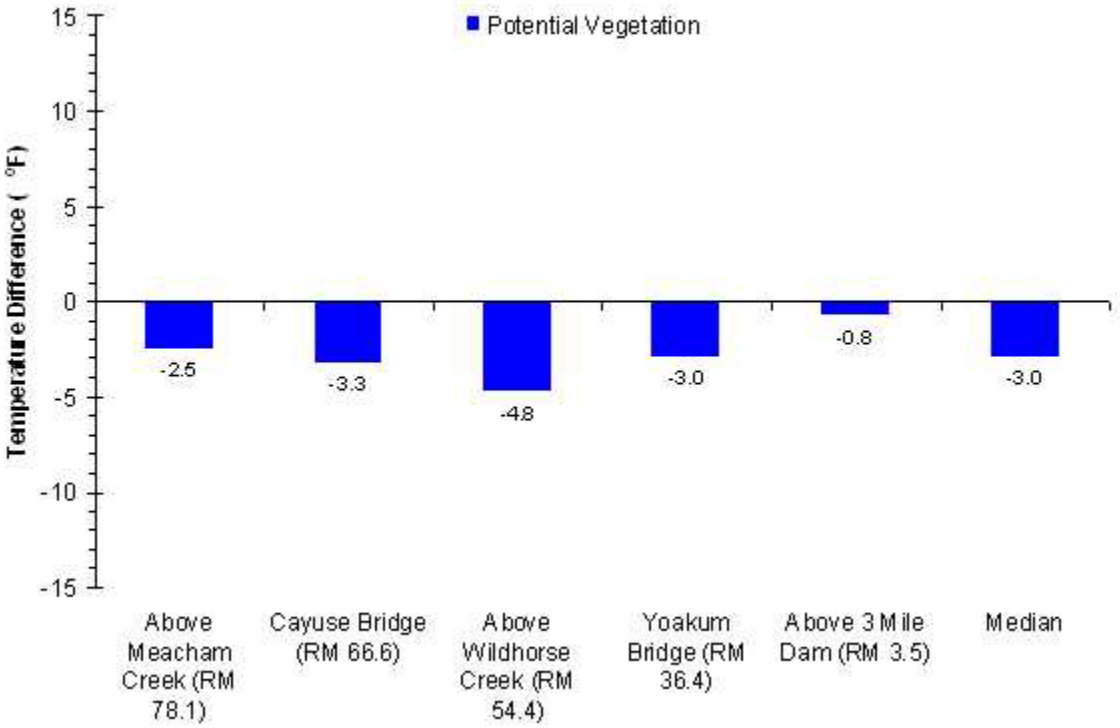

As previously illustrated, the combination scenarios resulted in the greatest Umatilla River temperature reductions. The combination scenario temperature deviations for fives sites along the Umatilla and their averages are summarized in **Figure A-65**. The Umatilla River system potential appears to be approximately 13°F cooler (than current conditions) above McKay Creek and about 5°F cooler below McKay Creek.

Figure A-65. Combination Scenario Sensitivity

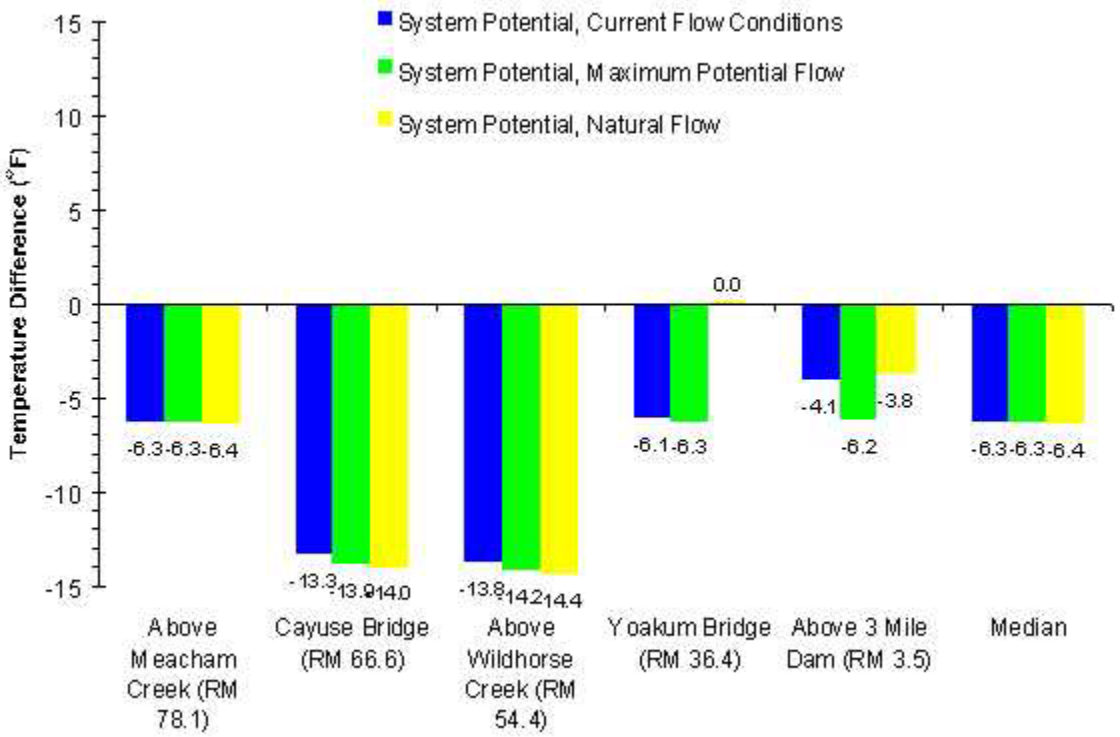

REFERENCES

Beschta, R.L, R.E. Bilby, G.W. Brown, L.B. Holtby, and T.D. Hofstra. 1987. Stream temperature and aquatic habitat: Fisheries and forestry interactions. Pp. 191-232. *In*: E.O. Salo and T.W. Cundy (eds), Streamside Management: Forestry and Fishery Interactions. University of Washington, Institute of Forest Resources, Contribution No. 57. 471 pp.

Beschta, R.L. and J. Weatherred. 1984. A computer model for predicting stream temperatures resulting from the management of streamside vegetation. USDA Forest Service. WSDG-AD-00009.

Beschta, R.L., S.J. O'Leary, R.E. Edwards, and K.D. Knoop. 1981. Sediment and Organic Matter Transport in Oregon Coast Range Streams. Water Resources Research Institute. OSU. WRRI-70.

Bowen, I.S. 1926. The ration of heat loss by convection and evaporation from any water surface. Physical Review. Series 2, Vol. 27:779-787.

Boyd, M.S. 1996. Heat Source: stream temperature prediction. Master's Thesis. Departments of Civil and Bioresource Engineering, Oregon State University, Corvallis, Oregon.

Brown, G.W. 1983. Chapter III, Water Temperature. Forestry and Water Quality. Oregon State University Bookstore. Pp. 47-57.

Brown, G.W. 1970. Predicting the effects of clearcutting on stream temperature. *Journal of Soil and Water Conservation.* 25:11-13.

Brown, G.W. 1969. Predicting temperatures of small streams. *Water Resour. Res.* 5(1):68-75.

Brown, L.C. and T.O. Barnwell. 1987. *The enhanced stream water quality models qual2e and qual2e-uncas: documentation and user manual*. U.S. Environmental Protection Agency, Athens, Georgia.

Chen, D.Y. 1996. Hydrologic and water quality modeling for aquatic ecosystem protection and restoration in forest watersheds: a case study of stream temperature in the Upper Grande Ronde River, Oregon. Ph.D. Dissertation. University, of Georgia. Athens, Georgia.

Chow, V.T. 1959. *Open Channel Hydraulics*. New York: McGraw-Hill Co.

Clarke, S.E. and S.A. Bryce. 1997. Hierarchical subdivisions of the Columbia Plateau and Blue Mountain Ecoregions, Oregon and Washington. Gen. Tech. Rep. U.S. Department of Agriculture Forest Service, Portland, OR.

Crowe, E.A. and R.R. Clausnitzer. 1997. Mid-Montane Wetland Plant Associations of the Malheur, Umatilla and Wallowa-Whitman National Forests. United States Department of Agriculture Forest Service, Pacific Northwest Region. Technical Paper R6-NR-ECOL-TP-22-97.

Everest F.H., R.L. Beschta, J.C. Scrivener, K.V. Koski, J.R. Sedell, and D.J. Cederholm. 1987. Fine Sediment and salmonid production a paradox. in *Streamside Management Forestry and Fishery Interactions*. Salo and Cundy Eds. College of Forest Resources. University of Washington, Seattle WA.

Halliday D. and R. Resnick. 1988. *Fundamentals of Physics*. 3rd Edition. John Wiley and Sons, New York. pp. 472-473.

Harbeck, G.E. and J.S. Meyers. 1970. Present day evaporation measurement techniques. J. Hydraulic Division. A.S.C.E., Prceed. Paper 7388.

Harvey, G.W. 1993. Technical review of sediment criteria. Idaho Department of Health and Welfare, Division of Environmental Quality. Boise, ID.

Ibqal, M. 1983. An Introduction to Solar Radiation. Academic Press. New York. 213 pp.

Irving, J.S. and T.C. Bjornn. 1984. Effects of substrate size composition on survival of Kokanee salmon and cutthroat and rainbow trout embryos. Univ. of Idaho Coop. Fish. Res. Unit. Tech. Re., pp. 84-96. Moscow, ID.

Iwamoto R.N., E.O. Salo, M.A. Madej, R.L. McComas. 1978. Sediment and water quality: A review of the literature including a suggested approach for water quality criteria. EPA 910/9-78-048.

Jobson, H.E. and T.N. Keefer. 1979. Modeling highly transient flow, mass and heat transfer in the Chattahoochee River near Atlanta, Georgia. Geological Survey Professional Paper 1136. U.S. Gov. Printing Office, Washington D.C.

Kagan, J.S., R. Morgan, and K. Blakely. 1999. *Umatilla and Willow Creek Basin Assessment for Shrub Steppe, Grasslands, and Riparian Wildlife Habitats*. EPA Regional Geographic Initiative Draft Final Report.

Kovalchik, B.L. 1987. Riparian zone associations of the Deschutes, Ochoco, Fremont and Winema National Forests. R6ECOLTP279/87. Portland, OR:U.S. Department of Agriculture, Forest Service, Pacific Northwest Region. 171 pp.

Newcombe C.P. and D.D. MacDonold. 1991. Effects of suspended sediment on aquatic ecosystems. North American Journal of Fishery Management. 11:72-82

Oregon Department of Environmental Quality. 1995. 1992-1994 Water Quality Standards Review. DO issue paper.

Park, C. 1993. SHADOW: stream temperature management program. User's Manual v. 2.3. USDA Forest Service. Pacific Northwest Region.

Parker, F.L. and P.A. Krenkel. 1969. Thermal pollution: status of the art. Rep. 3. Department of Environmental and Resource Engineering, Vanderbilt University, Nashville, TN.

Rishel, G.B., Lynch, J.A. and E.S. Corbett.. 1982. Seasonal stream temperature changes following forest harvesting. *J. Environ. Qual.* 11:112-116.

Rosgen, D. 1996. *Applied River Morphology*. Wildland Hydrology. Pagosa Springs, CO.

Rosgen, D. 1994. A Classification of Natural Rivers. Catena, Vol 22: 169-199. Elsevier Science, B.V. Amsterdam.

Sattterland, D.R. and P.W. Adams. 1992. *Wildland Watershed Managemet*. 2nd edition. John Wiley and Sons, Inc., New York.

Sellers, W.D. 1965. Physical Climatology. University of Chicago Press. Chicago, IL. 272 pp.

Sinokrot, B.A. and H.G. Stefan. 1993. Stream temperature dynamics: measurement and modeling. *Water Resour. Res.* 29(7):2299-2312.

Stowell, R.A., A. Espinosa, T.C. Bjornn, W.S. Platts, D.C. Burns, and J.S. Irving. 1983. A guide for predicting salmonid response to sediment yields in Idaho batholiths watersheds. Unpubl. Rept. UDS-FS.

Tappel, P.D. 1981. A new method of relating spawning gravel size composition to salmonid embryo survival. MS Thesis, Univ. of Idaho, Moscow, ID.

Tappel, P.D. and T.C. Bjornn. 1993. A new method of relating size of spawning gravel to salmonid embryo survival. *N. Am. Journal Fish Mgmt*. 3:123-135.

U.S. Forest Service (USFS) and Bureau of Land Management (BLM). 1995. "Interim Strategies for Managing Anadromous Fish-Producing Watersheds in Eastern Oregon and Washington, Idaho, and portions of California [**PACFISH**]".

Waters, T.F. 1995. Sediment in streams: sources, biological effects and control. American Fisheries Society Monograph 7.

Wunderlich, T.E. 1972. Heat and mass transfer between a water surface and the atmosphere. Water Resources Research Laboratory, Tennessee Valley Authority. Report No. 14, Norris Tennessee. Pp 4.20.